The RNA-associated splicing-factor p54^{nrb} regulates survival of human cells after UV irradiation

Aoife Corduff

Cell Cycle Control Laboratory, Centre for Chromosome Biology,

Discipline of Biochemistry, School of Natural Sciences,

National University of Ireland, Galway

A thesis submitted to the National University of Ireland, Galway for the degree of

Doctor of Philosophy

Supervisor: Professor Heinz-Peter Nasheuer

April 2013

TABLE OF CONTENTS

LIST OF FIGURES

LIST OF TABLES

ACKNOWLEDGEMENTS

I would first and foremost like to thank my supervisor, Prof. Heinz-Peter Nasheuer for giving me the opportunity to carry out a Ph.D project in his group and for all of his support, advice and encouragement over the years.

I would like to say a special thank you to Heinrich Anhold for all of his help throughout the years, especially in the beginning in helping me with the project, teaching me the minichromosome preparation method, and giving me some fantastic ideas.

I owe a great deal of gratitude to Prof. Brian McStay for all of his help and useful advice throughout my Ph.D. studies, especially for his time and use of his laboratory equipment to prepare the purified nucleoli.

I would also like to thank Prof. Juhani Syväoja and Miiko Sokka for their kind gift of the TopBP1 antibody that I used for this project.

I would like to thank all the members of the Cell Cycle Control group, past and present, for all of their helpful advice, friendly chats and encouragement over the years, especially Kristina Rehmet and Ronan Broderick.

Thanks to everyone in the Centre for Chromosome Biology and Biochemistry department for all of their support and helpful ideas and most of all being good friends both in and out of the lab. A special thanks to Mary, Sarah, Elaine, Róisín and Becca for all of their many cups of tea, wonderful help and friendship during the last number of years.

Finally, massive thanks to my family, without whom none of this would be possible, especially my wonderful parents, Pádraic and Mary and siblings, Ciara and Pádraic, who have supported me in every way and kept me positive and helped me to escape from the world of science when I needed to.

Go raibh míle maith agaibh,

Aoife

DECLARATION

I, Aoife Corduff, declare that the work presented in this thesis has been acquired and analysed by myself.

ABBREVIATIONS

53BP1	p53 binding protein 1
6-4 PP	6-4 pyrimidone photoproduct
9-1-1	Rad9-Rad1-Hus1
ATM	ataxia telangiectasia mutated
ATR	ATM- and Rad3-related
ATRIP	ATR-interacting protein
Bcl11a	B-cell chronic lymphoid leukemia 11a
BER	base excision repair
BLAP75	BLM-associated peptide 75
BLM	bloom syndrome helicase
BRCA1	breast cancer susceptibility gene 1
Cdc	cell division cycle
CDK	cyclin-dependent kinase
Cdt1	Cdc10-dependent target 1
CF	cleavage factor
CFIm68	cleavage factor Im 68
Chk1	checkpoint kinase 1
Chk2	checkpoint kinase 2
Col2AI	collagen, type II, A I
CPD	cyclobutane pyrimidine dimer
CS	Cockayne syndrome
CTD	carboxyl-terminal domain
D. melanogaster	*Drosophila melanogaster*
DAPI	6-diamidino-2-phenylindole
DBHS	*Drosophila* behaviour and human splicing
DDB	damaged DNA-binding protein
DDK	Dbf4-dependent kinase
DDR	DNA damage response
DFC	dense fibrillar centre
DMEM	Dulbecco's modified eagles medium
DMSO	dimethysulphoxide
DNA	deoxyribonucleic acid
Dna2	DNA replication helicase 2 homolog
DNA-PK	DNA-dependent protein kinase
DNA-PKcs	DNA-dependent protein kinase catalytic subunit
DOC	deoxycholate
DSB	double strand break
dsDNA	Double-stranded DNA
DTT	dithiothreitol
E. coli	*Escherichia coli*
E2F	adenovirus E2 promoter binding factor
E3UL	E3 ubiquitin ligase

ECL	enhanced chemiluminesence
EDTA	ethylenediaminetetraacetic acid
ERCC1	excision repair cross-complementing rodent repair deficiency, complementation group 1
Exo1	exonuclease 1
FBS	fetal bovine serum
FC	fibrillar centre
Fen1	flap endonuclease 1
FUS	Fused in Sarcoma (RNA-binding protein)
g	gravity
GC	granular component
GEN1	gen homologue, endonuclease 1
GFP	green fluorescent protein
GGR	global genome repair
GINS	go-ichi-ni-san
GT	guanyltransferase
H.H3	Histone H3
HEPES	4-(2-Hydroxyethyl) piperazine-1-ethanesulfonic acid
HJ	Holliday junction
HMGN1	high mobility group nucleosome binding domain 1
hnRNP M	heterogeneous nuclear ribonucleoprotein M
HR	homologous recombination
HRP	horseradish peroxidase
ICL	intrastrand crosslink
IF	immunofluorescence
IGAZ	interchromatin granule-associated zone
IR	ionizing radiation
LB	lysogeny broth
lcRNA	long non-protein-coding RNA
MATR-3	matrin-3
mCAT2	mouse cationic amino acid transporter 2
MCM	minichromosome maintenance
MDC1	mediator of DNA damage checkpoint protein 1
MMR	mismatch repair
MRN	Mre11, Rad 50 and Nbs1 complex
mRNA	messenger RNA
NBS1	Nibrin
NEAT	nuclear enriched abundant transcript
NEB	New England Biolabs
NER	Nucleotide excision repair
NHEJ	Non-homologous end joining
NonA	no-on-transient A
NOR	nucleolus organizer region
Nucp	nucleophosmin

ORC	origin recognition complex
$p54^{nrb}$	p54 nuclear RNA binding protein (also called `nono`)
PARP	Poly (ADP-ribose) polymerase
PBS	phosphate buffered saline
PCNA	Proliferating cell nuclear antigen
PCR	Polymerase chain reaction
Pen/Strep	Penicillin/Streptomycin
PFA	Paraformaldehyde
PIKK	Phosphatidylinositol 3-kinase-related kinase
PML	promyelocytic leukemia protein
PNK	polynucleotide kinase
Pol α/primase	DNA polymerase α/primase
PPM1G	Protein phosphatase Mg2+/Mn2+ dependent, 1G
pre-RC	pre-replicative complex
PSF	polypyrimidine tract-binding protein (PTB)-associated splicing factor
PSP	paraspeckle protein
Rad	radiation sensitive
Rb	retinoblastoma
RBMX	RNA-binding motif protein, X chromosome
RFC	replication factor C
RNA pol	RNA polymerase
RNA	ribonucleic acid
RNase	ribonuclease
RNP	ribonucleic protein
ROS	reactive oxygen species
RPA	replication protein A
RRM	RNA recognition motif
rRNA	ribosomal RNA
RTP	RNA 5’ triphosphatase
Sae2	sumo activating enzyme subunit 2
SDS	sodium dodecyl sulphate
SDS-PAGE	SDS polyacrylamide gel electrophoresis
SF-1	steroidogenic factor
Sgs1	salivary gland secretion 1
siRNA	small interfering RNA
snRNA	small nuclear RNA
snRNP	small nuclear ribonucleoproteins particle
Sox9	SRY-box containing gene 9
SS	Seckel syndrome
SSB	single-stranded break
SSC	sodium chloride trisodium citrate
ssDNA	single-stranded DNA
TAE	tris-acetate EDTA buffer
TAg	T antigen

TBP	TATA-binding protein
TCR	transcription-coupled repair
TEMED	tetramethylethylenediamine
TFIID	transcription factor II D
TFIIH	transcription factor II H
TG	Tris-glycine
THRAP3	thyroid hormone receptor-associated protein 3
TopBP1	topoisomerase II DNA binding protein 1
Tris	tris(hydroxymethyl)aminomethane
tRNA	transfer RNA
TTD	tricothiodystrophy
U2OS	human osteosarcoma cell line
UBF	upstream binding factor
UV	ultraviolet
WRN	Werner syndrome
XAB2	XPA binding protein 2
XLF	XRCC4-like factor
XP	xeroderma pigmentosum
XPA	xeroderma pigmentosum complementation group A
XPV	XP variant
XRCC4	X-ray repair cross complementary protein 4

ABSTRACT

UV radiation causes several forms of DNA damage; the most prominent of these are cyclobutane pyrimidine dimers (CPDs) and 6-4 pyrimidine-photoproducts (6-4 PPs). Nucleotide excision repair (NER) is a repair process that repairs these DNA lesions. Defects in the NER pathway lead to cancer-related diseases such as xeroderma pigmentosum (XP) that is caused by a defect in the XPA to XPG genes that are involved in the NER pathway. To investigate protein recruitment to chromatin after DNA damage, SV40 minichromosomes containing pyrimidine-rich DNA were established to create a tool with high sensitivity to UV for *in vivo* studies. Using this tool these findings suggest that $p54^{nrb}$, which exhibits multi-functional characteristics in a variety of cellular processes, including DNA and RNA binding, nuclear RNA processing and regulation of transcription, is a novel protein putatively involved in UV DNA damage response. The objective of this study was to gain a better insight into the mechanism(s) by which $p54^{nrb}$ is involved in the DNA damage response following UV irradiation, primarily using human cells as a model system. Immunofluorescence microscopy using human cells showed that $p54^{nrb}$, a 54-kDa nuclear RNA-binding protein, is recruited to nucleoli after UV irradiation. This recruitment is evident in a number of cell lines and depends on transcription since inhibition of transcription abolishes the DNA damage-dependent recruitment of $p54^{nrb}$. Fusion constructs of green fluorescent protein (GFP) with N- and C-terminal domains of $p54^{nrb}$ deleted have been constructed to determine that the coiled-coil domain (C-terminal) of $p54^{nrb}$ is required for its localisation to nucleoli. By performing local UV irradiation "micropore" experiments, whereby specific areas of the cell are irradiated with UV, it was determined that $p54^{nrb}$ does not localise to sites of DNA damage and nucleoli specifically do not need to be irradiated for the nucleolar localisation of $p54^{nrb}$. DNA damage signalling (PIK kinases) drug inhibitors reduce $p54^{nrb}$ nucleolar localisation following UV irradiation that suggests that $p54^{nrb}$ could be a downstream target of these factors. Notably, the use of ATM- and ATR-specific inhibitors revealed that both DNA damage response kinases cooperate in the regulation of $p54^{nrb}$ recruitment to the nucleolus after UV treatment. Depletion of $p54^{nrb}$ demonstrates higher cell viability following UV irradiation. Model consistent with data is that sequestering of $p54^{nrb}$ to the nucleolus could be a cellular mechanism to allow an optimal response of cells to repair DNA damage.

Chapter 1- Introduction

The cell is the fundamental unit of life. The study of cell biology allows us to contemplate the various systems that interact in the cell, particularly molecular and biochemical pathways that are essential for the cell to survive. This chapter will introduce the main types of DNA, RNA and protein associated molecular and biochemical pathways currently recognised in eukaryotic organisms. Several of these metabolic processes are described in detail with particular focus on DNA repair pathways and the process of transcription both of which are vital for the cells' viability.

1.1 The cell cycle

For the cell to duplicate, it must undergo the cell cycle. The cell cycle can be divided into four different phases: G_1 phase (Gap 1), S phase (Synthesis), G_2 phase (Gap 2) and M phase (Mitosis and cytokinesis) (Blow and Quan Ge, 2009). These distinct phases can be grouped into two major phases: M phase and interphase. M phase includes the processes of mitosis and cytokinesis in which the cell divides into two daughter cells. G_1, S and G_2 phase are collectively known as interphase and it is the period between cell division where the cell grows in size and engages in metabolic activities (Karp, 2007). Alternatively, cells may enter the quiescent G_0 state from G_1 and can remain there for a long period of time (Karp, 2007). The transition of the cell into the G_0 phase is not permanent and it can re-enter the G_1 phase at any time, although this is tightly regulated. M phase consists of mitosis (nuclear division) and can be broken down into four distinct phases, sequentially known as prophase, metaphase, anaphase and telophase, each characterised by a particular series of events. These processes are closely followed by cytokinesis, a process by which a dividing cell splits into two forming two daughter cells (Karp, 2007).

During the first stage of mitosis, prophase, the duplicated chromosomes are prepared for segregation, and the mitotic machinery is assembled. Firstly, the chromosomal material is condensed into compact mitotic chromosomes; each chromosome consists of two sister chromatids, bound together at the centromere by a cohesin protein complex (Karp, 2007). Next the cytoskeleton is disassembled and the mitotic spindle machinery is assembled, this consists of a bipolar structure consisting of microtubules and associated proteins (Karp, 2007). Finally, at late prophase, the nuclear envelope of the nucleus disassembles. The breakdown of the nuclear envelope marks the start of pro-metaphase. Here, the spindle

microtubules enter the nuclear space and attach to the condensed chromosomes at the kinetichore, a complex protein structure that attach the microtubules to the chromosomes (Karp, 2007). Finally, the chromosomes are positioned along the centre of the cell, midway between the spindle poles. Once the chromosomes are aligned in the centre of the cell (this is termed the metaphase plate) and one chromatid of each chromosome is connected by its kinetichore to microtubules from one pole and its sister chromatid is connected by its kinetichore to a microtubule from the opposite pole, the cell is said to be in metaphase (Karp, 2007). Anaphase begins when the sister chromatids of each chromosome split apart and start their movement towards opposite poles. This process is initiated by microtubules shortening, causing each chromatid to be pulled slowly towards the centrosome the microtubules are attached to (Karp, 2007). As the chromosomes cluster at opposite spindle poles, it marks the beginning of telophase. In this phase, the chromosomes become dispersed and the nuclear envelope reassembles surrounding the chromosome clusters (Karp, 2007). Finally, the cell is divided into two daughter cells by a separate process called cytokinesis. In cytokinesis, a cleavage furrow (pinch) containing a contractile ring develops, where the metaphase plate used to be, pinching off the separated nuclei. Each daughter cell has a complete copy of the genome of its parent cell. The end of cytokinesis marks the end of M phase (Nanninga, 2001).

As described earlier, interphase is divided into three phases: G_1, S and G_2. During all three phases, the cell grows by producing proteins and cytoplasmic organelles. However, chromosomes are replicated only during the S phase. S phase is also the period when the cell synthesises additional histones that are required as the cell doubles the number of nucleosomes in its chromosomes (Karp, 2007). Thus, a cell grows (G_1), continues to grow as it duplicates its chromosomes (S), propagates more, and prepares for mitosis (G_2), and finally it divides (M) before restarting the cell cycle. The progression of the cell through the cell cycle is a highly regulated process and is monitored by members of the cyclin family of proteins. Cyclins bind to and activate members of the cyclin-dependent kinase family (CDK), which in turn effects cell cycle progression. The progression of a cell through the cell cycle is controlled by relative levels of individual cyclin family members including cyclin D, E, A and B (Karp, 2007). CDK activity is relatively low during G_1 phase to allow the formation of pre-replicative complexes at the origins of replication (see DNA

replication, section 1.2). The cyclin D family members are G_1 phase cyclins that monitor the entry of cells into G_1 from G_0 quiescent phase. The cyclin D family associate with Cdk4 and Cdk6 that enforce commitment to enter S-phase (Sherr and Roberts, 2004). The G_1/S transition is driven by the activity of cyclin E and cyclin A binding to Cdk2 (Coverley et al., 2002). The cyclin B family trigger the assembly of the mitotic spindle and sister-chromatid pair alignment on the spindle. Cyclin E and cyclin A play a role in DNA synthesis during S phase which is described in more detail below (Coverley et al., 2002).

1.2 Eukaryotic DNA replication

In eukaryotes, DNA replication takes place throughout the S phase of the cell cycle, during which time the entire genome is precisely duplicated (Blow and Quan Ge, 2009). The highly coordinated process of eukaryotic DNA replication is initiated once and only once per cell cycle at distinct origins of replication on chromosomal DNA (Nasheuer et al., 2002). The initiation of DNA replication begins with the binding of the multisubunit origin recognition complex (ORC) to the origin of replication, at the early G1-phase of the cell cycle (Rytkönen et al., 2006). Following the binding of the ORC to the origin, Cdc6 (cell division cycle 6) and Cdt1 (Cdt6-dependent target 1) bind to the ORC complex (Rytkönen et al., 2006). This multimeric Cdc6–Cdt1–ORC–DNA complex, enables the loading of the MCM 2-7 (minichromosome maintenance 2-7) complex to chromatin, forming the pre-replicative complex (pre-RC) (Rytkönen et al., 2006). CDKs and DDK (Dbf4-dependent kinase) activate the pre-RC complex to allow the formation of the initiation complex that is made up of a large complex containing RPA (replication protein A), Cdc45 and the GINS [go-ichi-ni-san (five-one-two-three)] complex, leading to activation of the replicative helicase complex and causing the unwinding of the DNA double helix (Masai et al., 2005; Rytkönen et al., 2006).

The MCM 2-7 protein complex forms a clamp around the DNA and facilitates in the separation of the double helix ahead of the replication forks (Blow and Quan Ge, 2009). As the DNA helix is unwound, the single-stranded DNA (ssDNA) becomes coated with the trimeric protein, RPA (Blow and Quan Ge, 2009). RPA protein facilitates in the chromatin association of the DNA polymerase-α/primase (Pol α/primase), triggering the initiation of DNA replication (Nasheuer et al., 2002). In order to relieve torsional stress on the DNA

backbone during replication, topoisomerase I is recruited to sites ahead of the progressing replication fork (Broderick and Nasheuer, 2009).

Figure 1.1 Overview of the proteins involved in eukaryotic DNA replication
The diagram represents the proteins that play a role in DNA replication with particular attention on the origin of replication and the formation of the lagging and leading strand. Figure adapted from (Broderick and Nasheuer, 2009).

Pol α is the only DNA polymerase that can start DNA replication *de novo*, it consist of four subunits, p180, p68, p58, and p48 (Nasheuer et al., 2002). The major function of the Pol α/primase complex is synthesizing a short RNA-DNA primer of ~30-40 nucleotides that serves to initiate DNA replication (Rytkönen et al., 2006). The RNA-DNA synthesized primer is then recognized by replication factor C (RFC) that loads the replicative sliding clamp, PCNA (proliferating-cell nuclear antigen), onto the DNA (Broderick and Nasheuer, 2009). A DNA polymerase switch takes place from Pol α/primase to either DNA polymerase δ or ε (Pol δ and ε) with the cooperative binding of RFC, PCNA and RPA, this allows continuous DNA synthesis on the leading strand and discontinuous DNA synthesis on the lagging strand (Broderick and Nasheuer, 2009). On the lagging strand, the repetitive priming of Pol α/primase followed by RFC and PCNA mediated polymerase switch leads to the formation of Okazaki fragments (~200 nucleotides long) (Rytkönen et al., 2006). These fragments are then matured and ligated into a continuous new strand by the actions

of RNAse H, Fen1 (flap endonuclease 1), Dna1, Pol δ and DNA ligase 1 (Broderick and Nasheuer, 2009).

1.3 The DNA damage response and genome instability

The inability to repair DNA damage properly results in genomic instability and enhances the rate of tumour formation. Organisms are continuously under attack by exogenous (external agents such as ultraviolet (UV) light and ionizing radiation (IR)) and endogenous (such as reactive oxygen species (ROS)) cytotoxic agents (Ciccia and Elledge, 2010). UV radiation is a form of direct DNA damage that induces the formation of crosslinking between adjacent cytosine and thymine bases creating pyrimidine dimers. The most prominent of these pyrimidine dimers are cyclobutane pyrimidine dimers (CPDs) and the (6-4) pyrimidone photoproducts (6-4 PPs). UV light from sunlight can induce up to 10^6 DNA lesions per cell per day (de Boer and Hoeijmakers, 2000). Both CPD and 6-4 PP formation occur between any two adjacent pyrimidines and they cause severe structural distortion in the DNA helix thus compromising cellular viability (Friedberg, 2006). The presence of these DNA lesions represents physical obstacles for replication and transcription, thus greatly affecting DNA metabolic processes (Lazzaro et al., 2009).

Figure 1.2 Lewis structures of photoproducts induced by ultraviolet (UV) light
The most prominent of these photoproducts are cyclobutane pyrimidine dimers (CPDs) and the (6-4) pyrimidone photoproducts (6-4 PPs). Image adapted from (Li et al., 2006)

1.4 DNA repair pathways in eukaryotes

In response to DNA damage caused by the cytotoxic agents described previously, organisms have developed various DNA repair and signal transduction pathways. Mispaired DNA bases are replaced with correct bases by mismatch repair (MMR), and small chemical alterations of DNA bases are repaired by base excision repair (BER) through excision of the damaged base (Lindahl and Barnes, 2000). The more complex lesions, such as pyrimidine dimers are corrected by nucleotide excision repair (NER) resulting in the excision of approximately 20-30 bp of the damaged DNA (described in detail further on). Similarly, intrastrand crosslinks (ICLs) are excised by ICL repair and are assisted by proteins involved in the genetic syndrome Fanconi anaemia (de Boer and Hoeijmakers, 2000). Single-strand breaks (SSBs) are repaired by single-strand break repair (SSBR). Double strand breaks (DSBs) are processed by one of two processes, either NHEJ (non-homologous end joining) or HR (homologous recombination) (Ciccia and Elledge, 2010).

1.4.1 Non-homologous end joining (NHEJ)

Non-homologous end joining (NHEJ) is the predominant DSB repair pathway in G_1/G_0 cells. In the initial step of NHEJ, the Ku heterodimer (Ku70 and Ku80) binds to the DNA. The Ku heterodimer has a toroidal structure with a hole through it that loads onto DSB ends (Ciccia and Elledge, 2010). Once the Ku heterodimer localises to DSBs, it recruits and activates the catalytic subunit of DNA-PK (DNA-PKcs) to initiate NHEJ (Mahaney et al., 2009). After the DNA ends have been detected, the DNA ends are processed by Artemis, DNA polymerase μ and λ, PNK and WRN (Mahaney et al., 2009). After the DNA has been processed, the DNA ends are then religated by the co-operative binding of DNA ligase IV in a complex with XRCC4 and the stimulatory factor XLF (Ciccia and Elledge, 2010; Mahaney et al., 2009).

1.4.2 Homologous recombination (HR)

Homologous recombination (HR) is a critical mode of DNA repair that is utilised predominantly in S and G_2 phase of the cell cycle (Ciccia and Elledge, 2010). In the first step of the HR repair pathway, MRN (Mre11-Rad50-Nbs1) and CtIP (Sae2) induce initial

resection of the DSB, resulting in 50–100 nucleotide ssDNA 3' overhangs. In the second step, these DNA overhangs can serve as templates for long-range DNA end resection. End resection can occur by two independent mechanisms: one that uses Sgs1/BLM and Dna2 and the other using Exo1. Following resection, the exposed ssDNA is coated by RPA, which recruits the Rad52 to enable Rad51 strand exchange (Ciccia and Elledge, 2010). After the search for homology, a joint DNA structure is formed. The resulting double Holliday junctions (HJs) are then resolved by crossover or non-crossover events (Bernstein and Rothstein, 2009). The resolution of the junctions by the BLM-TOP3-RMI1 (BLAP75) complex leads to a non-crossover product of DSB repair. HJ resolution by the nucleases GEN1 and SLX1/SLX4, which associates with MUS81/EME1, can lead to both crossover and non-crossover events (Ciccia and Elledge, 2010).

1.4.3 PARP activation

Poly (ADP-ribose) polymerase (PARP) structures act as sensors upon which DNA repair factors are recruited to initiate DNA repair (Ciccia and Elledge, 2010). Poly (ADP-ribose) polymerases (PARPs) constitute a superfamily of 18 proteins, encoded by different genes and display a common conserved catalytic domain. PARP-1 and PARP-2 are both involved in DNA-break sensing and signalling when SSBR or base excision repair (BER) pathways are activated (Huber et al., 2004). PARP-1 has been shown to play a role in DSB repair by interacting with Ku proteins, mediating the accumulation of the MRN complex at γH2AX foci at DSBs and facilitates in the activation of ATM (Ciccia and Elledge, 2010).

Figure 1.4.3.1 DNA repair pathways involved in the repair of double strand breaks.
(A) Schematic representation of DSB repair by NHEJ and the key proteins involved in the process. The DSB is recognised by the Ku heterodimer, which in turn recruits repair factors, such as DNA-PKcs and Artemis to the DSB for end-processing. The final end-joining is carried out by the XLF-XRCC4-DNA ligase IV complex and involves DNA pol μ and λ. **(B)** Schematic representation of DSB repair carried out by PARP-1 mediating the accumulation of the MRN complex at DSBs and facilitates in the activation of the HR pathway. The MRN complex and Sae1 are recruited to the DSB, for the initial resection of the DNA, resulting in ssDNA overhangs. These overhangs serve as templates for long-range DNA resection, using either Sgs1-Dna2 or Exo1. The exposed ssDNA is then coated with RPA, which recruits the Rad52 group of proteins, to enable Rad51 filament formation. After finding a homologous sequence, a joint DNA structure and Holliday junction is formed, which is resolved by the BLAP75 complex and involves GEN1. Adapted from (Ciccia and Elledge, 2010)

1.4.4 Nucleotide excision repair (NER)

Nucleotide excision repair (NER) is a highly conserved pathway that deals with bulky helix-distorting lesions, mainly UV induced photoproducts, but also with several kinds of bulky adducts induced by chemical agents. The process of NER is accomplished in two sub pathways for the recognition of DNA photoproducts. The first subpathway is global genome repair (GGR) that takes place when the DNA damage occurs in non-transcribed regions and on the non-transcribed strand of transcription-active genes. Transcription-coupled repair (TCR) takes place on the transcriptionally active strand of transcription-active genes (Mullenders, 2001). Both of these sub pathways GGR and TCR use the same pathway for the repair of the lesions and only differ in the process in which they recognise DNA damage. 6-4 PPs that distort the DNA more than CPDs are recognised more rapidly and predominantly by GGR. The repair of CPDs by GGR is a slow process and is more efficiently carried out in active genes by TCR (de Lima-Bessa et al., 2008).

1.4.4.1 Recognition of a DNA lesion

GGR is initiated when XPC protein forms a heterodimer complex with HR23B and is vital for the recognition of DNA lesions in the GGR pathway. The XPC-HR23B complex is preceded by the heterodimeric UV-DDR (UV-damaged-DNA-binding protein) complex that consists of the 127 kDa (DDB1) and 48 kDa (also known as XPE (DDB2)) subunits (Hwang et al., 1998)). Mutations in the DDB2 gene have been found to cause the XP group E phenotype (Vrouwe and Mullenders, 2009). This heterodimer is also part of an E3 ubiquitin ligase (E3UL) that has many substrates relevant for the activation of repair of damaged sites including histones and XPC protein (Vrouwe and Mullenders, 2009). UV-DDB has a higher affinity for damaged DNA (100-1000 fold) than the XPC-HR23B heterodimer, although the specific affinity for 6-4 PP is comparable (Batty et al., 2000).

For the TCR repair pathway the XPC-HR23B and DDB complexes are not required for recognition of damaged DNA suggesting a different method is used (Costa et al., 2003). The TCR repair pathway is initiated by the stalling of RNA pol II on the actively transcribed DNA strand. RNA pol II stops when it encounters damage on the template strand such as CPDs (de Lima-Bessa et al., 2008). Since TCR is initiated on transcriptionally active DNA, lesions are repaired more efficiently than in the case of GGR

(de Lima-Bessa et al., 2008). The stalled RNA pol II then colocalises with the proteins Cockayne Syndrome A (CSA) and Cockayne Syndrome B (CSB) that in turn triggers the assembly of the remaining NER factors including the nucleosomal binding protein HMGN1 (high mobility group nucleosome binding domain 1) and XAB2 (XPA binding protein 2) (Kamileri et al., 2012).

Figure 1.4.4.1 Proteins involved in the GGR pathway.
The XPE-DDB1 complex is involved with the XPC-HR23B recognition complex that binds to sites of DNA damage (depicted above in red). The resulting protein complex is used to stabilise the binding of the TFIIH complex containing XPB and XPD that unwinds the damaged DNA double helix. Subsequently the incision proteins are recruited and the lesion is processed. Adapted from (Vilmar and Sorensen, 2009).

1.4.4.2 Damage demarcation

Once lesions have been recognised by either GGR or TCR the DNA is unwound by the DNA helicase activities of transcription factor II H (TFIIH). TFIIH is a multiprotein complex that consists of at least 10 different subunits that also plays a role in the transcription initiation process (Vrouwe and Mullenders, 2009). The XPB and XPD subunits of TFIIH are ATP-dependent helicases that mediate unwinding of the DNA, XPB in the 3'-5' direction and XPD in a 5'-3' direction (Vrouwe and Mullenders, 2009).

Following the activity of TFIIH, RPA together with XPA stabilize the DNA "bubble" around the damage (Leibeling et al., 2006). RPA is a eukaryotic ssDNA-binding protein that binds to the undamaged DNA strand partially unwound by TFIIH but has also been shown to interact with pre-incision and post-incision proteins (Moser et al., 2007). XPA is an essential factor for GGR and associates with ERCC1-XPF, TFIIH and together with RPA allows for the identification of DNA lesions to form the pre-incision complex (Vrouwe and Mullenders, 2009).

Figure 1.4.4.2 Transcription-coupled repair: Recognition of damaged DNA.
When RNA pol II on actively transcribed DNA meets a lesion such as a UV photoproduct (depicted in red) it is stalled and a damage response in initiated. Adapted from Vilmar and Sorensen, 2009.

1.4.4.3 Single strand incision at both sides of the DNA lesion

The two endonucleases, XPG and XPF-ERCC1, incise the damage containing DNA strand. The XPG protein specifically incises the DNA strand on the 3' side ~6 nucleotides downstream of the DNA damage (Vrouwe and Mullenders, 2009). This is followed by strand incision ~20-22 nucleotides upstream of the DNA damage performed by the XPF-ERCC1 complex on the 5' side of the damage DNA (Mullenders, 2001). The XPG protein

interacts with RPA and TFIIH and the recruitment of XPG to the preincision complex is dependent on the functional TFIIH complex (Vrouwe and Mullenders, 2009). The recruitment of XPF-ERCC1 to the pre-incision complex is dependent on XPA and this interaction is essential for the activity of NER (Volker et al., 2001).

1.4.4.4 Repair syntheis

Following the removal of the damaged oligonucleotide, the remaining gap in the DNA backbone is filled with a newly synthesised oligonucleotides using the complementary strand as a template (Leibeling et al., 2006). Repair synthesis requires PCNA, RF-C, RPA, DNA ligase I, Pols δ and ε repair the remaining nick in the DNA backbone (Vrouwe and Mullenders, 2009).

Figure 1.4.4.4 The unwinding, incision, and gap-filling steps of nucleotide excision repair. After recognition NER proceeds with DNA unwinding and excision of the damaged nucleotides. RPA coats the exposed ssDNA and DNA polymerases move in to fill the remaining gap. Adapted from (Vilmar and Sorensen, 2009).

1.4.4.5 XPA protein and checkpoint activation

XPA is a ubiquitously expressed nuclear protein that is an essential factor in NER as described previously. It has been shown that XPA protein has a higher affinity for damaged DNA (UV-induced photoproducts) relative to undamaged DNA, indicating that XPA protein is a damage recognition protein (Friedberg, 2006). More recently, XPA protein has been shown to be an essential factor in checkpoint activation and this activity is conserved from yeast to humans (Bomgarden et al., 2006; Giannattasio et al., 2004).

Recent reports have shown a role for XPA protein in the activation of the intra-S-phase checkpoint (Bomgarden et al., 2006). The study demonstrated that XPA was required for successful Chk1 activation in human cells and further to this, they demonstrated that XPA was the only NER protein required for this activation highlighting the importance of XPA in this activation process. Bomgarden et al also observed that ATRIP forms foci with CPDs in response to UV and that this colocalisation is both cell cycle dependent, and XPA-sensitive (Bomgarden et al., 2006). Further to this, it was demonstrated that XPA was a direct target of ATR kinase for its relocalisation and phosphorylation following UV irradiation and this interaction promotes DNA repair (Shell et al., 2009; Wu et al., 2007). These data taken together signify the versatility of XPA protein in the DNA damage response and not just as a fundamental target for NER.

1.4.4.6 Nucleotide excision repair and human disease

Defects in the NER pathway are demonstrated by three rare autosomal-recessive inherited model diseases including xeroderma pigmentosum (XP), Cockayne syndrome (CS), and tricothiodystrophy (TTD). Each inherited defect can arise from mutations in more than one gene, and conversely, different mutations in one gene can give rise to more than one clinical phenotype (de Boer and Hoeijmakers, 2000).

As far back as the late sixties, xeroderma pigmentosum was established as the first human disorder defective in the repair of DNA damage, caused by UV-induced photoproducts (Cleaver, 1969). XP affects about 1 in 250,000 people in Europe and the United States and this incidince is higher in Japan with 1 in 40,000 people diagnosed with the disease (Friedberg, 2006; Takebe et al., 1977). XP is caused as a result of mutations in the eight

genes involved in NER, XPA through XPG and XPV (XP-Variant) (Mullenders, 2001). Mutations in these genes leads to the inability to cope properly with UV-induced DNA lesions. Patients with XP show severe photosensitivity, abnormal pigmentation and develop skin cancer at a very young age (van Hoffen et al., 2003). Patients with XP also exhibit abnormal gait, sensorineural deafness and the lack of deep tendon reflexes. Structural neurological abnormalities such as microcephaly, cerebellar atrophy and enlarged ventricles are also apparent in some XP complementation groups (Kerzendorfer and O'Driscoll, 2009).

Cockayne syndrome (CS) patients generally show dwarfism, mental retardation and photosensitivity (van Hoffen et al., 2003). CS patients shows defects in the CSA and CSB genes resulting in the defecting processing of UV-induced DNA damage (van Hoffen et al., 2003).

Tricothiodystrophy (TTD) patients display facial abnormalities, short stature, brittle hair and ichthyosis (Mullenders, 2001). TTD patients show defects in the XPD and XPB genes (Leibeling et al., 2006). More recently a defect in the TTD-A gene, a subunit of TFIIH has beeen identified in TTD patients (Leibeling et al., 2006).

1.4.5 DNA damage response and signal transduction pathway

Organisms respond to cytotoxic agents by activating a signal transduction pathway that consists of sensors, signal transducers, and effectors that leads to cell cycle checkpoint activation, apoptosis, transcription, DNA repair, and chromatin remodelling (Zhou and Elledge, 2000).

Figure 1.4.5.1 Schematic model of the signal transduction pathway in response to DNA damage or replication stress.
DNA damage triggers a signal transduction pathway that consists of sensors, signal transducers, and effectors and leads to cell cycle checkpoint activation, apoptosis, transcription, DNA repair, and chromatin remodelling (Figure adapted from (Zhou and Elledge, 2000)).

Signal transducers consist of members of the PIKK (phosphatidylinositol 3-kinase-related kinase) family. The highly conserved PIKK family includes ataxia telangiectasia mutated (ATM), ATM- and Rad3-related (ATR), and DNA-dependent protein kinase (DNA-PK) in humans (Yang et al., 2003). These proteins share the phosphatidylinositol 3-kinase-related domain and function as serine-threonine protein kinases (Yang et al., 2003).

ATM in a complex with its regulator MRN (MRE11-Rad50-NBS1) responds primarily to double-strand breaks (DSBs) induced by IR (Kastan and Bartek, 2004). Mediators of DNA damage signaling through ATM include 53BP1 (p53 binding protein 1), BRCA-1 (Breast cancer susceptibility gene 1), and MDC1 (Mediator of DNA damage checkpoint protein 1) (Zhou and Elledge, 2000). 53BP1 is a BRCT domain protein that plays a role in the DNA damage response and associates with Mre11, BRCA-1 and γH2AX (Yang et al., 2003). ATM forms a complex with BRCA-1 that partakes in the recognition and repair of aberrant DNA structures (Yang et al., 2003). ATM phosphorylates H2AX which is called γH2AX, and is required for the formation of MRN foci formation and also acts as docking site for MDC1 (Furuta et al., 2003). MDC1 in turn facilitates the recruitment 53BP1, BRCA-1 and MRN to damaged-induced (γH2AX) foci (Yang et al., 2003).

ATR with its regulator ATRIP (ATR-interacting protein) is primarily activated by bulky adduct formations on DNA induced by UV radiation, processing of DSBs (resulting in the formation of ssDNA), or stalled replication forks (Zhou and Elledge, 2000). The ATR-

ATRIP complex is recruited to RPA-coated ssDNA and stimulates the phosphorylation of Rad17 that is bound to DNA (Zou and Elledge, 2003). Independently, the Rad17-RFC complex (which is made up of Rad17 and RFC2-5) is loaded onto the sites of DNA damage. The Rad17-RFC complex facilitates the loading of the 9-1-1 (Rad9-Rad1-Hus1) clamp onto DNA, where it functions in the DNA damage response and is necessary for Chk1 activation and subsequent checkpoint signalling (Zou et al., 2002). TopBP1 (Topoisomerase II DNA binding protein 1) is a BRCT domain-rich protein that has been shown to physically interact with ATR and enhance its kinase activity in response to DNA damage (Kumagai et al., 2006). Once activated, ATM and ATR activate a plethora of downstream proteins to initiate a signalling cascade that results in DNA repair and cell growth arrest, which may occur at the G_1, S or G_2 stages of the cell cycle (Furgason and Bahassi, 2012).

This DNA damage response involves the activation of the structurally unrelated Chk1 (cell cycle checkpoint 1) and Chk2 (cell cycle checkpoint 2) kinases. Chk1 is a serine/threonine kinase and is responsible for initiating cell cycle arrest, thus allowing for DNA repair and cell survival (Zhou and Sausville, 2003). ATR is predominantly responsible for the phosphorylation of the Chk1 on Ser317 and Ser345 on its C-terminus (Leung-Pineda et al., 2006). Chk2 is a serine/threonine kinase phosphorylated by ATM at Thr68 near its N-terminus (Matsuoka et al., 2000). Chk2 is primarily activated by factors that induce double strand breaks (DSBs). Both of these kinases play a role in activating cell cycle checkpoints in order to give the cell sufficient time to repair the damage caused.

There are four main checkpoints activated in response to DNA damage: the G_1 and G_1-S checkpoint, the intra-S checkpoint and, the G_2-M checkpoint (Kastan and Bartek, 2004). The G_1 and G_1-S phase checkpoint arrest occurs when cells receive damage to their DNA during G_1 phase and are prevented from entering S phase (Sorensen et al., 2003). Damage induced by either DSBs caused by IR or radiomimetic agents activate the ATM-Chk2-Cdc25a pathway, while DNA damage caused by UV light, or UV-mimetic agents activate the ATR-Chk1-Cdc25a pathway. ATM/ATR directly phosphorylate p53 at Ser15, while Chk1 and Chk2 are capable of phosphorylating p53 at Thr18 and Ser20 (Hirao et al., 2000). These kinases also target the activity of MDM2, and together with p53 activity results in the inhibition of the cyclin B/Cdk2 complex, thereby preventing entry into S phase (Kastan

and Bartek, 2004). p53 also targets p21, which in turn binds to the cyclin D/Cdk4 complex, thus preventing cyclin D/Cdk4 from phosphorylating Rb. The phosphorylation of Rb prevents its association with the E2F transcription factor and allows cells to progress through the cell cycle.

The intra-S-phase checkpoint is activated when DNA damage caused by genotoxic insults occur during S-phase and results in the inhibition of the initiation of DNA replication at the origins of replication. One of the pathways that slows down DNA synthesis is activated through the Cdc25a degradation (either by ATM or ATR) cascade that prevents the activation of Cdk2 thus preventing the loading of Cdc45 onto chromatin (Kastan and Bartek, 2004). As discussed previously, Cdc45 is an important protein for the initiation of DNA replication. Another process by which the intra-S-phase checkpoint is activated is the recruitment of the MRN and BRCA1 complex by ATM to sites of DSBs thus triggering a signalling cascade to repair the damage induced (Kastan and Bartek, 2004).

The G2-M checkpoint prevents cells form entering mitosis in the presence of damaged DNA. The critical target of the G_2 checkpoint is Cdc25C, which is activated by the ATM/ Chk1-ATR/Chk2 pathway (Peng et al., 1997). Cdc25C promotes the activity of the cyclin B/Cdk1 complex, thus blocking entry into mitosis. Similarly to the S-phase checkpoint BRCA1 and p53 are involved in the G_2-M checkpoint response by upregulating the activation of CDK inhibitors such as p21.

Similar to ATM and ATR, DNA-PK is a nuclear serine/threonine kinase that consists of a catalytic subunit (DNA-PKcs) and the DNA binding subunits Ku70/Ku80 heterodimer (Yang et al., 2003). DNA-PK can be activated by DNA damage induced by IR or UV irradiation. DNA-PK plays a key role in DSB repair via NHEJ (Non-homologous end joining) (Yang et al., 2003). Following the induction of DBSs, the Ku heterodimer binds to the damaged DNA, which in turn then activates the catalytic subunit of DNA-PK, DNA-PKcs, to initiate NHEJ (Mahaney et al., 2009).

Figure 1.4.5.2 Chk1 and Chk2 are serine/threonine kinases that are activated by the ATM and ATR kinases in response to DNA damage.
The checkpoint kinases are transducers of the DNA damage signal and both phosphorylate a number of substrates involved in the DNA damage response. Image adapted from (Ashwell and Zabludoff, 2008)

It has been suggested recently that there is a common underlying mechanism by which these PIK kinases detect and activate various DNA damage signals, and although they might signal different, but overlapping, types of DNA damage they interact with one another to signal DNA repair or further downstream proteins, (Yang et al., 2003). The ATR-Chk1 and ATM-Chk2 pathways are not parallel branches of the DNA damage response, but show a high level of 'cross-talk' and connectivity. Single-stranded regions of DNA produced at stalled replication forks can degenerate into accessible DSBs and shifts the emphasis from ATR activation to that of ATM (Stiff et al., 2006). Reciprocally, DSBs, at certain phases of the cell cycle, undergo resection to generate ssDNA and therefore induces ATR activation (Jazayeri et al., 2006). Another example highlights ATR and ATM to collaborate in the IR-induced G_2/M checkpoint (Brown and Baltimore, 2003). ATM has been shown to activate Chk1 in response to IR (Gatei et al., 2003). It has also been shown that ATR can substitute for ATM in the phosphorylation of Chk2 in response to IR when ATM is deficient (Wang et al., 2006). Further to this, it has been shown that defective Chk1

(via ATR directly), and Chk2 activation (indirectly via ATR-dependent, ATM activation), are required for failure of the UV-induced G_2/M cell cycle checkpoint (Stiff et al., 2008). Loss of Chk1 function alone is not sufficient for G_2/M checkpoint failure under these conditions, presumably as Chk2 can function as a redundant signalling pathway (Kerzendorfer and O'Driscoll, 2009). Nevertheless, whilst ATM and ATR control overlapping DNA damage response pathways, genetic defects in each kinase present clinically distinct human conditions highlighting their significance in the DNA damage response.

Figure 1.4.5.3 The functional overlap between ATR and ATM pathways in mediating the G_2/M arrest following replication fork stalling (UV irradiation) that activates ATR.
(A) Selective inhibition of Chk1 does not impair ATR-dependent G_2/M arrest, as Chk2 is still active under these conditions via ATR-dependent ATM activation. **(B)** Similarly, inhibition of Chk2 function specifically does not impair ATR-dependent G_2/M arrest. **(C)** Defective ATR-dependent G_2/M arrest is only seen when Chk1 and Chk2 function are abrogated. (Kerzendorfer and O'Driscoll, 2009).

1.5 Transcription

Transcription factories in the eukaryotic nucleus are units in which active gene transcription takes place. These factories contain various RNA polymerases that perform transcription on different genes. RNA polymerase I (RNA pol I) transcribes the genes that encode ribosomal RNAs (rRNAs), RNA polymerase III (RNA pol III) transcribes the genes for small RNA (sRNA), transfer RNA (tRNA) and small regulatory RNA molecules. RNA polymerase II (RNA pol II) transcribes messenger RNA (mRNA) that serves as a template for the production of proteins (Clancy, 2008). In eukaryotes, transcription of mRNA is carried out in three steps: initiation, elongation and finally termination, which are described in detail further on. As mentioned, RNA pol I transcribes ribosomal rRNA which takes place in the nucleolus of the cell.

1.5.1 Transcription of messenger RNA (mRNA)

In the first step of mRNA transcription, RNA pol II binds to the promoter region of DNA. The promoter region is found upstream (5' end) of the start site of the DNA transcription unit, most of these contain a sequence known as the TATA box (Berg, 2002). Several complexes termed transcription factors are required for successful transcription. The first transcription factor is TFIID (Transcription Factor II D), the largest of the general factors, that contains a component called TBP (TATA-binding protein) that binds to the DNA using the TATA box to position the TFIID complex near the transcription initiation site (Berg, 2002). Other transcription factors, including TFIIA and TFIIB, then attach to and prepare the DNA for the successful binding of RNA polymerase II (Berg, 2002). Other transcription factors bind to form the pre-initiation complex, including the TFIIH transcription factor that contains helicases that unwind the DNA strands (Cooper, 2000).

RNA pol II then synthesizes an RNA template from the template strand of DNA. Most of the factors mentioned above are released once transcription begins. As the RNA template is being synthesized, RNA pol II clears away from the promoter sequence. mRNA transcription can involve multiple RNA polymerases on a single DNA template and multiple rounds of transcription (amplification of a particular mRNA), so many mRNA molecules can be rapidly produced from a single copy of a gene (Proudfoot et al., 2002).

When the end of transcription unit is reached, RNA pol II dissociates and the newly formed strand of RNA is released. This allows the RNA pol II enzyme complex to begin further rounds of transcription, highlighting that the activity of mRNA processing and transcription are coupled events (Proudfoot et al., 2002).

1.5.2 Processing of pre-mRNA

Shortly after RNA pol II initiates mRNA transcription, a 5' cap of modified guanine nucleotide is added to the 5' end of the eukaryotic mRNA (Proudfoot, 2000). Firstly, a RNA 5' triphosphatase (RTP) hydrolyzes the triphosphate of the first nucleotide to a diphosphate. Then, a guanylyltransferase (GT) catalyzes the merging of a GMP moiety from GTP to the initial nucleotide of the pre-mRNA transcript. To finalise the cap structure, a methyltransferase (MT) methylates the transferred GMP (Neugebauer and Roth, 1997). The addition of the 5' cap is essential for the recognition of the transcript by ribosome machinery and its protection from RNases. Cap addition is coupled to transcription, and occurs co-transcriptionally, such that each influences each other (Neugebauer and Roth, 1997). Once the process of transcription reaches completion, RNA pol II releases the 5' capped mRNA for further modifications.

Splicing of mRNAs is an important step in eukaryotic gene expression; in which non-coding sequence called introns are removed from the primary RNA pol II transcript (Proudfoot et al., 2002). Pre-mRNA splicing is performed by the spliceosome, a large complex whose assembly requires a series of binding and rearrangement events involving small nuclear ribonucleoproteins particles (snRNPs), U1, U2, U4/U6 and U5. In the first step of this assembly pathway, U1 snRNP binds to the 5' splice site at the GU sequence of the intron to initiate the assembly of the spliceosome (Proudfoot et al., 2002). Next, U2 snRNP binds to the A branch site that is ~100 bp upstream of the 3' splice site, determined by its AG sequence, of the intron with the addition of the SF1 branchpoint binding protein and the U2AF splicing factor (Proudfoot et al., 2002). Together, this assembly process generates the pre-spliceosome complex A and initiates the RNA to loop. Upon association with U4/U6 and U5, complex B is formed, and a conformational change takes place. U4 does not directly bind to the mRNA but plays a crucial role in assembling U5 and U6 onto the spliceosome (Proudfoot et al., 2002). Following this, the intron is cleaved at the 5' site

and forms a lariat with the A branch site that results in the formation of complex C and the removal of U4. The U2, U5 and U6 snRNPs remain bound to the lariat and the 3' site of the intron is then cleaved. Cleavage of the mRNA sequence is aided by many factors including cleavage factor I (CFI) and II (CFII) that directly bind to the mRNA sequence (Proudfoot et al., 2002). The exons are then ligated and the spliced RNA is released followed by the degradation of the removed intron.

In eukaryotes, most mRNAs are polyadenylated at the 3' end. Polyadenylation is the addition of a long sequence of adenine nucleotides to the 3' end of the mRNA directed by sequences present on the pre-mRNA (Proudfoot et al., 2002). The poly (A) tail and the proteins bound to it aid in protecting the mRNA from degradation by exonucleases. Polyadenylation is also important for the termination of transcription, export of the mRNA from the nucleus, and translation. Eukaryotic mRNA that has been processed and transported from the nucleus to the cytoplasm is then recognised and translated by ribosomes.

1.5.3 $p54^{nrb}$ and its role in RNA biogenesis

The 54 kDa protein $p54^{nrb}$ (nuclear RNA binding protein) has a high affinity for RNA via its N-terminus and partakes in numerous processes regarding RNA biogenesis (Yang et al., 1993). $p54^{nrb}$ can bind to various pre-mRNA and RNA sequences and has been found to act in the binding and nuclear retention of defective RNAs (Hallier et al., 1996; Zhang and Carmichael, 2001).

$p54^{nrb}$ binds to the carboxyl-terminal domain (CTD) of RNA pol II at both the initiation and elongation stages of transcription (Emili et al., 2002). The CTD domain of the largest subunit of RNA pol II has many important roles in transcription and processing of pre-mRNA (Hirose and Manley, 2000; Neugebauer and Roth, 1997). $p54^{nrb}$ directly interacts with hnRNP M (heterogeneous nuclear ribonucleoprotein M), a protein that associates with pre-mRNA at early stages of spliceosomal assembly (Marko et al., 2010). Various studies have shown that $p54^{nrb}$ is involved in splicing of mRNA. Initially $p54^{nrb}$ was detected in a screen designed to identify proteins that cross react with antibodies against Prp18, a yeast splicing associated factor (Dong et al., 1993; Horowitz and Abelson, 1993). $p54^{nrb}$ has also been shown to bind to the 5' splice site of the mRNA transcript, this interaction was found

to take place with a number of complexes including RNA pol II and snRNPs, highlighting that splicing occurs co-transcriptionally (Kameoka et al., 2004). Overexpression of Spi-1/PU.1, an Ets related transcription factor, blocks $p54^{nrb}$ from binding to RNA that correlates with an effect on *in vitro* splicing (Hallier et al., 1996).

$p54^{nrb}$ recruits the exonuclease XRN2 to sites of 3' end processing and termination to facilitate its activity in RNA processing (Kaneko et al., 2007). $p54^{nrb}$ can induce the binding of several transcription factors to their response elements. $p54^{nrb}$ has been shown to repress basal transcription of the human *CYP17* gene involved in steroidogenesis and is found in complex with Sin3A, HDAC 1 and SF-1 (steroidogenic factor) (Dammer et al., 2007; Sewer et al., 2002). In 2008, Hata et al demonstrated that $p54^{nrb}$ interacted with Sox-9, a transcription factor that plays an essential role in promoting chondrogenesis, thus stimulating its activity (Hata et al., 2008). Further to this, they demonstrated that $p54^{nrb}$ regulates both transcription and splicing of the collagen, type II, a 1 (Col2a1) mRNA during chondrocyte differentiation (Hata et al., 2008). $p54^{nrb}$ in a complex with PSF and matrin 3, a nuclear matrix protein, functions in nuclear retention of edited transcripts containing inosine residues (Zhang and Carmichael, 2001). $p54^{nrb}$ binds to an enhancer element in the long terminal repeats of murine intracisternal A particles and activates transcription indicating its role in transcriptional control (Basu et al., 1997).

Figure 1.5.5.1 p54^{nrb} protein has various roles in RNA biogenesis.
p54^{nrb} binds to the carboxyl-terminal domain (CTD) of RNA pol II at both the initiation and elongation stages of transcription (Emili et al., 2002) and associates with pre-mRNA at the early stages of spliceosomal assembly (Marko et al., 2010). p54^{nrb} binds to the 5' splice site of the mRNA transcript, this interaction was found to take place with a number of complexes including RNA pol II and snRNPs (Kameoka et al., 2004). p54^{nrb} influences the transcriptional activity of various other factors (Dammer et al., 2007; Sewer et al., 2002). Image adapted from (Karp, 2007).

1.5.4 Structure and function of the nucleolus

One of the most well characterised nuclear bodies of higher eukaryotes is the nucleolus, it is a large organelle can be visualised by light microscopy. Other subnuclear bodies include nuclear speckles, PML bodies, Polycomb bodies, Cajal bodies, histone locus bodies, and nuclear stress bodies, most of which reside in the interchromatin space and are enriched in splicing factors (Fox and Lamond, 2010; Spector and Lamond, 2011). The structured formation of these nuclear bodies is considered essential for the intricate regulation of gene expression and the subsequent higher-order biological processes typically found in higher eukaryotes (Nakagawa and Hirose, 2012).

As mentioned, the nucleolus is a sub-nuclear compartment of the nucleus and it is here that ribosome biogenesis is performed. In the nucleolus, ribosomal RNAs (rRNAs) are

synthesized, transcribed and assembled into 40S and 60S ribosomal subunits (Raska et al., 2006). The rRNA genes are clustered in tandem head-to-tail repeats. These rRNA clusters are formed around genetic loci on the chromosomes called nucleolar organising regions (NORs) that are distributed across five pairs of chromosomes in humans (chromosomes 13, 14, 15, 21, and 22). rRNA synthesis is carried out at the end of mitosis and initiates the assembly of the nucleolus by the clustering of rDNA repeats (~400) from more than one NOR-containing chromosome (Dellaire and Bazett-Jones, 2007). Nucleolar transcription of rDNA is initiated by RNA pol I. However, evidence has shown that around half of the r-gene repeats are transcriptionally silent in mammalian cells (Grummt, 2003). When the cells enter mitosis, nucleoli disassemble as RNA pol I subunits dissociate from rDNA, and rRNA synthesis is arrested (Dellaire and Bazett-Jones, 2007). The assembly of 28s, 18s, and 5.8s rRNAs along with 5s RNA with r-proteins is an essential step in ribosomal biogenesis (Gerbi, 2000). RNA pol II transcribes the genes that encode the ribosomal proteins. The organisation of rRNAs with ribosomal proteins results in the formation of RNP (ribonucleoprotein) precursors. The RNP precursors then mature into the 40s and 60s subunits of the ribosome and are exported from the nuclear pore into the cytoplasm (Raska et al., 2006).

Electron microscopy analysis has indicated that the nucleolus is made up of three major structures: fibrillar centres (FC), dense fibrillar components (DFC) and the granular component (GC) (Raska et al., 2006). The transcription of rRNA takes place in the FC and it consists of tandem repeats of these genes. The DFC surrounds the FC and harbours matured rRNAs (pre-RNA transcripts). Assembly of pre-ribosomal particles and late RNA processing take place in the GC (Raska et al., 2006). In a typical eukaryotic cell, the GC makes up ~75% of the nucleolar space, the DFC accounts for ~17% and FC only accounts for ~2% of the nucleolar space (Shaw and Jordan, 1995).

Proteomic analysis of the human nucleolus has identified more than 700 proteins that participate in molecular functions in the nucleolus other than ribosome biogenesis indicating that the nucleolus contributes to many diverse processes (Andersen et al., 2005; Dellaire et al., 2003). These processes include the maturation of non-nucleolar RNAs and RNPs, mRNA export and nonsense-mediated decay, regulation of cell senescence, control of viral infection, cell cycle progression, tumour suppression and DNA repair, as well as

regulation of telomerase function and the cell stress response (Pederson, 1998; Raska et al., 2006).

Cellular stress causes a dramatic reorganisation of the nucleolar structure, function and its proteins. The dramatic change in response to stress can be caused by abnormal ribosome biogenesis, heat shock, hypoxia, transcriptional inhibition and DNA damage (Pederson, 1998; Raska et al., 2006). In response to transcriptional arrest by RNA pol I inhibitor treatment (Actinomycin-D), nucleolar components segregate and form structures termed nucleolar caps that surround the nucleolar body (Shav-Tal et al., 2005). DNA damage caused by UV irradiation or induction of DSB's by topoisomerase II inhibitors causes nucleolar segregation and is characterised by the separation of nucleolar compartments (Govoni et al., 1994). The structural changes induced by UV irradiation are also accompanied by the redistribution of nucleolar proteins such as nucleolin, nucleophosmin and RNA pol I (Al-Baker et al., 2004; Daniely et al., 2002; Kurki et al., 2004).

1.5.5 $p54^{nrb}$ is a core protein of paraspeckles

One of the most recent subnuclear bodies that have been identified are paraspeckles and are located in the interchromatin region of mammalian cells (Andersen et al., 2002). The term paraspeckles was coined by A. Lamond's laboratory at the University of Dundee, UK, because of their close positional association with nuclear speckles. Paraspeckles are small, irregularly sized and unevenly distributed subnuclear bodies. The number of paraspeckles varies between 5 and 20 foci per nucleus (Clemson et al., 2009). In 2002, Fox et al showed that the nuclear proteins $p54^{nrb}$ (nuclear RNA binding protein, also known as NONO (Non-Pou domain containing octamer binding), NMT55 and NRB54), PSF (Polypyrimidine tract-binding protein (PTB)-associated splicing factor, also known as SFPQ), PSP1 (Paraspeckle Protein 1) and PSP2 (Paraspeckle Protein 2, also known as COAA, RBM14, SIP, and SYTIP1) accumulated at these structures (Fox et al., 2002). In association with these nuclear proteins, CFIm68 (cleavage factor Im 68 kDa, also known as CPSF6) and FUS (fused in sarcoma, RNA binding protein) have been identified as factors associated with paraspeckles (Dettwiler et al., 2004; Page et al., 2011) along with the transcription factors Sox9 (SRY-box containing gene 9) and Bcl11a (B-cell chronic lymphoid leukaemia 11a) (Fox et al., 2002).

Reports have shown that the number of paraspeckles varies with the cell cycle, the number of paraspeckles increase in number during interphase, disappear at telophase, when paraspeckle proteins translocate to the perinucleolar compartment, and reappear early in G_1 phase (Fox et al., 2005). Upon the inhibition of RNA pol II transcription, paraspeckle proteins redistribute and accumulate at perinucleolar caps (Fox et al., 2002; Shav-Tal et al., 2005) highlighting their role in transcription and/or RNA processing.

$p54^{nrb}$, PSF and PSP1 are the core protein components of paraspeckles and are members of the DBHS (*Drosophila* behaviour and human splicing) family. $p54^{nrb}$, PSF and PSP1 share ~50% sequence identity, however PSF has an additional N-terminal domain ($p54^{nrb}$ and PSF share a 71% sequence similarity (Peng et al., 2002)). The DBHS domain comprises of two RRM (RNA recognition motif) domains and a carboxy-terminal helix-turn-helix (HTH) domain (also termed the coil-coiled domain) (Fox et al., 2005). All three paraspeckle proteins are ubiquitously expressed and are conserved in vertebrates, see figure 1.5.2.1. Invertebrate species such as *Drosophila melanogaster*, *Caenorhabditis elegans*, and mosquitoes only have one gene representing the $p54^{nrb}$/PSF/PSP1 family. In *D. melanogaster*, nonA (no-on-transient A), is required for normal eye development and courtship song behaviour (Jones and Rubin, 1990). In *Chironomus tentans,* the homologue Hrp65 is expressed in three isoforms and has two classical RNA-binding domains (Kiesler et al., 2005). The DBHS domain appears to play a key role in the structural integrity of these proteins and together they are termed "core paraspeckles proteins" (Bond and Fox, 2009). $p54^{nrb}$ and PSF are essential for the formation and the maintenance of paraspeckles, and their depletion leads to disassembly of paraspeckles (Souquere et al., 2010). $p54^{nrb}$ forms a heterodimer with PSP1 via its helix-turn-helix domain and this is targeted to paraspeckles in a RNA-dependent manner (Fox et al., 2005). The specificity of DBHS dimerisation is highlighted by the fact that PSP1 forms a dimer with $p54^{nrb}$ but not with PSF (Fox et al., 2005). $p54^{nrb}$ interacts with PSF via its DBHS domain (Peng et al., 2002; Zhang et al., 1993). $p54^{nrb}$ and PSF are often co-purified in biochemical studies as a heterodimer and have been shown to bind to specific nucleic acids or protein factors (Bladen et al., 2005; Kameoka et al., 2004; Marko et al., 2010; Zhang et al., 1993).

Figure 1.5.2.1 Structural elements in p54^{nrb}.
p54^{nrb} is conserved throughout vertebrates. p54^{nrb}, PSF and PSP1 share ~50% sequence identity. For comparison the human p54^{nrb}, PSP1, PSF, *Drosophila* (nonA) and *Chironomus tentans* (hrp65) are shown. The C-terminus harbours the RRMs (RNA recognition motif). In addition, N- and C-termini contain regions rich in proline (P), glutamine (Q), histidine (H), glycine (G) and asparagine (N). p54^{nrb} has a region predicted to form a HTH structure followed by a basic/acidic (±) stretch of amino acids which together form the predicted DNA binding domain (DBD). The RRM domains and the DBD form the DBHS (*Drosophila* Behaviour Human Splicing) domain, the homologous element in these proteins and is conserves throughout the species. The C-terminus of p54^{nrb} is implicated in the protein-protein interaction with PSF and PSP1. Adapted from (Shav-Tal and Zipori, 2002).

Most of the paraspeckles proteins have been shown to be sensitive to transcriptional inhibition and RNase treatment, suggesting that ribonucleic acids play a role in their structural integrity (Fox et al., 2002). Two specific RNA components are enriched in paraspeckles, the first one, A-to-I hyper-edited CTN RNA, is a long isoform transcribed from mCAT2 (mouse cationic amino acid transporter 2). CTN RNA is regulated within paraspeckles, and is implicated in the control of gene expression by RNA nuclear retention (Fox et al., 2002). The A-to-I hyper-edited CTN-RNAs are retained in the nucleus and the majority of them are associated with paraspeckles (Prasanth et al., 2005). The paraspeckle

protein p54^{nrb} recognises A-to-I hyper-edited edited RNAs over non-modified RNAs, which coincide with A-to-I hyper-edited CTN-RNAs that are associated with paraspeckles (Zhang and Carmichael, 2001).

Another of the RNA components is NEAT1 (nuclear enriched abundant transcript 1), an abundant nuclear long non-protein-coding RNA (lcRNA) that is essential for the formation and the maintenance of paraspeckles (Sunwoo et al., 2009). The NEAT1 locus generates short (3.7 kb in human; 3.2 kb in mouse) and long (23 kb in human; 20 kb in mouse) non-coding RNA isoforms. These isoforms are termed NEAT1_1 and NEAT1_2 (previously referred to as MENε and MENβ) (Nakagawa and Hirose, 2012). These isoforms are transcribed from the same RNA pol II promoter but differ in the location of their 3' ends (Sasaki et al., 2009). NEAT1_2 but not NEAT1_1, plays an architectural role in the formation of paraspeckles (Sunwoo et al., 2009) although both transcripts localise to paraspeckles and associate with protein members of the DBHS family. The specific deletion of NEAT1_2 leads to the reductions or disappearance of paraspeckles (Sasaki et al., 2009; Sunwoo et al., 2009). The disruption of the paraspeckles upon knockdown of PSF or p54^{nrb} is accompanied by a dramatic down-regulation of NEAT1_2, whereas the level of NEAT1_1 is affected minimally (Sasaki et al., 2009).

The assembly of paraspeckles begins when NEAT1 reaches a high concentration, this normally occurs only at a transcription site (Nakagawa and Hirose, 2012). Paraspeckle components accumulate and bind to newly synthesised NEAT1 transcripts at the transcription site to form paraspeckles (Souquere et al., 2010). The formation and maintenance of paraspeckles are dependent on active transcription of NEAT1; this was observed when NEAT1 transcripts were destabilised by transcriptional inhibition whereby paraspeckle proteins redistributed to nuclear structures termed perinucleolar caps (Fox et al., 2002). NEAT1_1 has three binding sites for p54^{nrb}; these are located in the 5' and 3' regions of the transcript (Murthy and Rangarajan, 2010). However, no conserved sequences or structural motifs are found in the three binding sites of p54^{nrb} indicating that it recognises a higher order of NEAT1_1 (Nakagawa and Hirose, 2012). Paraspeckles possess a highly ordered structure with a regular arrangement of architectural noncoding RNAs and associated protein components (Nakagawa and Hirose, 2012). The paraspeckle components p54^{nrb}, PSF, and PSP1 are distributed uniformly throughout the IGAZ (interchromatin

granule associated zone) (Souquere et al., 2010). The IGAZ is a nuclear structure closely associated with interchromatin granules known as nuclear speckles that contains U1 snRNA (small nuclear RNA) (Cardinale et al., 2007).

As described, paraspeckles function in retaining A-to-I hyper edited mRNAs and this retention mechanism may play a role in cellular processes such as stress responses, viral infection, and circardian rhythm maintenance (Souquere et al., 2010). There are numerous proteins associated with paraspeckles that play various roles in RNA processing/degradation and/or protein modification/degradation that may be dependent on paraspeckle association (Nakagawa and Hirose, 2012). Paraspeckle formation may also counter regulate the function of paraspeckle-localising factors that normally regulate distinct nuclear functions outside the paraspeckle (Nakagawa and Hirose, 2012). As an example, $p54^{nrb}$ protein has been implicated in a number of various processes including splicing regulation, mRNA control, the DNA damage response, transcriptional regulation and DNA pairing (Bladen et al., 2005; Marko et al., 2010; Shav-Tal and Zipori, 2002; Zhang et al., 1993; Zhang and Carmichael, 2001).

1.6 Proteins that possess dual roles RNA biogenesis and DNA damage response

In the past few years, growing interest has been shown in proteins that possess dual roles in gene regulation and genome stability through RNA biology and DNA repair. RNA pol II plays a central role in transcription, however when it encounters a UV induced photoproduct, cyclobutane pyrimidine dimer (CPD), it stalls and results in transcriptional inhibition and the initiation of transcription-coupled repair, as described previously (Laine and Egly, 2006; Selby et al., 1997)

Beli et al showed that the protein phosphatase PPM1G, which promotes pre-mRNA splicing, is phosphorylated in response to DNA damage and is promptly and temporarily recruited to sites of laser induced DNA damage (Beli et al., 2012). Another factor, THRAP3, which functions in RNA processing and in regulating RNA stability was shown to be phosphorylated in response to DNA damage, with this primarily being mediated by ATR (Beli et al., 2012). They reported that THRAP3 is excluded from sites of laser microirradiated regions in a manner that parallels transcriptional inhibition. Adamson et al performed a genome-wide siRNA screen; and through this screen and identified proteins

that localise to sites of laser induced DNA damage. One of the candidates they identified as positive regulator of HR was RBMX; a heterogeneous nuclear ribonucleoprotein (hnRNP) that associates with the spliceosome binds RNA and influences alternative splicing. They found that RBMX is required for resistance to DNA damage and accumulates at sites of DNA damage in a PARP-1-dependent manner (Adamson et al., 2012).

Several members of the hnRNP family have recently been linked to the DDR and further to this human heterogeneous nuclear ribonucleoprotein U-like (hnRNPUL) 1 and 2 proteins are recruited to sites of DNA damage in a MRN-dependent and RNA-independent manner and promote effective DNA resection, a process required for ATR-dependent signalling from DSB sites and for DSB repair by HR (Haley et al., 2009; Polo et al., 2012). The catalytic subunit of DNA-PK (DNA-PKcs), and Ku proteins, central proteins in NHEJ as described, have been shown to arrest RNA pol II transcription (following DSBs) and have been implicated in transcriptional reinitiation and control of mRNA expression respectively (Woodard et al., 2001).

Further to this, Guo et al showed that the transcription factor E2F1 localises to sites of UV-induced DNA damage to enhance NER. They showed that the depletion of E2F1 did not effect the expression of repair factors such as XPA and XPC, however, the depletion of E2F1 did impair the recruitment of NER factors to sites of DNA damage thus reducing DNA repair efficiency (Guo et al., 2010).

1.7 p54^{nrb} and its role in DNA damage response

As described previously, p54^{nrb} protein is a multifunctional protein that has been implicated in a number of different processes such as RNA processing. In recent years, growing attention has been shown in p54^{nrb} and its implication in the DNA damage response pathway. In 2004, William Dynan and his colleagues, identified p54^{nrb} in a heterodimer with PSF as a stimulator for DNA end joining *in vitro*, that the heterodimer directly bound to the DNA substrates of the end joining reaction, and that the heterodimer cooperates with Ku proteins to establish a functional preligation complex (Bladen et al., 2005). Dynan and his colleagues established a functional assay in which biochemical fractions, derived from HeLa cell nuclear extracts, were tested for their ability to stimulate end joining in the presence of recombinant Ku heterodimer and L4.X4. In previous work they recognised two

stimulatory fractions, one fraction contained a >500-kDa complex of human Mre11, Rad50, and NBS1 polypeptides, all of which are implicated in DSB repair. The other fraction contained a >200kDa complex that does not crossreact with any of the antibodies raised against the proteins implicated in DSB repair and only this fraction is capable of binding to DNA-PK to perform a phosphorylation-regulated end joining reaction (Huang and Dynan, 2002; Pang et al., 1997). Further purification was carried out on this fraction and they identified two major polypeptides with mobility corresponding to ~55 and 100 kDa that co-eluted with peak stimulatory activity (Bladen et al., 2005). Following mass spectrometry analysis, these polypeptides were identified as PSF and $p54^{nrb}$. They went on to identify that absorption of a crude stimulatory fraction with monoclonal antibodies to PSF and $p54^{nrb}$ depleted end joining activity and that activity was restored following the addition of a purified PSF/$p54^{nrb}$ complex and that the complex participated in NHEJ in vitro (Bladen et al., 2005). Prior studies have also shown PSF protein, the $p54^{nrb}$ binding partner, to cooperate *in vitro* with the HR protein, Rad51, to promote homologous DNA pairing. PSF was shown to bind to RAD51 via its N-terminus, which also contains its DNA binding region. However, the RRM domain region of PSF does not bind to RAD51 or DNA, indicating that PSF has dual functions in binding to RAD51 for homologous recombination and RNA processing (Morozumi et al., 2009; Rajesh et al., 2011).

Dynan and his colleagues went on to elucidate $p54^{nrb}$ protein in the DNA damage response *in vivo* (Li et al., 2009). They implicated that the attenuation of $p54^{nrb}$ expression by siRNA caused a deficiency in DSB repair by evidence of a delay in resolution of γH2AX foci in human cells. The finding that $p54^{nrb}$ siRNA treatment delayed, but did not abolish, DSB repair, suggests that it is involved in the initial phase of DSB repair, which is mediated by the NHEJ pathway (Li et al., 2009). They also went on to develop a stably transfected cell line with a markedly reduced level of $p54^{nrb}$ using an EmGFP-encoding mRNA that showed an increase in chromosome abnormalities following radiation exposure and a decrease in clonogenic survival (Li et al., 2009). This work, along with their previous studies, strongly supports the involvement of $p54^{nrb}$ in the DNA damage response and DNA repair. Dynan and his colleagues also reported that PSF was implicated in DNA repair *in vivo* (Ha et al., 2011). They identified that sequences required to rescue the radiosensitive

phenotype correlated with those required for localisation of PSF-containing protein complexes to sites DNA damage (Ha et al., 2011).

$p54^{nrb}$ has been shown to form complexes with proteins involved in DSB repair and accumulates to sites of laser induced DNA damage. Salton et al showed in a report that, $p54^{nrb}$ in a complex with PSF along with Matrin-3 (MATR-3) was involved in the early stages of DSB response via the NHEJ pathway (Salton et al., 2010). MATR-3 is a highly conserved, inner nuclear matrix protein of 125 kDa that, similar to $p54^{nrb}$ protein, partakes in a number of processes such as DNA replication, transcription, repair, RNA processing and transport (Cohen et al., 2008). MATR-3 was shown to be a downstream target of ATM and by immunoprecipitation, they found that $p54^{nrb}$ interacted with MATR-3 protein following DNA damage. They induced localised DNA damage by laser micro irradiation and found that $p54^{nrb}$ localised these sites. $p54^{nrb}$ was seen as early as 2 seconds following damage induction, with subsequent disappearance about 10 minutes later (Salton et al., 2010). The report also highlights that attenuation of PSF by siRNA showed a marked delay in the disappearance of 53BP1 foci, a DSB sensor, following damage (Salton et al., 2010). Ha et al reported that $p54^{nrb}$ localises to sites of laser induced DNA damage as early as 2 seconds and begins to decline after 2 minutes, emphasising the results obtained by Salton et al (Ha et al., 2011). Kuhnert et al showed that $p54^{nrb}$ interacts with TopBP1 (Kuhnert et al., 2012). Top-BP1 is a BRCT-rich domain protein that has been shown to interact with PARP-1 and NBS-1, proteins that are involved in sensing DNA damage as described (Morishima et al., 2007; Wollmann et al., 2007). By performing a coimmunoprecipitation assay, a yeast two-hybrid assay, and a GST pull-down assay, it was indicated that $p54^{nrb}$ interacts with TopBP1 *in vivo* and *in vitro* (Kuhnert et al., 2012). It was discovered that the RRM domains of $p54^{nrb}$ promote the heterodimerisation with PSF and TopBP1 (Kuhnert et al., 2012). Kuhnert et al also showed that $p54^{nrb}$ localises to sites of UV-A laser induced DNA damage at similar retention times to the reports previously discussed (Kuhnert et al., 2012).

Following a bioinformatics screen, Kriestch et al identified $p54^{nrb}$ as a PAR binding protein involved in the NHEJ repair pathway (Krietsch et al., 2012). PAR is the catalytically activated form of PARP-1 that is involved in the recruitment of DNA repair proteins to sites of damage. PARP-1 is an abundant nuclear chromatin–associated protein, well

characterised for its high DNA damage sensing ability, as described previously (Krishnakumar and Kraus, 2010). p54^{nrb} associates with PAR through its RRM1 (RNA recognition motif 1) for its activation in the response to double-strand breaks via the NHEJ pathway (Krietsch et al., 2012). It was also elucidated that p54^{nrb} localises to sites of laser induced DNA damage and that this localisation was dependent on PARP-1 activity (Krietsch et al., 2012). Collectively these results suggest an important role for p54^{nrb} in NHEJ and HR repair pathways, individually and in a heterodimer with PSF.

1.8 Hypothesis and objectives

p54^{nrb} protein has been shown to play a crucial role in RNA biogenesis, particularly, pre-mRNA splicing along with many other transcriptional activities, and recently some reports have identified p54^{nrb} as a target for DSB repair. Previous work performed by Dr. Heinrich Anhold, using SV40 minichromosomes as a model system, highlighted p54^{nrb} as a UV-DNA damage response protein. Our hypothesis was that p54^{nrb} is an important negative regulator in the UV DNA damage response pathway.

The objective of this study was to gain a better insight into the mechanism(s) by which p54^{nrb} is involved in the DNA damage response following UV irradiation, primarily using human fibroblast cells as a model system. To do this, extensive *in vivo* studies were performed to investigate the sub-cellular localisation of p54^{nrb} protein following UV irradiation. In addition to this, deletion mutants of p54^{nrb} were investigated to further characterise the crucial domain of the protein responsible for its localisation to the nucleolus following UV irradiation. We also gained further insight into the mechanism of how p54^{nrb} and the transcriptional machinery operate following UV irradiation using drug inhibitors that specifically target this pathway. Until now, little or no work has shown the regulation of p54^{nrb} following UV irradiation; here we sought to highlight the importance of the regulation of p54^{nrb} protein in this pathway. By using various drug inhibitors, including specific PIK kinase inhibitors that target the DNA damage response pathway we highlight that p54^{nrb} is a target of these kinases following UV irradiation. We also studied the impact the loss of p54^{nrb} by siRNA had on human cells following UV irradiation and the effect this had on cell survival of these cells.

Chapter 2 - Materials and Methods

2.1 Cell culture

2.1.1 Cell lines used

Epithelial human bone osteosarcoma cell line (U2OS) and HeLa S3 cells were received from ATCC (www.atcc.com). XP12RO is a human fibroblast cell line derived from a xeroderma pigmentosum type A patient homozygous for a stop codon in the XPA gene, and is transformed by SV40 TAg. XP12RO clone 5 cell line is derived from XP12RO but with the XPA gene knocked-in to produce XPA protein (Koberle et al., 2006). Both cell lines were kind gifts from Drs. Wood and Koberle, University of Pittsburgh. Human lymphoblastoid cells (Control) GM07521 (apparently normal), GM01525 (A-T) and GM18367 (Seckel syndrome (SS)) were kind gifts from Prof. Ciaran Morrison.

2.1.2 Cell culture

Cells were grown at 37°C, 5% CO_2 in Dulbecco's Modified Eagles Serum (Sigma Aldrich), supplemented with 2mM L-glutamine, 1U/ml Penicillin, 1µg/ml Streptomycin and 10% sterile filtered foetal bovine serum (FBS) (Lonza). Human lymphoblastoid cells were grown in RPMI serum (Sigma Aldrich) supplemented as above. Cells were grown to a confluency of 60-90% and split in a ratio of between 1:3 and 1:5 every 48-72 h using trypsin (Sigma) for all cell types.

2.1.3 Cell storage

For long term storage in liquid nitrogen or in the -80°C freezer, cells were grown to near confluency, removed from the dish as outlined above with trypsin (Sigma) and pelleted at 160 x g for 5 min (Hettich Rotanta 460 centrifuge). The cells were resuspended in sterile FBS supplemented with 20% dimethysulphoxide (DMSO) (Sigma) and transferred to storage vials. Vials and cells were frozen slowly to -80°C using a cryo 1°C freezing container (Nalgene) containing isopropanol and then either stored in an -80°C freezer or transferred to liquid nitrogen. To recover, a vial with cells was thawed quickly in a waterbath at 37°C, and cells mixed with 10 ml normal growth media containing 10% FBS. Upon becoming adherent, the media is changed to remove any adverse effects of DMSO.

2.2 Cell treatment

2.2.1 Cell transfection method using FuGENE 6™

For fibroblast cell lines the transfection reagent FuGENE 6™ (Roche) was used. Transfection procedure was carried out according to manufacturers guidelines. Briefly, for a 35 mm dish, 3 µl of FuGENE 6™ was added to 197 µl of DMEM (without Pen/Strep or FBS) and the mixture was allowed incubate at room temperature for 5 min. 2 µg of DNA was then added and the mixture was allowed to incubate at room temperature for a further 20 min. The transfection mixture was then added to the dish of cells in a dropwise manner while swirling the dish for equal distribution. For a 150 mm petridish for minichromosome purifications it was increased to 480 µl of DMEM (without Pen/Strep or FBS), 10.5 µl FuGENE 6™ and 7 µg of DNA.

2.2.2 Small interference RNA (siRNA) transfection procedure

Small interference RNAs (siRNAs) targeting human $p54^{nrb}$ and control RNA were purchased from Dharmacon RNAi Technologies (Lafayette, CO, USA), a subsidiary of Thermo Scientific. The products used are shown in table 2.2.2. Resuspension of siRNA reagents and transfection protocol was carried out according to manufacturers guidelines. Briefly, siRNA were resuspended in siRNA buffer (5x siRNA buffer - 20 mM KCl, 6 mM HEPES-KOH, pH 7.5, and 0.2 mM $MgCl_2$). Cells required for siRNA transfection were grown in antibiotic-free complete (with FBS) DMEM media 24 h before transfection. In separate tubes, 3 µl of Dharmafect was added to 197 µl of DMEM (without Pen/Strep or FBS) (Tube A) and 5 to 100 nM siRNA was added to a final volume of 200 µl of DMEM (without Pen/Strep or FBS) (Tube B) and the mixtures was allowed incubate at room temperature for 5 min. Tube A and tube B were then added together and were allowed incubate at room temperature for a further 20 min. The transfection mixture was then added to the dish of cells in a dropwise manner while swirling the dish for equal distribution and kept in DMEM (without Pen/Strep or FBS) for 24 h. Cell culture media was changed to antibiotic-free complete (with FBS) DMEM media 24 h after siRNA transfection mixture was added. Cells were then harvested 24-72 h after siRNA transfection.

Table 2.2.2. Products used for siRNA transfection procedure

Product	Description	Catalogue Number
DharmaFECT 1, 2, 3, 4	siRNA transfection reagents	T-2005-01
ON-TARGET*plus* Duplex (Human NONO, NM_007363)	Sense sequence - AAACAAACGUCGCCGAUACUU Antisense sequence - UAUCGGCGACGUUUGUUUUU	J-007756-09-0005
ON-TARGET*plus* GAPD Control siRNA (Human)	Positive silencing control for GAPD (GAPDH) mRNA in human cells. MW ~ 13,300 g/mol	D-001830-01-05
ON-TARGET*plus* Non-targeting Pool (Human)	Negative control siRNA with at least 4 mismatches to any human, mouse, or rat gene. Microarray tested. MW ~ 13.400 g/mol	D-001810-10-05
ON-TARGET*plus* Set of 4 (Human NONO, NM_007363)	Target sequences: AAACAAACGUCGCCGAUAC GGAUGGGUCAGAUGGCUAU GUCAAUUCUGUGUGGUAUA CAAAGUGGAUCCAGUUAGA	LQ-007756-01-0005
si*GENOME*™*SMART* pool (Human Chk1, NM_007363)	Target sequence: CAAGAUGUGUGGUACUUUA GAGAAGGCAAUAUCCAAUA CCACAUGUCCUGAUCAUAU GAAGUUGGGCUAUCAAUGG	M-003255-04-0005

2.2.3 UV irradiation

For UV irradiation analysis cells were irradiated in the laminar flow hood at 254 nm using a UVC lamp (Bender, Germany). The distance from the lamp was adjusted to give a constant rate of 0.5 J/m^2/s measured using a UVX dosimeter (UVP Inc. USA). Doses of between 1.25 J/m^2 and 100 J/m^2 were applied by varying the time of irradiation. For general UV irradiation experiments, cells grown on tissue culture dishes were rinsed with PBS to remove media before irradiation. After irradiation, media was added back to the dish and cells were incubated at 37ºC for the indicated times before fixation or harvesting for analysis.

For local irradiation experiments, cells were grown on glass coverslips and were incubated at 37ºC for 24 h before treatment. The coverslips were rinsed in PBS then individually covered with a piece of isopore polycarbonate 5.0 μm membrane filter (Millipore), and

irradiated with a dose of 100 J/m^2 as described above. The filters were removed and the coverslips were returned to the original media and incubated at 37ºC for the indicated times before fixation. Non-irradiated samples were processed identically, except the lamp was switched off. Cells were then put back in media and were incubated at 37ºC before the cells were fixed for analysis.

For laser-induced irradiation experiments, cells were grown on glass bottomed 35mm dishes (MatTek) and were incubated at 37ºC for 24 h. The cells were then irradiated with a 400 nm laser at 37°C on an integrated microscope system (DeltaVision). Then media was added back to the cells, which were incubated at 37ºC before fixation at 2 h post-irradiation.

2.2.4 Drug treatment

Table 2.2.4. Drug inhibitors

Drug	Source	Stock conc.	Final conc.
α –amanitin (6 h)*	ALX-350-270, Enzo Life Sciences	1 mg/ml	30 μg/ml
Actinomycin-D (2 h)*	A1410, Sigma-Aldrich	1 mg/ml	0.1 -1 μg/ml
ATM inhibitor	KU-55933, KuDOS Pharmaceuticals	1 mM	10 μM
ATR inhibitor	ETP-46464, Dr. Luis Toledo (Toledo et al., 2011)	1 mM	10 μM
Caffeine	C0750, Sigma-Aldrich	200 mM	5 - 10 mM
Chk1 inhibitor (UCN-01)	U6508, Sigma-Aldrich	1 mM	10 μM
Chk2 inhibitor	C3742, Sigma-Aldrich	1 mM	5 - 10 μM
DNA-PK inhibitor	NU 7441, KuDOS Pharmaceuticals	1 mM	10 μM
Roscovitine (30 min)*	R7772, Sigma-Aldrich		25-100 μM
Wortmannin	W1628, Sigma-Aldrich	1 mM	10 - 20 μM

All inhibitors listed above were made up as stock solutions in DMSO and used at a final concentration as shown above in complete DMEM media (with antibiotics and 10% FBS). Cells were pre-treated with the inhibitors 1 h prior to UV irradiation unless otherwise indicated (*). Cells that were subjected to UV irradiation as described previously, were placed back in the same drug-containing media and fixed or harvested at the indicated times for biochemical and cell biological analyses. Mock treated cells were processed identically to drug treated cells, except the cells were placed non-drug containing media throughout the experiment.

2.2.5 DNase I and RNase A treatment

Cells were grown in tissue culture on glass coverslips and were incubated overnight prior to treatment. Cells were rinsed in PBS to remove media before being UV irradiated as described previously (2.2.3), put back in complete media, and were incubated at 37ºC for 2 h. The cells were washed three times with PBS and were incubated in 0.05% Triton X-100 in PBS for 2 min with gentle rocking to permeabilise the cells. After washing three times with PBS, cells were treated with either DNase I enzyme (50 Units or 100 Units/ml) or RNase A enzyme (1mg/ml) for 10 min with gentle rocking. The cells were again washed three times with PBS to remove the enzymes and fixed in 4% paraformaldehyde for 10 min. The cells were again washed three times with PBS and then incubated at 4ºC until immunofluorescence staining was performed, as described in section 2.9.

2.3 Cell viability assay

Cells were seeded into 35 mm dishes (1.5 x 10^5 cells/dish) and were subjected to UV irradiation the following day, as described previously in 2.2.3. After 48 h post UV irradiation, cells were trypsinised. Cells were then resuspended in 1ml of PBS. A 50µl aliquot of cell suspension was added to 50µl of Trypan blue exclusion dye (0.4% Trypan Blue Solution (Sigma Aldrich). The bright, clear cells (excluding Trypan Blue) were counted using a hemocytometer. Each dose of UV irradiation was carried out in triplicate each time the experiment was carried out.

2.4 Antibodies

Table 2.4.1. Primary antibodies

Antibody	Raised against	Immunoblotting	Immunofluorescence microscopy	Source
β-actin	Mouse	1:10000	–	A5441, Sigma
Chk1	Mouse	1:1500	–	(DCS-300), Neomarkers
Chk1 pS317	Rabbit	1:1000	–	#2344, Cell Signalling Tech.
Chk2	Mouse	1:1500	–	(DCS-293), Neomarkers
Chk2 pThr68	Rabbit	1:1000	–	#2661, Cell Signalling Tech.
CPD*	Mouse	1:1000	1: 1000	NMDND001, Cosmo Bio Co. Ltd.
Fibrillarin	Mouse	–	1: 1000	Prof. B. McStay
GAPDH	Mouse	1: 5000	–	ab9484, AbCam
GFP**	Mouse	1:1000	–	11814460001, Roche
H.H3	Rabbit	1: 10000	–	ab1719, AbCam
γH2AX	Mouse	1: 3000	1: 3000	AbCam
Lamin β-1	Rabbit	–	1: 1000	ab16048, AbCam
Nucleophosmin	Rabbit	–	1: 500	ab15440, AbCam
PCNA	Mouse	1: 2000	–	(clone Pc 10), Neomarkers
$p54^{nrb}$	Mouse	1: 5000	1:1000	Affinity Bioreagents
$p54^{nrb}$	Rabbit	1: 5000	1:1000	ab45359, AbCam
RPA 32	Rat	1: 5	1: 5	(clone 4E4-11) Dr. E. Kremmer
RPA 43	Sheep	1: 1000	–	Prof. B. McStay
RPA 70	Rat	1: 5	–	(clone RAC-4D9) Dr. E. Kremmer
RPA pS4/S8	Rabbit	1: 4000	1: 4000	800-338-9579, Bethyl Laboratories
T-antigen	Mouse	1: 10000	–	PAB419, Dr. Alain Verreault
TopBP1	Rabbit	1: 2000	–	Prof. J. Syväoja
TT dimer	Mouse	1:1000	1: 1000	ab10347, AbCam
UBF 1/2	Sheep	–	1: 200	Prof. B. McStay
XPA	Rabbit	1: 5000	–	(CJ1), Dr. Christopher Jones

*Applied after denaturation in 1M HCl for 10 min prior to blocking step when used for local irradiation experiments in immunofluorescence microscopy
** Diluted in 0.01% PBS-Tween

Table 2.4.2. Secondary antibodies

Secondary antibodies used for immunoblotting (Horseradish peroxidase (HRP)-conjugated)		
Immuno-type	**Working dilution**	**Source**
Mouse	1: 10000	Jackson Immunoresearch Lab, Inc.
Rabbit	1: 5000	Jackson Immunoresearch Lab, Inc.
Rat	1: 10000	Jackson Immunoresearch Lab, Inc.
Sheep	1: 10000	9452, Sigma-Aldrich
Secondary antibodies used for immunofluorescence microscopy		
Immuno-type	**Working dilution**	**Source**
Mouse-Cy™2	1: 500	Jackson Immunoresearch Lab, Inc.
Mouse-Cy™3	1: 500	Jackson Immunoresearch Lab, Inc.
Rabbit-Cy™2	1: 500	Jackson Immunoresearch Lab, Inc.
Rabbit-Cy™3	1: 500	Jackson Immunoresearch Lab, Inc.
Rat-Cy™2	1: 500	Jackson Immunoresearch Lab, Inc.
Sheep-Cy™2	1: 200	Jackson Immunoresearch Lab, Inc.

2.5 DNA methods

2.5.1 Preparation of competent *E. coli* cells

E. coli strain Top 10 was used for all routine cloning procedures. Competent cells were prepared from 125 ml LB broth cultures with a typical A600 spectrophotometer reading of 0.6. The culture was chilled on ice for 10 min, centrifuged at 5000 x g for 15 min, and washed with ice-cold TB buffer (30 mM potassium acetate, 100 mM $RbCl_2$, 10 mM $CaCl_2$, 50 mM $MnCl_2$, 15% glycerol, pH 6.5). After a second centrifugation, cells were aliquoted, snap-frozen, and stored at -80ºC.

2.5.2 *E. coli* transformations

An aliquot of competent cells was thawed on ice. 1-5 µl ligation reaction or miniprep DNA was added to chilled Eppendorf tubes of 50 µl competent cells. After gently mixing, the transformation mixture was incubated on ice for 30 min, followed by a heat shock at 42ºC for 90 sec, and incubation on ice for 3 min. Subsequently, 950 µl of pre-heated LB (without antibiotic) was added, cells were incubated with shaking for 1 h at 37ºC, and samples were

plated onto LB plates supplemented with an appropriate antibiotic and incubated overnight at 37ºC.

2.5.3 Agarose gel electrophoresis

Agarose (Sigma Aldrich) gels were made at concentrations of 0.8-1.5% in 1 x TAE buffer **(**40 mM Tris-acetate, 1 mM EDTA) depending on the size of DNA fragments to be separated. DNA containing samples were prepared and 6x DNA loading dye (20% Sucrose, 0.1 M EDTA pH 8.0, 1% SDS, 0.25% Bromophenol blue, 0.25% Xylene cyanol) was added. Markers used were 100 bp and 1 kb ladders (New England Biolabs, NEB). Gels were run in 1x TAE buffer in mini (50 ml gel) or wide (100 ml gel) gel boxes (Biorad Systems), which were run at 80 - 100 V until the required separation was achieved. DNA was stained by soaking in 0.5 µg/ml Ethidium bromide (EtBr) for 30 min following this the gels were visualised with a UV transilluminator (Alpha Innotech ^{TM} Chemilmager 5500).

2.5.4 Restriction endonuclease digestions, plasmid purifications and gel extractions

Restriction digestions, gel extractions, and plasmid purifications were all carried out according to manufactures guidelines. New England Biolabs (NEB) supplied restriction enzymes. Plasmid purifications (GenElute^{TM} Plasmid Midi-prep kit and GenElute^{TM} Plasmid Mini-prep kit) and gel extraction kits (GenElute^{TM} Gel extraction kit, SigmaSpin^{TM} Post-reaction and Clean-up columns) were supplied by Sigma-Aldrich.

2.5.5 Ligation procedures

A molar ratio of vector and fragment DNA of 1:3 was calculated as follows:

$$\frac{\text{ng of vector x kb size of insert}}{\text{kb size of vector}} \times \frac{3}{1} \text{ (desired molar ratio)} = \text{ng of insert}$$

Ligations were carried out using T4 DNA ligase kit from NEB according to the manufacturer's recommendations for either 2 h at 25 °C or overnight at 4 °C. Ligations into pGEM-T Easy vector were carried out using pGEM-T Easy kit (Promega) according to the manufacturer's recommendations either for 2 h at 25 °C or overnight at 16 °C.

2.5.6 LR Clonase II reactions

The Gateway® LR Clonase® II enzyme mix kit was used according to the manufacturer's recommendations to recombine DNA fragments that were cloned into the pENTR3C entry vector into further destination vectors.

2.5.7 Polymerase chain reaction (PCR)

PCR was carried out using KOD polymerase (Novagen) or Taq polymerase (Sigma Aldrich) in the supplied buffer, supplemented with $MgCl_2$, DMSO, and dNTPs. 1 ng of template DNA and 10 µM of the required forward and reverse primer were used in the PCR reaction.

Table 2.5.7. Cycling profile for PCR programme

Cycling profile for 1 PCR cycle	
Temperature	Time
95°C	2 min
95°C	30 sec
63°C	30 sec
72°C	3 min
72°C	5 min
30 cycles were preceded by keeping the DNA heated to 72°C for 8 min, before allowing to cool down and stored at 4°C.	

2.5.8 Oligonucleotides

Oligonucleotides were designed using DNA Strider v1.4 software and oligonucleotides were ordered from Eurofins MWG Operon. Oligonucleotides were resuspended to a concentration of 100 pmol/µl in milli-Q H_2O and stored at -20°C. The sequences are listed below (Table 2.5.8).

Table 2.5.8. Oligonucleotides

Name	Amino acid	Sequence (5' – 3')
Fw $p54^{nrb}$ wt	wt, 1-471aa	CGCGGATCCATGCAGAGTAATAAAACTTTTAACTTGGAG
Rv $p54^{nrb}$ wt	wt, 1-471aa	CCGGAATTCTTAGTATCGGCGACGTTTGTTTG
Rv Δc-terminal domain	ΔCT, Δ1-229aa	CCGGAATTCTTATCCCTTGAATCCTTCCTGCTGTCGCCG
Fw ΔRNA recognition motif 1 & 2 domain	ΔRRM 1&2, Δ229-471aa	CGCGGATCCTTAGATGATGAAGAGGGACTTCCAGAGAAGC
Rv Δhelix-turn-helix domain	ΔHTH, Δ1-372aa	CCGGAATTCTTACTGGTCCATGGGCTCCACAGTCACAGGACG
Fwd NLS	-	TCGACTATGCCAAAAAAGAAGAGAAAGGTAG
Rv NLS	-	GATCCTACCTTTCTCTTCTTTTTTGGCATAG

2.5.9 Cloning and expression vectors

A full-length cDNA of $p54^{nrb}$ was obtained from Open Biosystems (Thermo Scientific). The cDNA was plated out on a LB agar plate supplemented with Chloramphenicol (25 mg/ml) and left O/N at 37°C. A single colony of bacteria was chosen and inoculated into 5 ml of LB broth supplemented with Chloramphenicol (25 mg/ml) and left O/N at 37°C. Bacterial cells were collected by centrifugation of 2 ml of culture at 4,000 x g for 10 min. A plasmid mini-prep was carried out with a GenElute^{TM} Plasmid Mini-prep kit (Sigma Aldrich).

GFP-tagged mutants of $p54^{nrb}$ were generated by PCR (see 2.5.7) and ligated into a pGEM-T Easy Vector, using the pGEM-T Easy Vector Systems kit (Promega). Following the ligation procedure, a transformation was carried out (see 2.5.2 and 2.5.5). The PCR products were then recombined into a peGFP-C1 or pENTR3C (Invitrogen) vector in frame between the *Bam*HI and *Eco*RI restriction sites.

The NLS sequence was cloned into the Gateway entry vector pENTR3C (Invitrogen) in frame between the *Bam*HI and *Sal*I restriction sites and recombined into the Gateway destination vector pIC113gw (Prof. Kevin Sullivan) using the LR-Clonase II enzyme mix (Invitrogen) according to the manufacturers recommendations.

Positive clones were confirmed by restriction digest diagnostic and sequencing (LGC genomics). GFP-tagged $p54^{nrb}$ mutant constructs were transiently transfected into cells using FuGENE 6^{TM} (Roche) as described in section 2.2.1 and immunofluorescence microscopy was carried out as described in section 2.9.

2.6 Cellular extracts

2.6.1 Minichromosome preparation

Cells were grown to ~ 4 x 10^6 confluency per 150 mm dish (Sarstedt) prior to transfection. Three 150 mm dishes were used for each sample preparation. After transfection, cells were incubated for 72-96 h at 37°C and 5% CO_2 before harvesting for minichromosome extraction. Minichromosome purification was carried out as described by Krude and Knippers (Krude and Knippers, 1991). Dishes were rinsed 3x with low salt (LS) buffer (20 mM HEPES-KOH, pH7.8, 5mM potassium acetate, 0.5mM magnesium chloride, 0.5mM dithiothreitol (DTT) in dH_2O) containing protease inhibitors (leupeptin, pepstatin A, PMSF, benzamidine, antipain, chymostatin) and phosphatase inhibitors (sodium fluoride, β-glycero-phosphate, sodium vanadate, EGTA, sodium pyrophosphate). Cells were then carefully scraped and pipetted into a Dounce homogeniser for physical disruption with a loose fitting pestle (15-20 strokes). Nuclei were then collected in a Beckman 22R benchtop microfuge centrifuge for 5 min at 1,000 x g at 4°C. Supernatant was discarded and nuclei were resuspended in 5 ml LS buffer before incubating on ice for 2 h (cellular integrity was checked by loading a small amount of extract onto a microscope slide and examining by microscopy). Subsequently, cellular and nuclear debris were collected by centrifugation at 20,000 x g for 5-10 min in a Beckman SW55Ti rotor. Pellet was discarded and supernatant was retained and transferred into a new tube (pre-cooled to 4°C). Minichromosomes were concentrated by centrifugation in a Beckman SW55Ti rotor through a 10 % sucrose cushion at 300,000 x g for 1 h. Supernatant was decanted and discarded. The pellet of minichromosomes was rinsed twice with 800 µl of LS buffer and then resuspended in the same buffer over a period of 1 h on ice with regular pipetting. Minichromosomes samples were stored at -80°C.

2.6.2 Nuclear extraction assay

The nuclear extraction assay was adapted from Burtelow et al (Burtelow et al., 2000). Briefly, ~4 x 10^6 cells were grown per 150 mm dish (Sarstedt). The media was poured off from the dishes and the cells were then rinsed three times with PBS (pre-cooled, kept at 4^{o}C). The cells were left in 500 µl of low salt (LS) buffer (see 2.6.1) for 5 min and then the dishes were scraped with a cell scraper. The cells were centrifuged at 1,000 x g in a Beckman 22R benchtop microfuge for 5 min at 4^{o}C. The supernatant was removed, snap frozen, and labelled 'Soluble protein fraction'. The pellet was resuspended in 250 µl of LS buffer and centrifuged at 1,000 x g for 5 min at 4^{o}C. The supernatant was removed, snap frozen, and labelled 'Low salt wash fraction'. The pellet was resuspended in 250 µl of medium salt (MS) buffer (20 mM HEPES-KOH**,** pH 7.4, 150 mM NaCl, 2.5 mM $MgCl_2$, the medium salt buffer was supplemented with either low (0.025%) or high (1%) triton x-100) and left at 4°C for 30 min on an oscillating rotor then centrifuged at 1,000 x g for 5 min at 4^{o}C. The supernatant was removed, snap frozen and labelled 'Medium salt fraction'. The pellet was then resuspended in 250 µl of medium salt buffer supplemented with DNase I (10,000 U/ml) for 30 min at room temperature then centrifuged at 9,500 xg for 5 min at 4^{o}C. The supernatant was removed, snap frozen and labelled 'DNase supernatant'. The pellet was resuspended in 250 µl of 1% SDS and sonicated at 40% amplitude for 10 second intervals twice and then centrifuged at 9,500 x g for 10 min. The supernatant was removed, snap frozen and labelled 'Sonicated supernatant'. The pellet was then resuspended in 150 µl of 1% SDS, snap frozen, and labelled 'Sonicated pellet'.

2.6.3 Nucleolar purification procedure

The nucleolar purification was adapted from Anderson et al (Andersen et al., 2002). Briefly, ~4 x 10^6 cells were grown per 150 mm dish (Sarstedt). Ten 150 mm dishes were used for each sample preparation. The media was poured off from the dishes and the cells were then rinsed three times with PBS (pre-cooled at 4°C). Following this, the cells were scraped into 40 ml of PBS using a cell scraper, applying gentle pressure to ensure the cells did not burst. After the cells were scraped from the dishes, they were rinsed with 40 ml of PBS to ensure all of the cells were collected. The cells were then centrifuged at 220 x g at 4°C for 5 min. The supernatant was removed; the pellet was washed 3 times with PBS. The

cell pellet was then resuspended in 10 ml of Buffer A (10 mM HEPES-KOH, pH 7.9, 10 mM KCl, 1.5 mM $MgCl_2$ and 0.5 mM DTT supplemented with protease inhibitors) and a dounce homogenizer (loose pestle) was used to burst the cells. After each 10 strokes, the cells were checked under a light microscope since it is important to verify at this step that the nuclei are not lysed. Once the nuclei were released the cells were centrifuged at 220 x g for 5 min at 4°C. The supernatant was removed and the cell pellet was resuspended in 3 ml of S1 buffer (0.25 M sucrose and 10 mM $MgCl_2$ supplemented with protease inhibitors). The resuspended solution was placed over 3 ml of S2 buffer (0.35 M sucrose and 0.5 mM $MgCl_2$ supplemented with protease inhibitors), ensuring that the two solutions form different layers and do not combine. The set-up was centrifuged at 1430 x g at 4°C for 5 min. The supernatant was removed and the pellet was resuspended in 4 ml of S2 buffer. The nuclei were burst open using a sonicator, 10 % amplitude for 10-second intervals, and monitored under a light microscope after each sonication, this step was repeated 10 times. The disrupted nuclei were then carefully placed over 3 ml of S3 buffer (0.88 M sucrose and 0.5 mM $MgCl_2$ supplemented with protease inhibitors), again ensuring that the two solutions form different layers and do not combine and centrifuged at 3000 x g at 4°C for 10 min.

2.7 Protein methods

2.7.1 Protein concentration determination

Whole cell lysates were prepared in lysis buffer (PBS containing 1% Triton X-100, 0.5% deoxycholate (DOC), 0.1% SDS supplemented with protease and phosphatase inhibitors) unless otherwise stated. Protein concentration of the samples was determined by doing a Bradford assay (2.7.2).

2.7.2 Bradford assay

A series of dilutions of bovine serum albumin (BSA) standard were prepared as a reference protein for total protein quantification (to generate a standard curve). 20 µl of each standard (BSA) and sample solution (1: 20 dilution) were prepared in triplicate. 280 µl of Bradford reagent (Sigma Aldrich) was added to each sample, incubated for 5 min at room temperature and the absorbance of each sample was read at 595 nm.

2.7.3 SDS-Polyacrylamide gel electrophoresis (SDS-PAGE)

Proteins were separated on the basis of their size using an SDS-Polyacrylamide Gel Electrophoresis (SDS-PAGE) system (BioRad). The table below shows the recipes used to prepare the gel.

Table 2.7.3.1. Recipe for SDS-Polyacrylamide resolving gel

SDS-Polyacrylamide resolving gel			
Solution	**8%**	**10%**	**15%**
37.5:1 ratio Acrylamide/Bis-acrylamide	3 ml	3.75 ml	5.625 ml
0.75 M Tris-HCl, pH 8.8	5.625 ml	5.625 ml	5.625 ml
20 % SDS	56.5 ml	56.5 µl	56.5 µl
Tetramethylethylenediamine (TEMED)	5.65 µl	5.65 µl	5.65 µl
H_2O	2.5 ml	1.75 ml	-
10% Ammonium PerSulfate (APS)	79 µl	79 µl	79 µl

Resolving gel was allowed to set for ~45 min with a layer of isopropanol on the surface to ensure a sharp interface between the resolving gel and the stacking gel. The recipe for the stacking gel is shown below.

Table 2.7.3.2. Recipe for SDS-Polyacrylamide stacking gel

SDS-Polyacrylamide stacking gel	
Solution	**5%**
37.5:1 ratio Acrylamide/Bis-acrylamide	835 µl
0.625 M Tris-HCl, pH 6.8	625 µl
20 % SDS	25 µl
TEMED	5 µl
H_2O	3.5 ml
10% APS	25 µl

6x SDS loading buffer (180 mM Tris-HCl, pH6.8, 40% glycerol, 3% SDS, and 3% 2-mercaptoethanol, 0.01% bromophenol blue in dH_2O) was added to protein samples and mixtures were boiled for 5 min before loading samples onto gels. A molecular weight marker (MWM) was also added to the gel (Pre-stained MWM, P7708, New England

Biolabs (NEB)). The gel was run in a 1x running buffer (25 mM Tris, 192 mM glycine and 0.1% SDS in dH_2O). Gels were run at constant voltage between 50 and 170 V, depending on the size of the gel and speed of separation required.

2.7.4 Coomassie Brilliant blue staining

For staining, the gel was transferred into a clean plastic box and Coomassie Brilliant blue stain (20% v/v Coomassie Brilliant blue (1:1 mixture of R250 & G250) stain, 20% v/v methanol in dH_2O) was added to cover the gel. The gel was incubated at room temperature with agitation for 1 h to overnight. Staining time depended on the gel thickness and constituency as well as protein concentration. The staining solution was removed and kept for re-use. Gels were then incubated in de-stain solution (40% methanol and 10 % acetic acid in dH_2O) until protein bands became clearly visible. Gels were either dried onto blot paper using a gel drying apparatus (DrygelSr.) or air dried between wetted, porous cellophane membrane sheets using a Perspex frame.

2.8 Immunoblot analysis

For immunoblot analysis proteins were transferred, from an SDS gel onto Polyvinylidene fluoride (PVDF) transfer membrane (Protran, Schleicher and Schuell) using the BioRad transfer system and 1x transfer buffer (25 mM Tris, 190 mM glycine and 20% (v/v) methanol in dH_2O). Prior to transfer, the PVDF membrane was soaked in methanol to activate the membrane. Transfers were carried out at 0.8 mA-1.5 mA for 90 min to 4 h depending on specific protein sizes.

The blocking step was performed using 20 ml blocking buffer (5% (w/v) dried low-fat milk powder in PBS) at room temperature with agitation for 1 h. Primary antibody incubation volumes varied from 3 – 10 ml, and were applied from 2 h at room temperature to overnight at 4°C with agitation. Primary antibodies were diluted according to table shown previously (2.4.1) in 5% fetal bovine serum (FBS) in PBS-Tween 20 (0.05%). Following incubation, the primary antibody was rinsed three times 15 min washes using PBS-Tween 20 (0.05%). The membrane was subsequently incubated with horseradish peroxidase-conjugated (HRP) secondary antibody. Secondary antibodies were diluted according to table 2.4.2, in 5% dried low-fat milk powder in PBS-Tween 20 (0.05%) and incubated for 2

h at RT. Secondary antibody was removed and rinsed off by three 15 min washes using PBS-Tween 20 (0.05%). For detection of the antibody, the membrane was developed using an enhanced chemiluminescence (ECL) kit (GE Healthcare), according to the manufacturer's protocol.

2.9 Co-immunoprecipitation procedure

Cells were grown to ~ 4 x 10^6 confluency per 150 mm dish (Sarstedt) prior to co-immunoprecipitation procedure. One 150 mm dish was used for each sample preparation. The cells were then harvested and lysed with IP lysis buffer (50 mM Tris-HCl, pH 8.0, 150 mM NaCl, 1% Triton X-100 supplemented with protease and phosphatase inhibitors). Lysates were cleared by centrifugation at 12,000 x g at 4°C for 15 min. Protein concentration of the samples was determined by doing a Bradford assay (2.7.2). 100 µl slurry (~30 µl bed volume) of Protein G plus/protein A-Agarose beads (Calbiochem) were used for each sample preparation. 100 µl slurry (~30 µl bed volume) of beads were washed three times in 500 µl IP lysis buffer (centrifuged at 1,000 x g for 5 min at 4°C). The beads (~30 µl bed volume) were then blocked in 200 µl IP lysis buffer supplemented with 1% BSA for 2 h at 4°C with constant rotation. 1 µg of a $p54^{nrb}$ monoclonal antibody (Affinity Bioreagents) or non-specific mouse IgG serum (Sigma Aldrich) were incubated with the blocked beads in 200 µl final volume of IP lysis buffer overnight at 4°C with constant rotation. The beads were then centrifuged at 1,000 x g for 5 min at 4°C, the supernatant was removed and the beads were resuspended in 1.5 mg lysate for 2 h at 4°C. The supernatant (flow through) was removed by centrifugation and the beads were then washed three times in 500 µl IP lysis buffer (centrifuged at 1,000 x g for 5 min at 4°C). Co-immunoprecipitated proteins were eluted by boiling the beads in 40 µl 2x SDS loading buffer (1:1 ratio) for 5 min.

2.10 Immunofluorescence staining procedure

Cells were grown in tissue culture on glass cover slips and were allowed to recover overnight. The media was removed from the dishes and the cells were washed twice with PBS. Afterwards, cells were fixed using 4% formaldehyde in PBS for 10 min at 37°C and permeabilised by 0.2% Triton X-100 in PBS for 10 min at 37°C. Slides were rinsed twice

with 500 µl PBS between each step. Cells were blocked for 30 min at 37°C with 10% goat serum, 5% BSA and 0.05% Tween in PBS. Incubation with appropriate primary antibody was then carried out, diluted as described previously in table 2.4.1 in 5% goat serum and 0.05% Tween in PBS for 1 h at 37°C. Cells were rinsed with 2.5% goat serum, 0.05% Tween in PBS and then probed with secondary antibody. Secondary antibodies against rabbit, mouse and rat coupled with cy-2 or cy-3 (Jackson Immunochemicals) were typically applied for 45 min at 37°C in 5% goat serum, 2.5% BSA and 0.05% Tween in PBS, dilutions described as in table 2.4.2. Cells were rinsed again with 2.5% goat serum, 0.05% Tween in PBS. DNA was then subsequently stained with DAPI (100 ng/ml), and the cells were then mounted on slides for examination. Immunofluorescence was detected using an Olympus IX51 microscope.

2.11 EdU labelling

EdU labelling was carried out using a Click-iT™ EdU imaging kit (Invitrogen). The labelling procedure was carried out according to manufacturers guidelines. Briefly, cells were grown in tissue culture on glass cover slips and allowed to recover overnight. A 20 µM solution of EdU (Component A) was prepared in complete medium from the 10 mM stock solution. The solution was pre-warmed and an equal volume of the 20 µM EdU solution was added to the volume of media containing cells to be treated (final concentration of EdU used was 10 µM). After a 1 h incubation with 10 µM EdU, the media was removed cells were fixed using 4% formaldehyde in PBS for 10 min at 37°C and permeabilised with 0.2% Triton X-100 in PBS for 10 min at 37°C. A Click-iT™ reaction cocktail was prepared according to manufacturer's protocol and was added to the glass cover slips within 15 min of preparation. The glass cover slips were incubated with the reaction cocktail for 30 min at room temperature and protected from light. Following incubation, the glass cover slips were subjected to immunofluorescence staining procedure as describe above in section 2.9.

2.12 Dot blot Immunoassay

Cells were subjected to UV irradiation as described previously (2.2.1) and harvested at various timepoints (0h – 24h post-UV). Genomic DNA was isolated using the GenElute kit

(Sigma-Aldrich). DNA was quantified using nanodrop (Thermo scientific 2000). 0.5 μg of DNA was denatured at 60°C for 1 h in an equal volume of 0.3 M NaOH. The DNA samples were then transferred onto nitrocellulose transfer membrane using a dot blot apparatus (Bio-Rad microfiltration apparatus). Each well was then washed with 600 μl of 0.3 M NaOH followed by sterile SSC buffer (3 M NaCl, 0.3M trisodium citrate, pH 7.0).

The nitrocellulose transfer membrane was fixed by heating the membrane to 80°C for 1 h in the dark. The blocking step was performed using 20 ml blocking buffer (5% (w/v) dried low-fat milk powder in PBS) at room temperature with agitation for 1 h. Primary antibodies were applied overnight, at 4°C with agitation in the dark. Primary antibodies were diluted according to table 2.4.1 shown previously in 5% fetal bovine serum (FBS) in PBS-Tween 20 (0.05%). Following incubation, primary antibody was rinsed by three 5 min washes using PBS-Tween 20 (0.1%). The membrane was subsequently incubated with an HRP-conjugated secondary antibody. Secondary antibodies were diluted according to table 2.4.2 in 5% milk in PBS-Tween 20 (0.05%) and applied for 2 h at RT. Secondary antibody was removed and the membrane was rinsed by three 5 min washes using PBS-Tween 20 (0.1%). For detection of the antibody, the membrane was developed using an enhanced chemiluminescence ECL kit (GE Healthcare), according to the manufacturer's protocol.

2.13 Chemical reagents and solutions

The chemical reagents that were used in this study were of analytical grade and were purchased from Sigma-Aldrich, BDH, Fisher, or Amersham Biosciences. All solutions were prepared in Milli-Q purified H2O unless otherwise specified. Solutions used in this study are shown in the table below.

Table 2.12. List of chemical reagents and solutions

Name	Composition
Blocking Solution	10% goat serum, 5% BSA and 0.05% Tween in PBS
Blocking solution for immunoblotting	5% w/v dried low-fat milk powder and 0.05% Tween 20 in PBS
Buffer A	10 mM HEPES-KOH, pH 7.9, 10 mM KCl, 1.5 mM $MgCl_2$ and 0.5 mM DTT supplemented with protease and phosphatase inhibitors
Coomassie Brilliant Blue stain	20% v/v colloidal Coomassie Brilliant blue stain (1:1 mixture of R250 & G250) 20% v/v methanol, in dH_2O
DNA loading dye (6x)	20% sucrose, 0.1 M EDTA pH 8.0, 1% SDS, 0.25% Bromophenol blue, 0.25% Xylene cyanol
Destain solution	40% methanol and 10 % acetic acid in dH_2O
Fixing solution for IF	4% paraformaldehyde in PBS
IP lysis buffer	50 mM Tris-HCl, pH 8.0, 150 mM NaCl, 1% Triton X-100 supplemented with protease and phosphatase inhibitors
Low Salt (LS) Buffer for nuclear extraction assay	20 mM HEPES-KOH, pH7.8, 5 mM potassium acetate, 0.5mM magnesium chloride, 0.5 mM dithiothreitol (DTT) in dH_2O supplemented with protease and phosphatase inhibitors
Lysis buffer	PBS containing 1% Triton X-100, 0.5% DOC, 0.1% SDS supplemented with protease and phosphatase inhibitors
Medium Salt (MS) Buffer for nuclear extraction assay	20 mM HEPES-KOH, pH 7.4, 150 mM NaCl, 2.5 mM $MgCl_2$, the medium salt buffer was supplemented with either low (0.025%) or high (1%) triton x-100 supplemented with protease and phosphatase inhibitors
Permeabilisation buffer for IF	0.05% Triton X-100 in PBS
Ponceau S stain	1 g Ponceau S, 15 g trichloroacetic acid, 15g sulphosalicylic acid, dH_20 to 500ml
Primary antibody solution for immunoblotting	5% fetal bovine serum (FBS) in PBS-Tween 20 (0.05%)
Primary antibody solution for IF	5% goat serum and 0.05% Tween in PBS
S1 Buffer	0.25 M sucrose and 10 mM $MgCl_2$ supplemented with protease inhibitors

S2 Buffer	0.35 M sucrose and 0.5 mM $MgCl_2$ supplemented with protease inhibitors
S3 Buffer	0.88 M sucrose and 0.5 mM $MgCl_2$ supplemented with protease inhibitors
SDS loading buffer (6x)	180mM Tris-HCl pH6.8, 40% glycerol, 3% SDS, and 3% 2-mercaptoethanol, 0.01% bromophenol blue, in dH_2O
SDS PAGE running buffer	25 mM Tris, 19 2mM glycine, 0.1% SDS in dH_2O
Secondary antibody solution for immunoblotting	5% dried low-fat milk powder in PBS-Tween 20 (0.05%)
Secondary antibody solution for IF	5% goat serum, 2.5% BSA in PBS-Tween 20 (0.05%)
SSC buffer (2x)	3M NaCl, 0.3M trisodium citrate, pH 7.0
TAE	40mM Tris-acetate, 1mM EDTA.
TFB buffer for transformations	30 mM potassium acetate, 100 mM $RbCl_2$, 10 mM $CaCl_2$, 50 mM $MnCl_2$, 15% glycerol, pH 6.5
Transfer buffer for immunoblotting	25mM Tris, 190mM glycine, and 20% v/v methanol in dH_2O.

Chapter 3 - Biochemical characterisation of p54^{nrb} following UV irradiation

The maintenance of genome integrity is vital for the survival of all organisms. Cells and organisms are continuously under attack by genotoxic agents, both endogenous and exogenous. DNA damage activates a cascade of DNA damage response pathways that activate cell-cycle checkpoints, apoptosis, transcription, and chromatin remodelling. These processes are tightly monitored so that the genetic material is faithfully maintained, duplicated, and segregated within the cell. The inability to repair DNA damage causes genomic instability and may cause carcinogenesis.

To investigate protein recruitment to chromatin after DNA damage *in vivo* SV40 minichromosomes having pyrimidine-rich DNA sequences were established to create a vector with a higher sensitivity to UV than currently available DNA sequences, effectively a UV "Hot-Spot" *in vivo*, (H. Anhold, PhD thesis). Subsequent to UV irradiation, minichromosomes were purified and associated proteins were identified by mass spectrometry. Several proteins were shown to have a greater association with purified minichromosomes after the UV treatment of cells. Of these proteins, p54^{nrb} that exhibits multi-functional characteristics in multiple nuclear processes including nuclear RNA processing, and regulation of transcription was selected for further analyses as a potential participant in the UV DNA damage repair or signal transduction pathways.

3.1 p54^{nrb} is associated with minichromosomes following UV irradiation

XP12RO is a human fibroblast cell line derived from a xeroderma pigmentosum type A patient lacking the expression of XPA protein whereas the XP12RO clone 5 cell line is derived from XP12RO by producing an isogenic cell line of XP12RO expressing XPA protein. XP12RO is an SV40-transformed cell line that is highly UV-sensitive and deficient in DNA repair however its isogenic cell line is proficient in DNA repair, see figure 3.9.2 for cell viability assays performed. By performing clonogenic survival assays, it was observed that the XP12RO cells were highly sensitive to UV irradiation (~20% survival rate at 1 J/m^2), in comparison, XP12RO C5 cells and SV40-transformed normal human skin fibroblast cell lines (GM00637), showed similar survival rates (~20% survival rate at 10 J/m^2) indicating that the isogenic cell line behaved similar to normal cells and have normal XPA expression (data not shown). These observations are in agreement with other published work (Cleaver et al., 1987; Muotri et al., 2002).

Asynchronous XP12RO (XPA$^-$) and XP12ROC5 (XPA$^+$) cells were subjected to UV irradiation (30 J/m^2), a minichromosome preparation was carried out as described in 2.6.1, and the association of p54^{nrb} with minichromosomes was determined by western blot. Equal amounts of samples were loaded on to a 15% SDS gel and the blots were probed with selected antibodies. Anti-SV40 T antigen (TAg) served as a loading control and anti-XPA was used to distinguish between the two cell lines studied. In these experiments, p54^{nrb} associated with minichromosomes in XP12RO (XPA$^-$) and XP12ROC5 (XPA$^+$) cells following UV irradiation as early as 30 min (Figure 3.1). This observation is in agreement with previous findings Dr. Heinrich Anhold discovered. Heinrich Anhold also performed a minichromosome preparation and identified p54nrb associated with minichromosomes at 5 and 10 J/m^2 of UV irradiation (data not shown). Subsequent to this, we wanted to investigate p54^{nrb} and its role in the DNA damage response following UV irradiation.

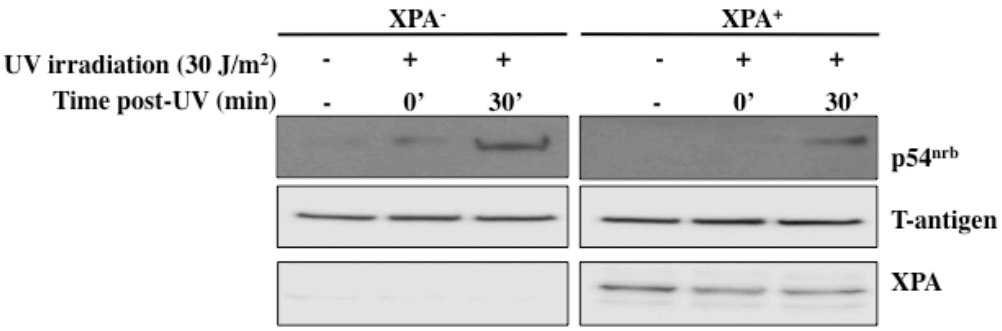

Figure 3.1 Western blot analysis of minichromosomes.
Minichromosomes prepared from XP12RO (XPA$^-$) and XP12RO clone 5 (XPA$^+$) cells, both non-irradiated and UV irradiated (30 J/m^2), were analysed by western blotting. An antibody specific to p54^{nrb} was used to detect the levels of the protein. T-antigen served as a loading control. XPA antibody was used to distinguish between the cell lines. Membranes were developed using a horseradish peroxidase-conjugated secondary antibody and ECL system. Signal was detected with a Fuji LAS 3000 imager.

3.2 Enrichment of p54^{nrb} in nucleoli following UV irradiation

3.2.1 Time- and dose-dependent enrichment of p54^{nrb} to nucleoli following UV irradiation

Following the discovery of p54^{nrb} being associated with minichromosomes after UV irradiation, it was our objective to investigate the cellular localisation of the protein after UV treatment in human cell lines. XP12RO (XPA^{-}), XP12ROC5 (XPA^{+}), U2OS (human epithelial bone osteosarcoma cell line) and HeLa S3 cells were exposed to 2.5 - 30 J/m^2 of UV irradiation and fixed 30 min to 8 h post-UV treatment for analysis by immunofluorescence microscopy.

In all non-irradiated cells, p54^{nrb} is dispersed throughout the nucleoplasm of the cell but is excluded from nucleoli (or at least shows a significantly reduced association with nucleoli) in all of the cell lines analysed. In the XP12RO (XPA^{-}) cells, p54^{nrb} shows a prominent subnucleolar localisation pattern as early as 30 min post 2.5 J/m^2 of UV irradiation (Figure 3.2.1 (B)). p54^{nrb} was observed in the nucleoli in about 10 % of cells (for quantifications of the nucleolar p54^{nrb} after UV treatment see figure 3.2.1 (K)). The number of cells showing p54^{nrb} nucleolar localisation increases with time and UV dose applied (see figure 3.2.1 (K)). p54^{nrb} persists to localise to the nucleolus up until 8 h post UV irradiation (Figure 3.2.1 (C) and (D)). In the XP12RO clone 5 (XPA^{+}) cells p54^{nrb} does not seem to target nucleoli at lower UV doses (see figure 3.2.1 (F) and (G)). p54^{nrb} begins to localise in nucleoli at later time points and a higher UV dose (10 J/m^2) relative to the XP12RO (XPA^{-}) cells (Figure 3.2.1 (H)). The data presented is a representative result of three independent experiments.

In U2OS and HeLa S3 cells p54^{nrb} localises in nucleoli after UV irradiation similarly to XP12RO (XPA^{-}) cells and can be observed in the nucleolus 2 h following 5 J/m^2 of UV irradiation. U2OS and HeLa S3 cells were also subjected to a higher UV dose (30 J/m^2) and showed p54^{nrb} nucleolar localisation (Figure 3.2.1 (I) and (J)). These findings suggest that p54^{nrb} moves to nucleoli in a time- and dose-dependent manner following UVC irradiation and that the phenomenon is evident in various human cell lines. The data presented are representative of three independent experiments.

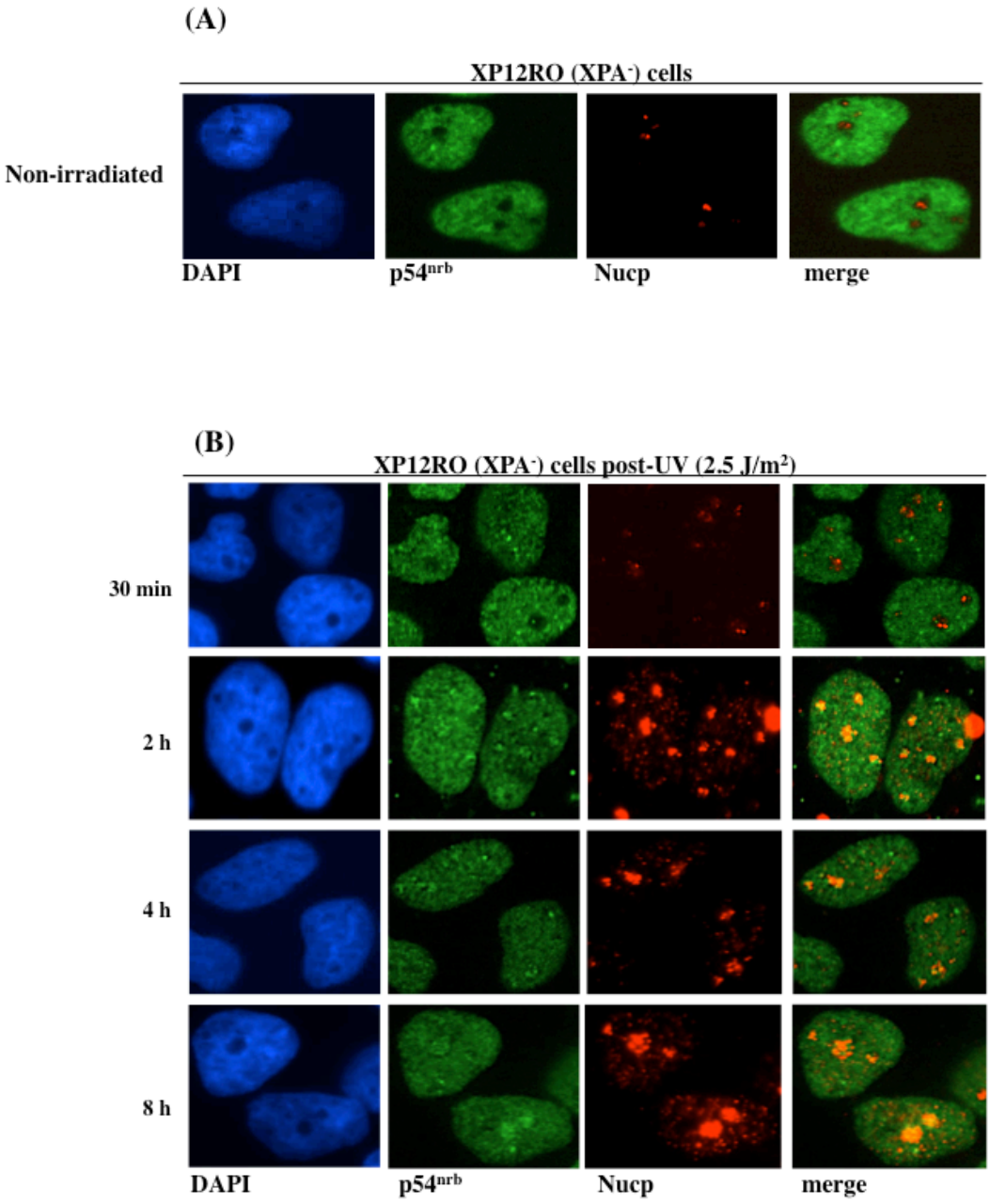
(A)
XP12RO (XPA-) cells
Non-irradiated
DAPI
p54nrb
Nucp
merge
(B)
XP12RO (XPA-) cells post-UV (2.5 J/m2)
30 min
2 h
4 h
8 h
DAPI
p54nrb
Nucp
merge

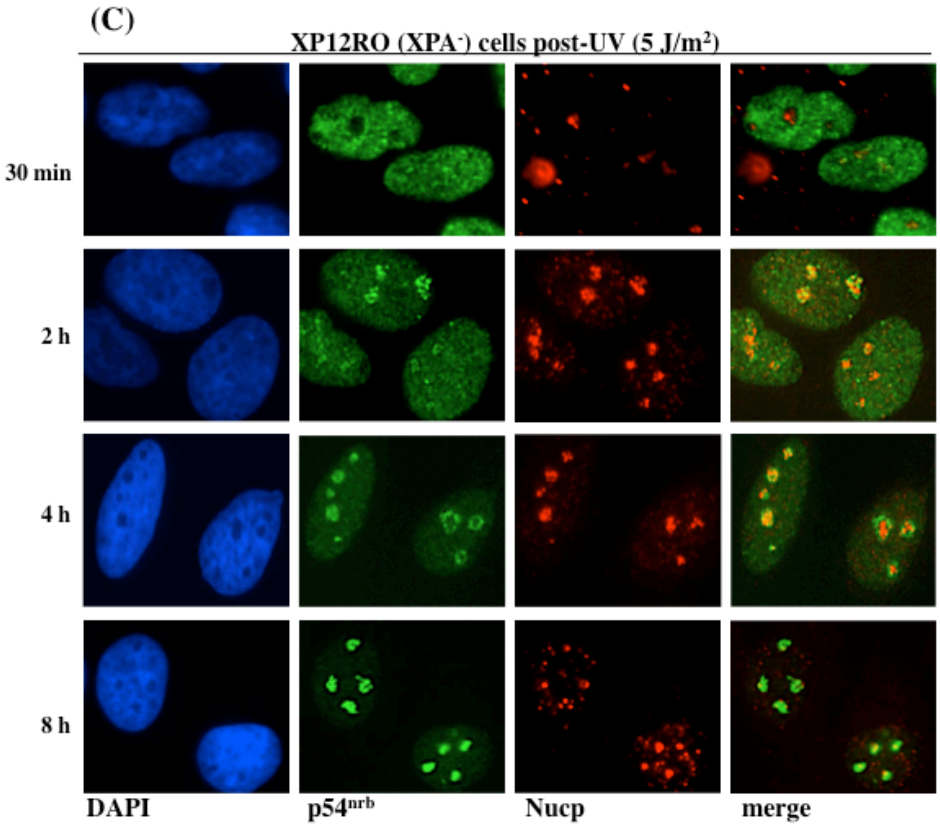
(C)
XP12RO (XPA-) cells post-UV (5 J/m2)
30 min
2 h
4 h
8 h
DAPI
p54nrb
Nucp
merge

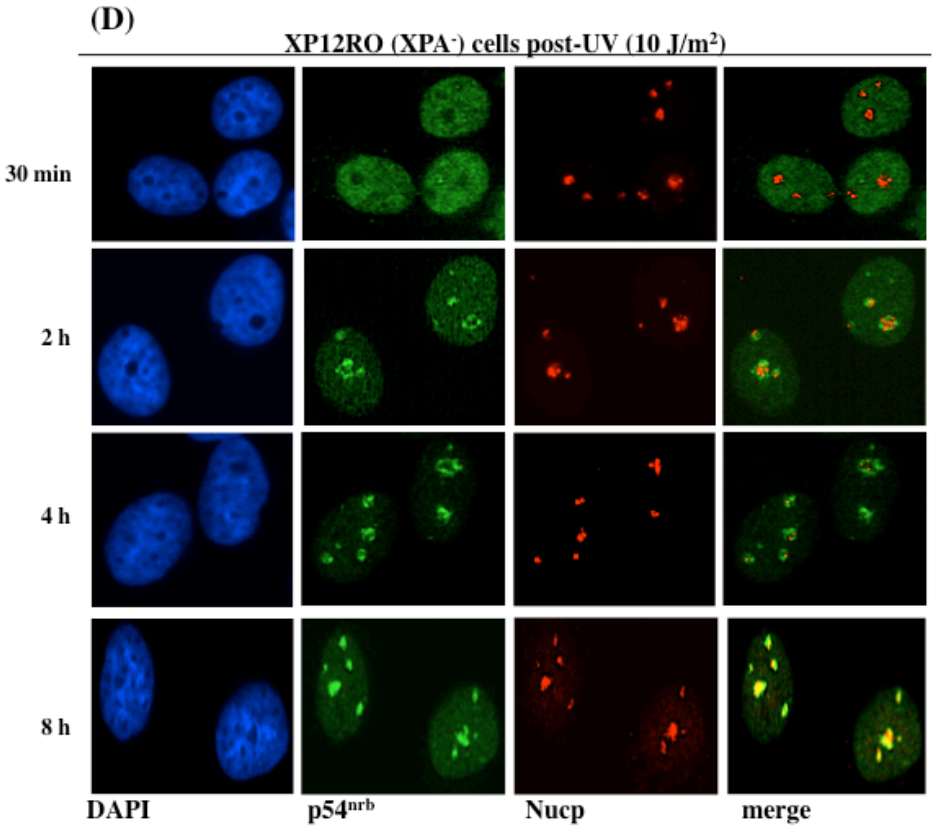
(D)
XP12RO (XPA-) cells post-UV (10 J/m2)
30 min
2 h
4 h
8 h
DAPI
p54nrb
Nucp
merge

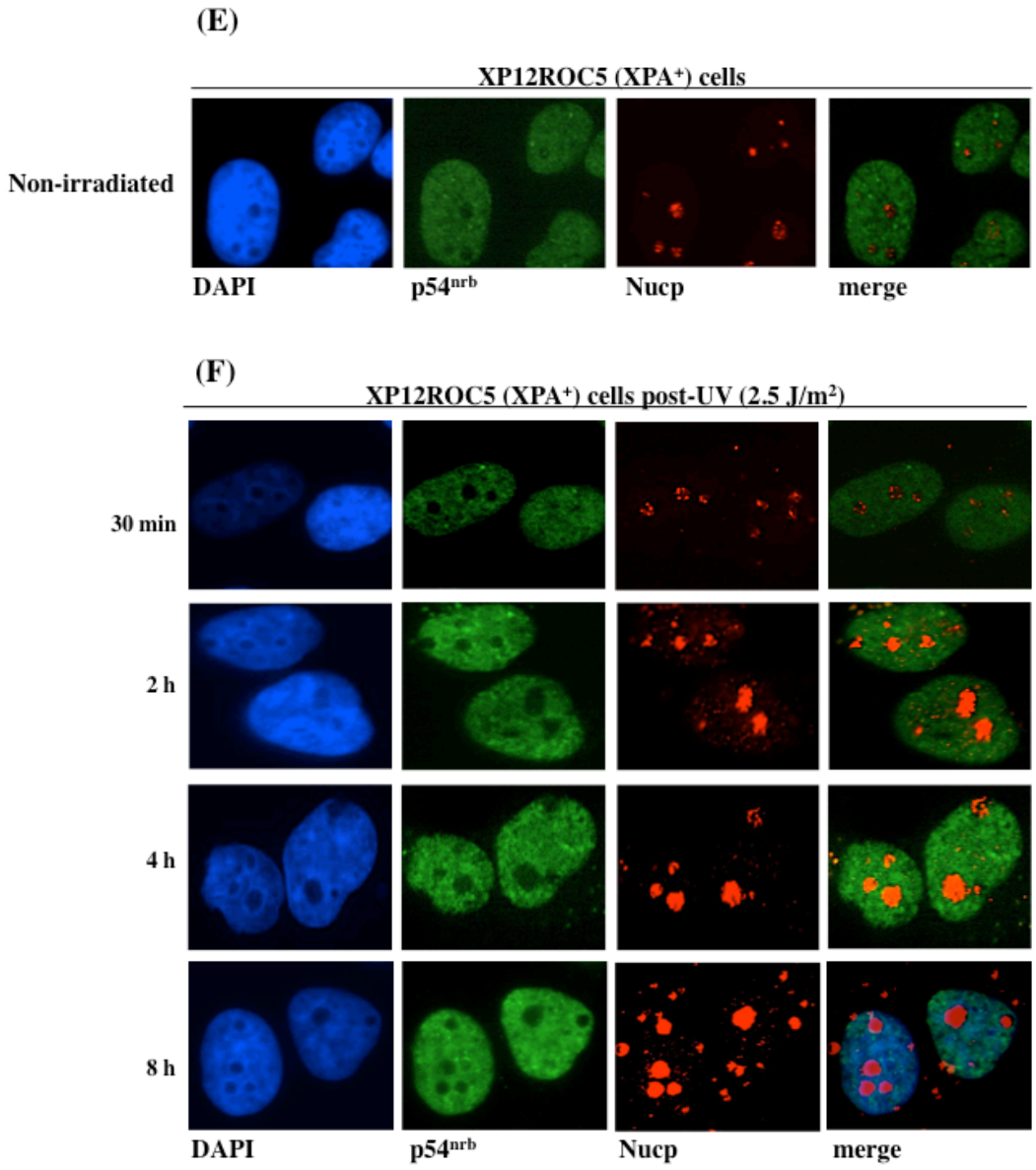
(E)
XP12ROC5 (XPA+) cells
Non-irradiated
DAPI
p54nrb
Nucp
merge
(F)
XP12ROC5 (XPA+) cells post-UV (2.5 J/m2)
30 min
2 h
4 h
8 h
DAPI
p54nrb
Nucp
merge

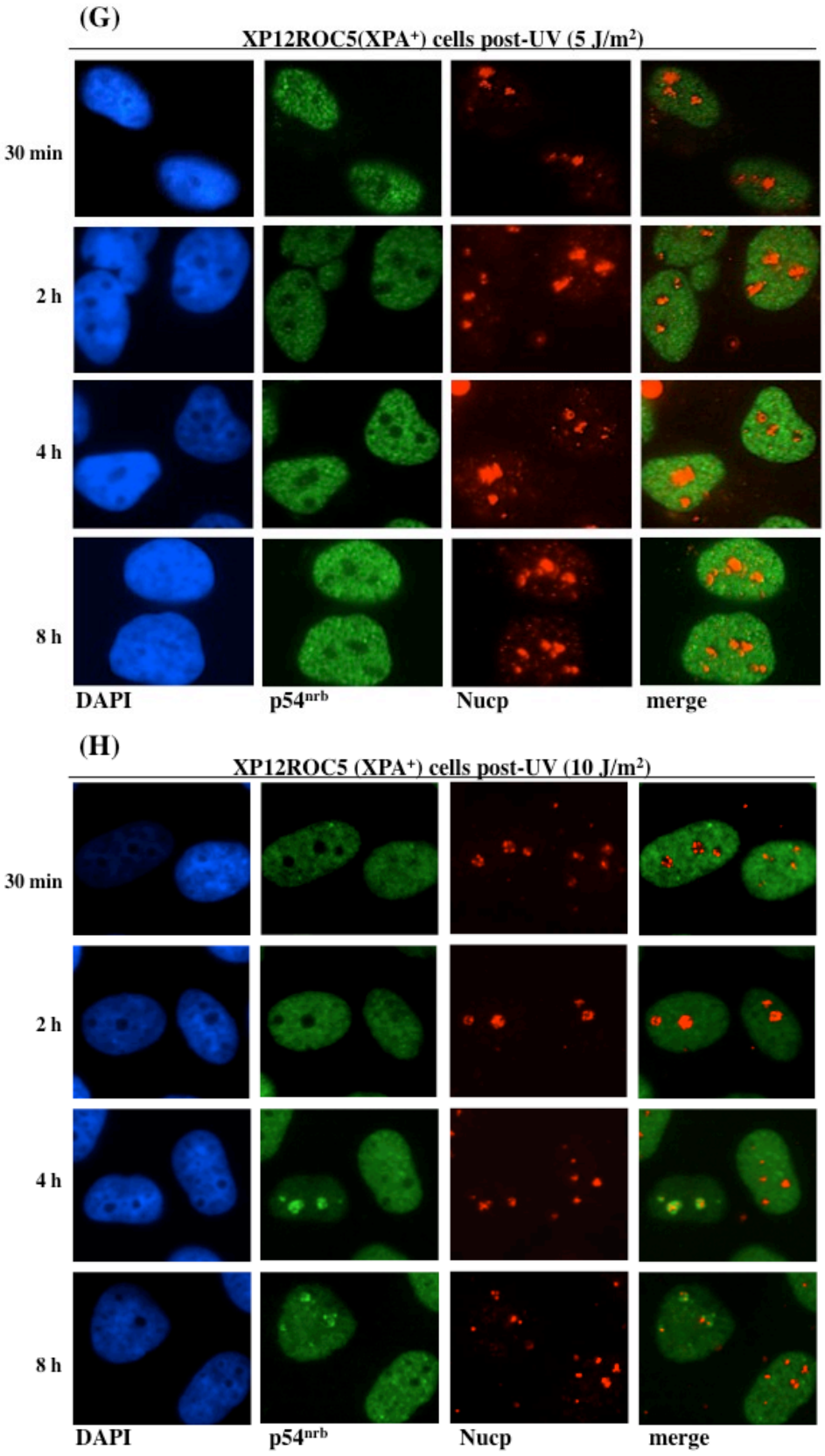
(G)
XP12ROC5(XPA+) cells post-UV (5 J/m2)
30 min
2 h
4 h
8 h
DAPI
p54nrb
Nucp
merge
(H)
XP12ROC5 (XPA+) cells post-UV (10 J/m2)
30 min
2 h
4 h
8 h
DAPI
p54nrb
Nucp
merge

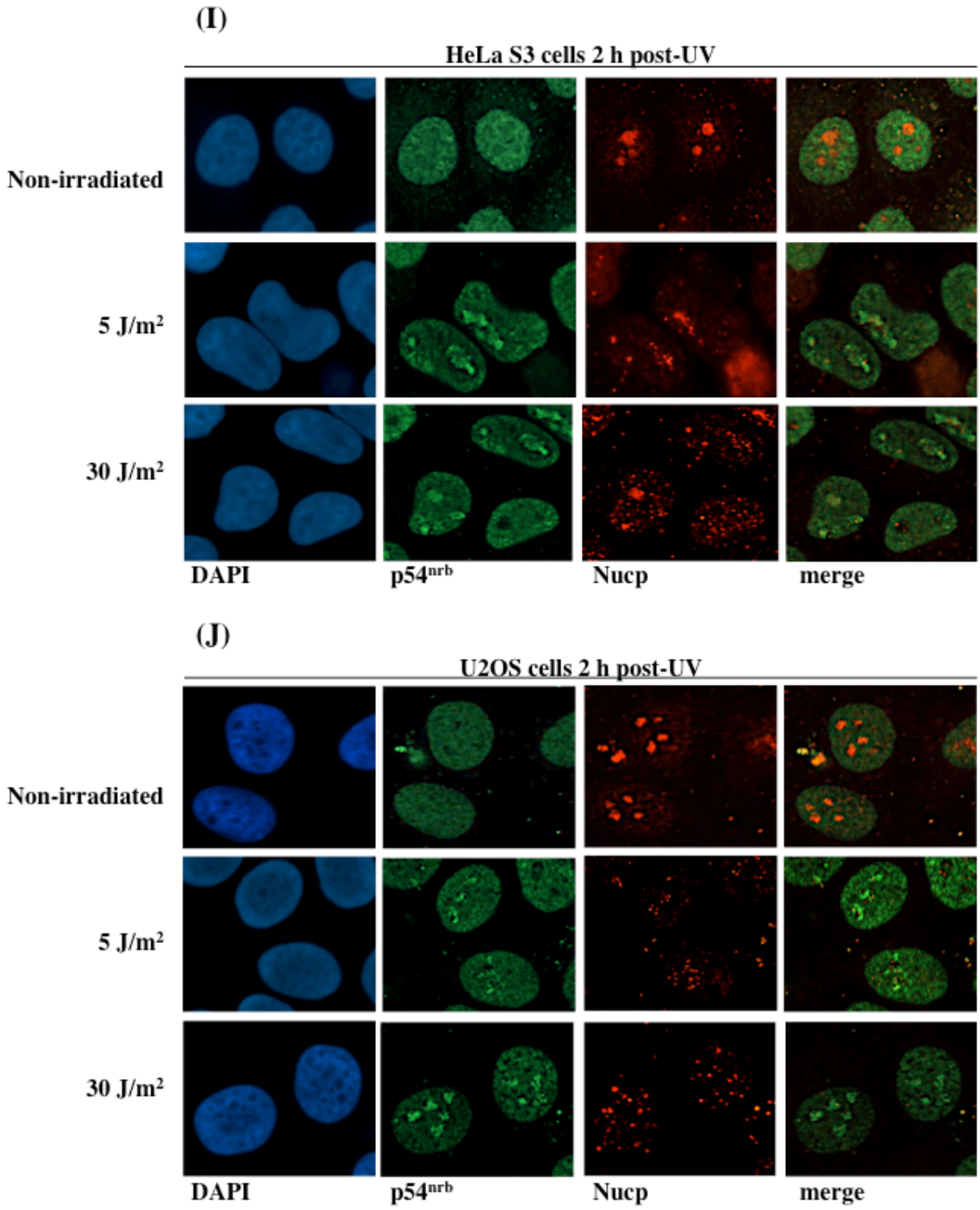
(I)
HeLa S3 cells 2 h post-UV
Non-irradiated
5 J/m²
30 J/m²
DAPI
p54nrb
Nucp
merge
(J)
U2OS cells 2 h post-UV
Non-irradiated
5 J/m²
30 J/m²
DAPI
p54nrb
Nucp
merge

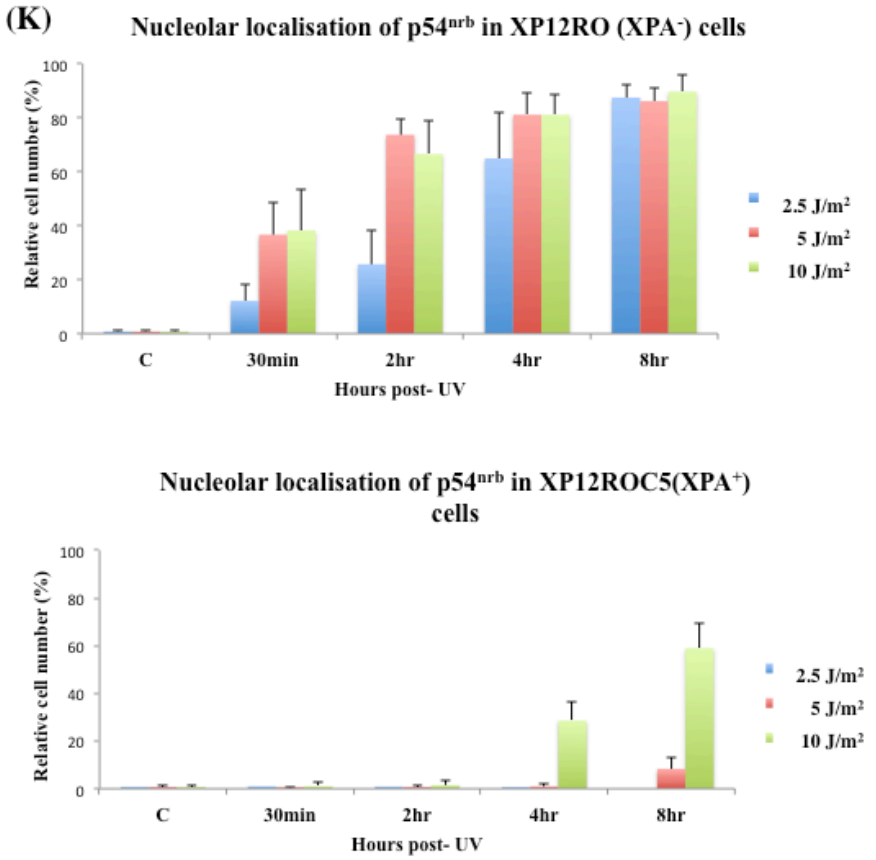

Figure 3.2.1 Multi-functional protein p54nrb localises to nucleoli following UV irradiation. XP12RO (XPA^-) and XP12RO clone 5 (XPA^+) cell lines were non-irradiated (panels **(A)** and **(E)** respectively) or UV irradiated with 2.5, 5 and 10 J/m^2 of UVC (in panels **B**, **C** and **D** for XPA^-, in panels **F**, **G** and **H** for XPA^+ cells). Cells were fixed 30 min, 2, 4 and 8 h post-UV and probed with p54nrb antibody followed by cy2-conjugated secondary mouse antibody (green). Nucleoli were stained with a nucleophosmin (Nucp) antibody followed by cy3-conjugated secondary rabbit antibody (red colour). Cell nuclei were stained with DAPI (blue). Immunofluorescence microscopy was performed using an Olympus IX51 microscope. U2OS and HeLa cell lines were non-irradiated or UV irradiated with 5 and 30 J/m^2 of UVC (panels **(I)** and **(J)** respectively). Cells were fixed 2 h post-UV and probed with p54nrb antibody followed by cy2-conjugated secondary mouse antibody (green). Nucleoli were stained with a nucleophosmin (Nucp) antibody followed by cy3-conjugated secondary rabbit antibody. Cell nuclei were stained with DAPI (blue). The immunofluorescence data of nucleophosmin and p54nrb were merged and presented in the fourth column highlighted as 'merge'. Immunofluorescence microscopy was performed using an Olympus IX51 microscope. Histogram representing the number of cells showing nucleolar localisation of p54nrb following UV irradiation in XP12RO (XPA^-) and XP12RO clone 5 (XPA^+) cells (obtained by immunofluorescence microscopy) (panel **(K)**). Data represents the mean of three independent experiments. Error bar represent one standard deviation.

3.2.2 p54^{nrb} is tightly bound to chromatin in XP12RO (XPA$^-$) and XP12RO clone 5 (XPA$^+$) cells

Following the discovery by immunofluorescence microscopy that p54^{nrb} localises to the nucleolus after UV irradiation, we wanted to investigate this observation biochemically. A nuclear extraction assay according to Burtelow et al (2000) was performed to determine the sub-cellular localisation of p54^{nrb} following UV irradiation as described in 2.6.2. The fractions represent soluble proteins; loosely chromatin bound proteins, and tightly bound chromatin proteins. Two different percentages of Triton X-100 detergent (0.025% and 1%) were used to vary the strength of the buffer.

Asynchronous XP12RO (XPA$^-$) and XP12RO clone 5 (XPA$^+$) cells were subjected to UV irradiation (5 J/m^2 of UVC) and harvested at 30 min and 2 h post-UV followed by cellular and nuclear extraction (Burtelow et al., 2000). The two time points were chosen because at these time points the change in p54^{nrb} nucleolar localisation is detected by immunofluorescence microscopy in XP12RO (XPA$^-$) cells (Figure 3.2.1). The samples obtained from the cellular and nuclear extraction were analysed by SDS PAGE and Coommassie Brilliant blue staining (Figure 3.2.2 (A) and (B)). The SDS PAGE easily distinguishes between the various fractions. The highest protein content is visible in the medium salt fraction. Histone bands are clearly seen in the sonicated supernatant fraction. Importantly XP12RO (XPA$^-$) and XP12RO clone 5 (XPA$^+$) cells show similar results when analysed by SDS PAGE.

The cellular and nuclear fractions were also subjected to SDS PAGE followed by western blotting. The blots were probed with anti-RPA 70, anti-lamin β antibody and anti-histone H3 antibody to distinguish between the different fractions. The data presented are representative of three independent experiments. These extraction assays revealed that p54^{nrb} protein was highly abundant in the tightly bound chromatin fractions (Figure 3.2.2 (C) and (D)). This observation suggests that p54^{nrb} is tightly DNA-associated. There were no changes observed in the levels of p54^{nrb} between the asynchronous XP12RO (XPA$^-$) and XP12RO clone 5 (XPA$^+$) cells (Figure 3.2.2 (C) and (D)). Moreover, no differences were detected in the levels of p54^{nrb} between the untreated and UV irradiated samples. These findings suggest that the nucleolar enrichment of p54^{nrb} observed by immunofluorescence microscopy could be due to a sub-cellular redistribution of p54^{nrb} and not an increase in the

overall amount of protein associated with chromatin following UV irradiation as determined by these biochemical assays.

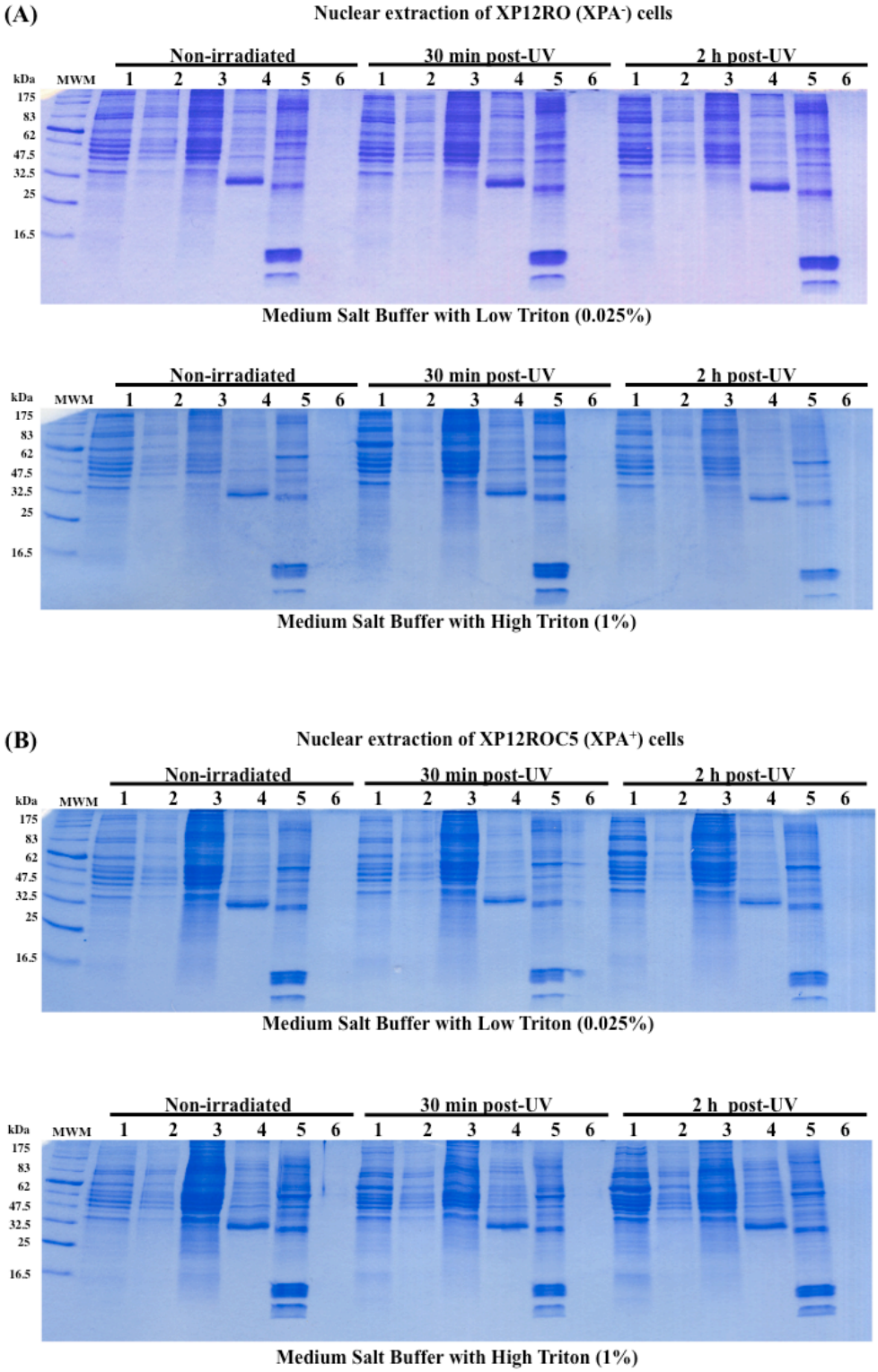

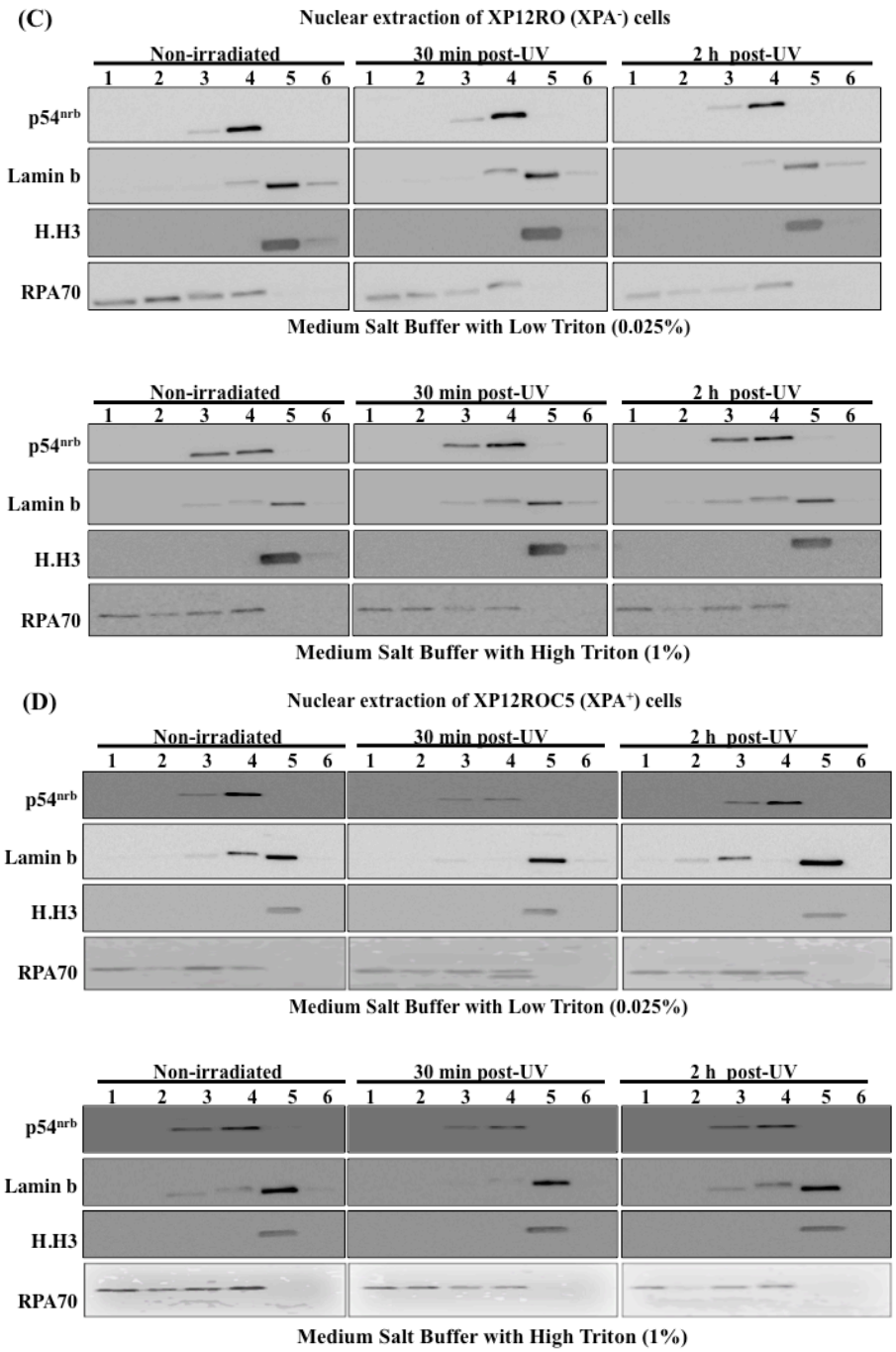

Figure 3.2.2 Cellular and nuclear extraction of XP12RO (XPA$^-$) and XP12RO (XPA$^+$) cells. Asynchronous XP12RO (XPA$^-$) and XP12RO clone 5 (XPA$^+$) cells were non-irradiated or UV irradiated (5 J/m^2), harvested at either 30 min or 2 h post-UV irradiation and subjected to nuclear extraction. The fractions obtained were normalised for protein content and analysed by 15% SDS polyacrylamide gels and Coommassie Brilliant blue staining (panels **(A)** and **(B)**). The fractions were further analysed by western blot using anti-RPA 70, anti-lamin β antibody and anti-histone H3 antibody to distinguish between the different cellular fractions (panels **(C)** and **(D)**). The fraction numbers corresponding to the above figures are as follows: 1. soluble protein, 2. low salt wash, 3. medium salt, 4. DNase supernatant, 5. sonicated supernatant, and 6. sonicated pellet solubilised in SDS loading buffer fraction.

3.2.3 Increased levels of p54^{nrb} observed in purified nucleoli following UV irradiation

p54^{nrb} localises to nucleoli following UV irradiation as characterised by immunofluorescence microscopy. Nuclear extraction assays showed that p54^{nrb} is tightly bound to chromatin although this very general procedure does not allow us to identify the increase of p54^{nrb} protein observed in nucleoli by immunofluorescence microscopy following UV irradiation. We therefore adapted a procedure from Andersen et al (2002) to purify nucleoli in an attempt to replicate the immunofluorescence data biochemically.

Asynchronous XP12RO (XPA^{-}) and XP12RO clone 5 (XPA^{+}) cells were subjected to UV irradiation (5 J/m^2 of UVC) and harvested at 2 h post-UV followed by purification of nucleoli as described in 2.6.3. This time point was chosen because it is at this time the change in p54^{nrb} nucleolar enrichment is observed in XP12RO (XPA^{-}) cells by immunofluorescence microscopy (Figure 3.2.1).

The purified nucleoli were subjected to SDS PAGE followed by quantitative western blotting. Purified nucleoli were loaded according to equal cell numbers (~1 x 10^6 cells) along with whole cell lysate samples. Anti-RPA43 and anti-UBF 1/2, which are involved in ribosomal transcription, were used as positive controls to detect for nucleoli and anti-RPA 32 was used to clarify the purity of the nucleoli prepared. The data presented is a representative result of three independent experiments. Following UV irradiation, we observed an increase in the levels p54^{nrb} protein in purified nucleoli in the XP12RO (XPA^{-}) cells (Figure 3.2.3 (A)). As determined by densitometry analysis, there is more than a two-fold increase of p54^{nrb} present in purified nucleoli following UV irradiation (Figure 3.2.3 (C)). There was an increase observed in the levels of p54^{nrb} protein in the XP12RO clone 5 (XPA^{+}) cells, although higher basal levels of p54^{nrb} were detected relative to that of XP12RO (XPA^{-}) cells (Figure 3.2.3 (A)). The increase of p54^{nrb} observed in nucleoli following UV irradiation by densitometry analysis was significantly less than that observed in XP12RO (XPA^{-}) nucleoli (Figure 3.2.3 (C)). The marked increase of p54^{nrb} protein in XP12RO clone 5 (XPA^{+}) nucleoli relative to that of XP12RO (XPA^{-}) nucleoli could be due to the presence of XPA protein, and perhaps the XP12RO (XPA^{-}) cells have a reduced level in functional transcription as observed by the lower levels of RPA43 and UBF 1/2. The higher level of these nucleolar transcription factors in XP12RO clone 5 (XPA^{+}) cells could

mark a higher level of nucleolar transcription and rRNA in these cells. p54nrb binds to RNA under these conditions in XP12RO clone 5 (XPA+) cells indicating higher levels of p54nrb would be recruited to nucleoli under normal growth conditions, thus resulting in higher levels of p54nrb in nucleoli than that of XP12RO (XPA-) nucleoli. However, it is still visible in the immunofluorescence analysis that association of p54nrb is lower than that of the nucleoplasm. These observations taken together suggests that p54nrb is retained in XP12RO (XPA-) and XP12RO clone 5 (XPA+) cell nucleoli after UV irradiation indicating that it partakes in a DNA damage response pathway in nucleoli.

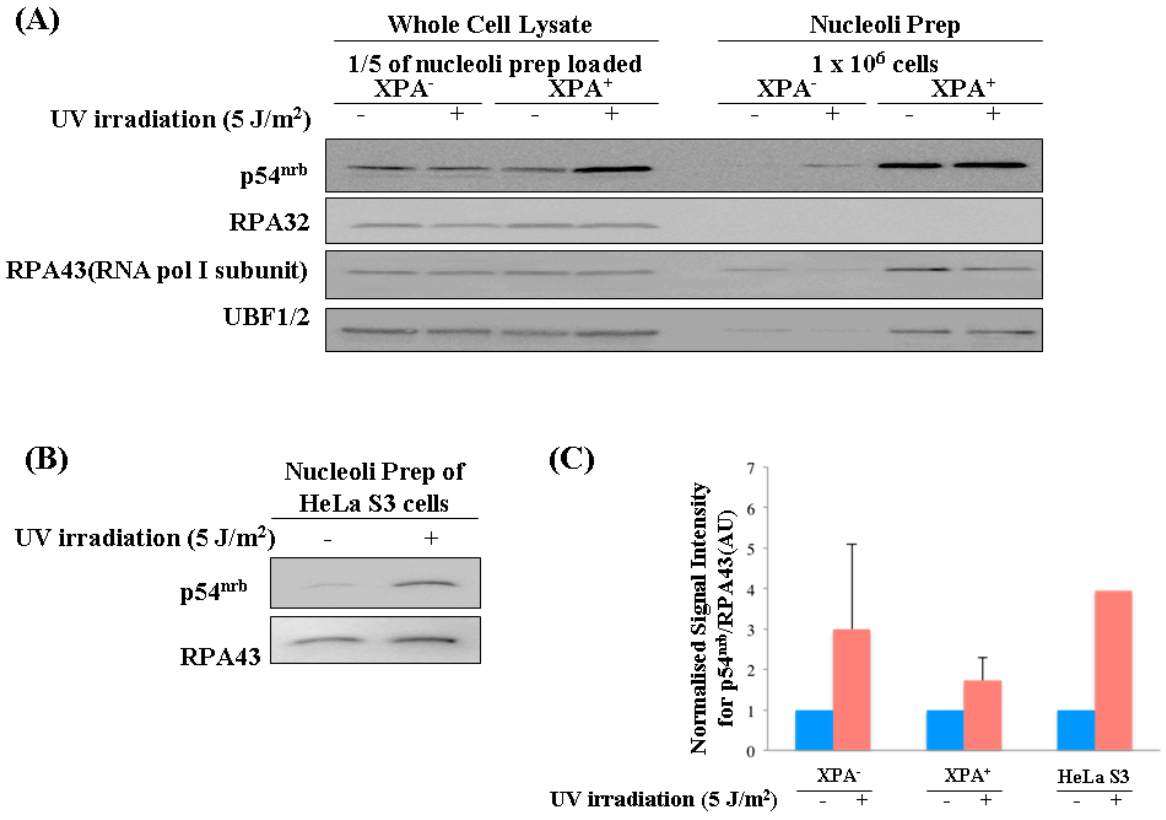

Figure 3.2.3 Nucleolar purification with and without UV treatment.
Asynchronous XP12RO (XPA-) and XP12RO clone 5 (XPA+) cells were subjected to UV irradiation (5 J/m^2 of UVC) and harvested at 2 h post-UV followed by a nucleolar purification. Western blot analysis was performed using an antibody specific to p54nrb to detect the levels of the protein. Purified nucleoli were loaded according to equal cell numbers (~1 x 10^6 cells) along with whole cell lysate samples. Anti-RPA43 and anti-UBF 1/2 were used as positive controls to detect for nucleoli and anti-RPA 32 was used to clarify the purity of the nucleoli prepared (panel **(A)**). HeLa S3 cells were also subjected to a nucleolar purification following UV irradiation (5 J/m^2) Anti-RPA43 was used as positive controls to detect for nucleoli (panel **(B)**). The ratios of signal intensities for p54nrb (minus background)/RPA43 (minus background) from three different nucleoli

preparation experiments of XP12RO (XPA^{-}) and XP12RO clone 5 (XPA^{+}) cells were determined by densitometry. The difference in ratio between untreated (UT, arbitrarily normalised to 1) and UV irradiated cells with standard deviation from the mean indicated by error bars are depicted. AU = Arbitrary Units. For comparison the experiment was also performed in HeLa S3 cells but this was only carried out once (panel **(C)**).

For comparison, HeLa S3 cells were also subjected to nucleolar purification following UV irradiation. In the HeLa S3 cells, an increase of p54^{nrb} protein was detected after UV irradiation (Figure 3.2.3 (B) and (C)). In conclusion, these observations allow us to biochemically represent the localisation of p54^{nrb} following UV irradiation. These biochemical purifications show an increase of p54^{nrb} association with nucleoli but also determined that there is a basic level of p54^{nrb} association with nucleoli in logarithmically growing cells in the absence of UV treatment and that this basic level may vary with the state of the cell. The reduced increase of association in XP12RO clone 5 cells could also be due to the time point chosen and the low level of irradiation used, perhaps these are not the optimal experimental conditions for the association of p54^{nrb} to nucleoli in XP12RO clone 5 cells.

3.3 The localisation of p54nrb to the nucleolus following UV irradiation is ablated by the deletion of its helix turn helix domain

p54nrb contains two RRM (RNA recognition motif) domains, a helix-turn-helix (HTH) domain and a highly basic C-terminal region, see figure 1.5.2.1. Subsequent to the discovery of nucleolar enrichment of p54nrb following UV irradiation we wanted to determine the domain required for relocalisation of the protein. A diagram representing the constructs produced is shown in figure 3.3 (A). GFP-tagged mutants of p54nrb were generated by PCR (Figure 3.3 (B)), finally ligated into a peGFP-C1 vector, and verified by sequencing and restriction digest, positive clones marked are with (*) (Figure 3.3 (C)). GFP-tagged p54nrb mutant constructs were transiently transfected into cells and immunofluorescence microscopy was performed as described previously (2.2.3). In parallel, transfected cells were lysed and subjected to western blotting to confirm the expression of the GFP-tagged constructs produced using an antibody raised against GFP and β-actin was used as a loading control. GFP constructs marked are with (*) (Figure 3.3 (D)).

Fluorescence microscopy analyses revealed that the full-length protein, GFP-p54nrbwt (1-471aa), and the C-terminal deletion mutant, GFP-p54nrbΔCT (1-372aa (Δ373-471)), localise to the nucleus and are excluded from nucleoli behaving like endogenous p54nrb protein. In contrast, GFP-p54nrbΔRRM1&2 (229-471aa (Δ1-228)) also highlights peri-nucleolar sites, which differs to the endogenously expressed p54nrb. Cell nuclei are stained with DAPI and nucleophosmin was used as a nucleolar marker (Figure 3.3 (E)). Following UV irradiation (5 J/m^2), GFP-p54nrbwt (1-471aa), GFP-p54nrbΔCT (1-372aa (Δ373-471)), and GFP-p54nrbΔRRM1&2 (229-471aa (Δ1-228)) are enriched in nucleoli thus behaving similar to endogenous p54nrb (Figure 3.3 (F)).

The transiently transfected GFP-p54nrbΔHTH (1-228aa (Δ229-471)) construct does not behave similarly to endogenous p54nrb in non-irradiated cells since it partially localises in the cytoplasm, and after UV treatment GFP-p54nrbΔHTH (1-228aa (Δ229-471)) does not localise in nucleoli (Figure 3.3 (E) and (F)). To direct the deletion mutant GFP-p54nrbΔHTH (1-228aa (Δ229-471)) into nuclei the nuclear localisation sequence (NLS) of SV40 large T-antigen (PKKKRKVG) was added to this polypeptide. The addition of the NLS to the GFP-p54nrbΔHTH (1-228aa (Δ229-471)) fusion protein efficiently directed the

GFP fusion protein into nuclei (Figure 3.3 (E) and (F)). However, UV irradiation of cells expressing NLS-GFP-p54^{nrb}ΔHTH (1-228aa (Δ229-471)) does not cause the localisation of the NLS fusion protein in nucleoli. To confirm that the transient transfection of GFP-p54^{nrb}ΔHTH (1-228aa (Δ229-471)) was successfully expressing in human cells, a co-transfection of the RFP-tagged human Raf protein was performed as a control experiment. Cell nuclei were stained with DAPI (blue), GFP-p54^{nrb}ΔHTH is shown in green and, RFP-hRAF is shown in red (Figure 3.3 (G)). The data presented is a representative result of three independent experiments.

These findings reveal that amino acids located at the C-terminal end of p54^{nrb} (229-471aa) are crucial for its nucleolar localisation following UV irradiation. Following the deletion of the RNA recognition motif (RRM) domains (1-229aa), p54^{nrb} is sequestered to peri-nucleolar sites, however, its localisation in the nucleolus following UV irradiation is not impaired suggesting that these domains do not play a role in it's localisation. The findings also suggest that amino acids in the helix-turn-helix (HTH) domain of p54^{nrb} are necessary for its localisation to the nucleolus following UVC irradiation.

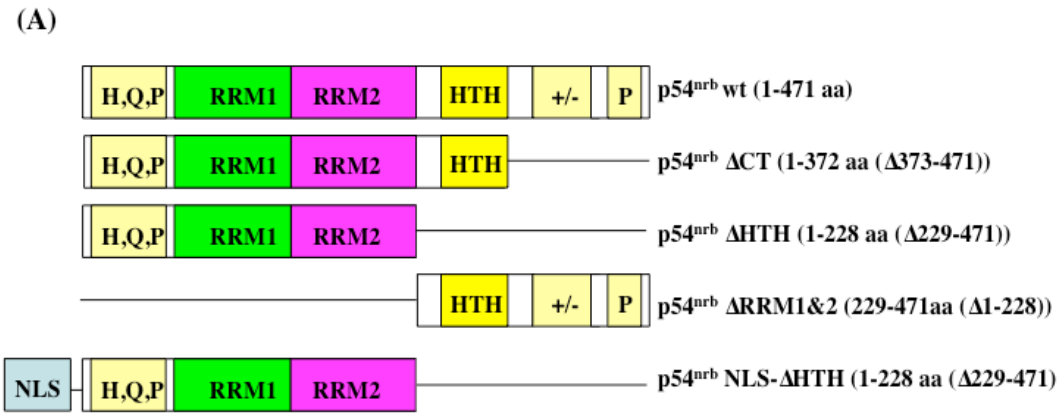

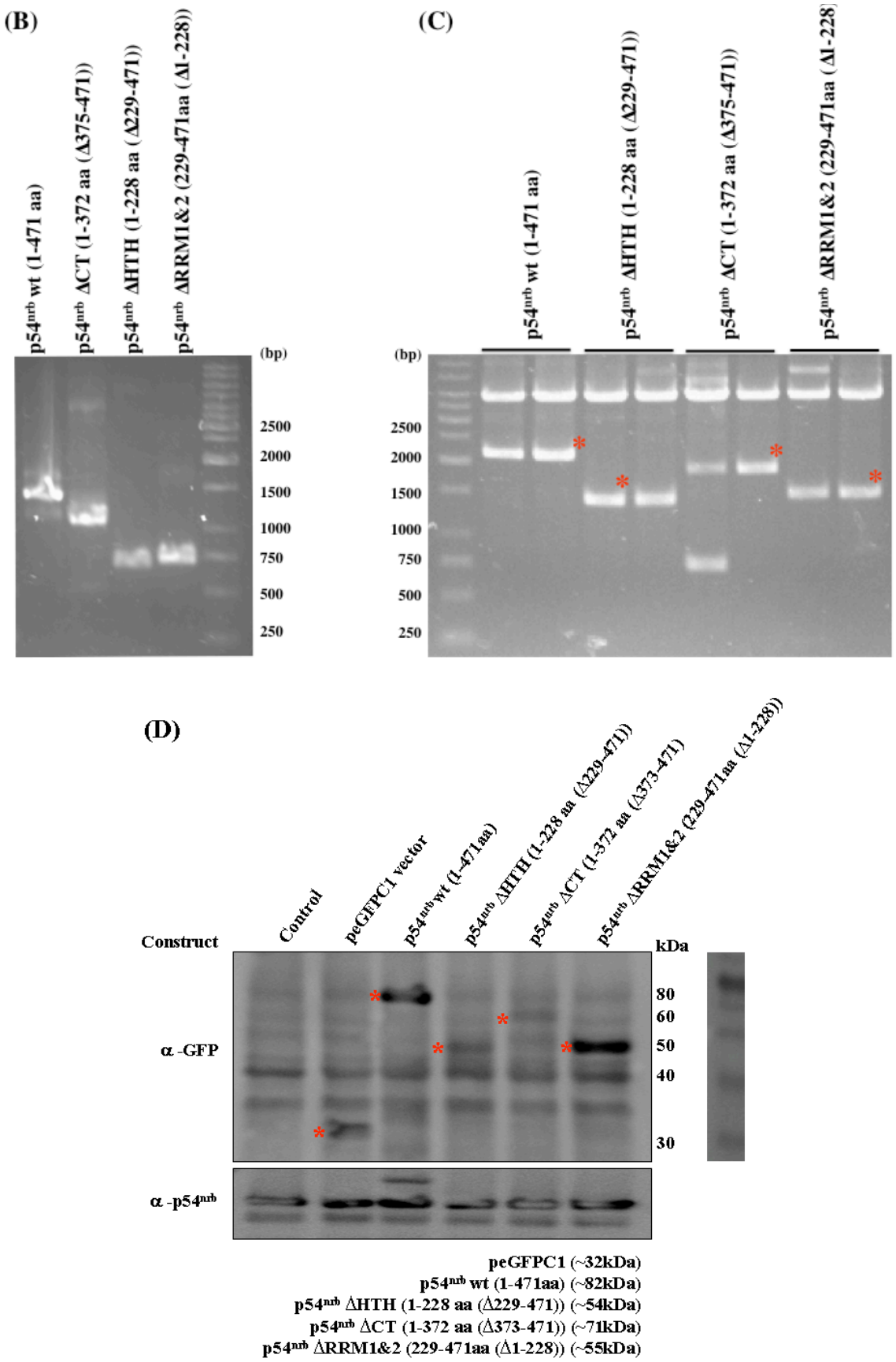
(B)
p54nrb wt (1-471 aa)
p54nrb ΔCT (1-372 aa (Δ375-471))
p54nrb ΔHTH (1-228 aa (Δ229-471))
p54nrb ΔRRM1&2 (229-471aa (Δ1-228))
(bp)
2500
2000
1500
1000
750
500
250
(C)
p54nrb wt (1-471 aa)
p54nrb ΔHTH (1-228 aa (Δ229-471))
p54nrb ΔCT (1-372 aa (Δ375-471))
p54nrb ΔRRM1&2 (229-471aa (Δ1-228
(bp)
2500
2000
1500
1000
750
500
250
(D)
Construct
Control
peGFPC1 vector
p54nrb wt (1-471aa)
p54nrb ΔHTH (1-228 aa (Δ229-471))
p54nrb ΔCT (1-372 aa (Δ373-471)
p54nrb ΔRRM1&2 (229-471aa (Δ1-228))
kDa
80
60
50
40
30
α -GFP
α -p54nrb
peGFPC1 (~32kDa)
p54nrb wt (1-471aa) (~82kDa)
p54nrb ΔHTH (1-228 aa (Δ229-471)) (~54kDa)
p54nrb ΔCT (1-372 aa (Δ373-471)) (~71kDa)
p54nrb ΔRRM1&2 (229-471aa (Δ1-228)) (~55kDa)

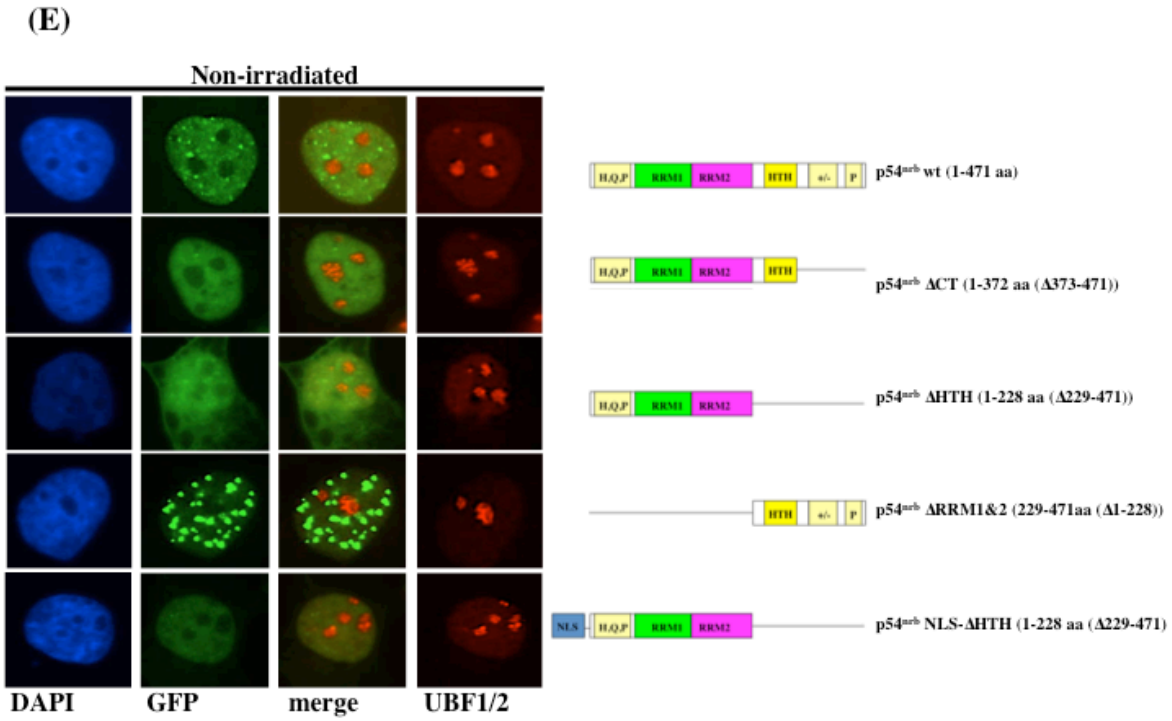
(E)
Non-irradiated
DAPI
GFP
merge
UBF1/2
H,Q,P
RRM1
RRM2
HTH
+/-
P
NLS
p54nrb wt (1-471 aa)
p54nrb ΔCT (1-372 aa (Δ373-471))
p54nrb ΔHTH (1-228 aa (Δ229-471))
p54nrb ΔRRM1&2 (229-471aa (Δ1-228))
p54nrb NLS-ΔHTH (1-228 aa (Δ229-471)

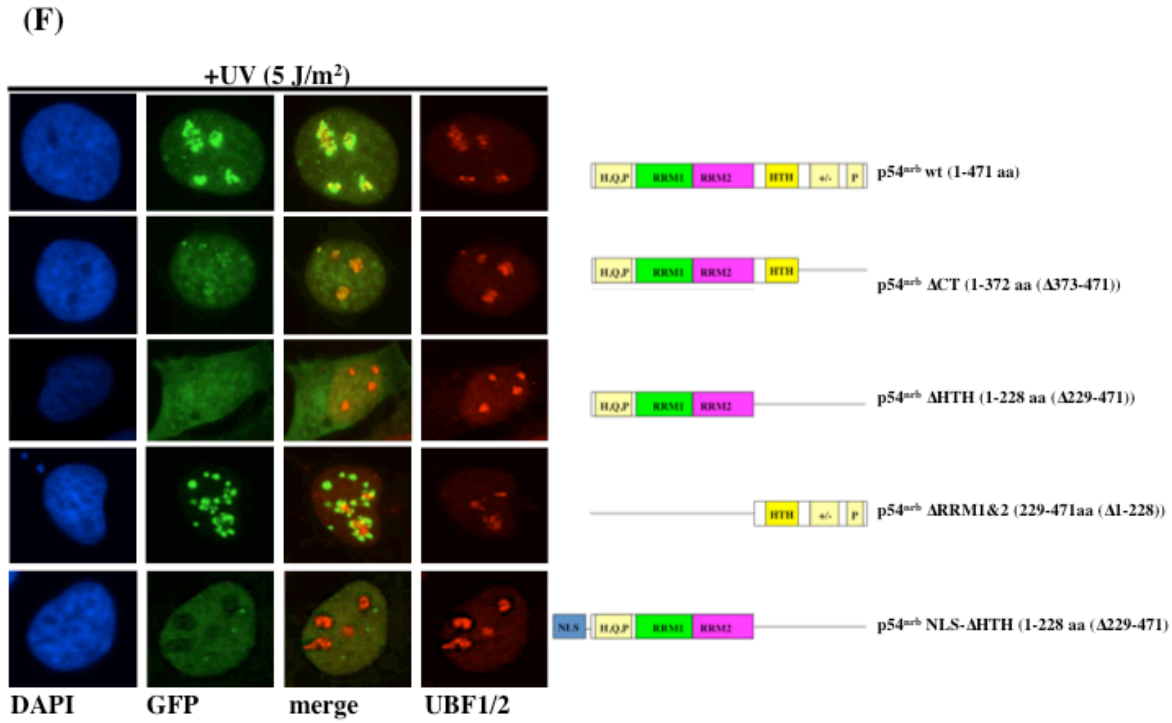
(F)
+UV (5 J/m²)
DAPI
GFP
merge
UBF1/2
H,Q,P
RRM1
RRM2
HTH
+/-
P
NLS
p54nrb wt (1-471 aa)
p54nrb ΔCT (1-372 aa (Δ373-471))
p54nrb ΔHTH (1-228 aa (Δ229-471))
p54nrb ΔRRM1&2 (229-471aa (Δ1-228))
p54nrb NLS-ΔHTH (1-228 aa (Δ229-471)

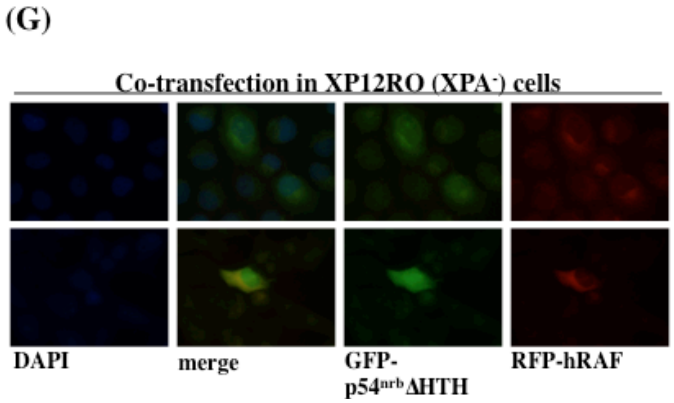

Figure 3.3 The helix-turn-helix domain (C-terminal) of p54^{nrb} is required for its localisation to nucleoli following UV irradiation.
A series of fusion constructs of green fluorescent protein (GFP) with N- and C-terminal domains of p54^{nrb} deleted were constructed (panel **(A)**). The p54^{nrb} protein contains two RRM (RNA recognition motif) domains, a HTH (helix-turn-helix) domain and a basic C-terminal region, see figure 1.5.2.1. GFP-tagged mutants of p54^{nrb} were generated by PCR. (wt) GFP-p54^{nrb}wt, 1-471aa, (~1416bp), (ΔCT). the C-terminal deletion mutant, GFP-p54^{nrb}ΔCT (1-372aa (Δ373-471)), (~1116bp), (ΔHTH), GFP-p54^{nrb}ΔHTH (1-228aa (Δ229-471)) (~687bp), (ΔRRM1&2) GFP-p54^{nrb}ΔRRM1&2 (229-471aa (Δ1-228)) (~729bp) (panel **(B)**). A restriction digest was performed on the positive PCR clones using *Ase*I and *Eco*RI restriction enzymes (panel **(C)**). The expression of the GFP constructs were analysed by western blotting using an antibody against GFP on XP12RO (XPA^{-}) whole cell lysates (panel **(D)**). Positive clones are marked with an asterisk (*) in panels **(C)** and **(D)**. Immunofluorescence data of GFP fusion deletion constructs of p54^{nrb}. XP12RO (XPA^{-}) human cell lines were transiently transfected using FuGENE 6 (Roche) with the indicated GFP-p54^{nrb} constructs and non-irradiated or UV irradiated (5J/m^2). Cells were fixed at 2 h post-UV treatment and cell nuclei were stained with UBF 1/2 (red) and DAPI (blue). GFP-p54^{nrb} constructs are shown in green. The immunofluorescence data of UBF 1/2 and p54^{nrb} were merged and presented in the fourth column highlighted as 'merge'. Fluorescence microscopy was performed using an Olympus IX51 microscope (panels **(E)** and **(F)**). A transient co-transfection of XP12RO (XPA^{-}) cells with RFP-hRaf (1µg DNA) and the GFP- p54^{nrb}ΔHTH (2µg DNA) construct using FuGENE 6 as a control to show the GFP-p54^{nrb}ΔHTH (1-228aa (Δ229-471)) construct was expressing. Cell nuclei were stained with DAPI (blue), GFP- p54^{nrb}ΔHTH is shown in green, and, RFP-hRAF is shown in red. Fluorescence microscopy was performed using an Olympus IX51 microscope (panel **(G)**).

3.4 DNA damage-dependent recruitment of p54^{nrb} to nucleoli is abolished following inhibition of transcription

3.4.1 The degradation of active RNA depletes p54^{nrb} nucleolar localisation following UV irradiation

The findings presented above strongly suggest that p54^{nrb} is enriched in nucleoli following UV irradiation and that it is HTH domain in the C-terminus that is required for the change in localisation of p54^{nrb}. p54^{nrb} protein is known to bind to single- and double-stranded RNA and DNA (Fox et al., 2005). Therefore, it was important to explore whether an interaction with RNA or DNA mediates the recruitment of p54^{nrb} to nucleoli following UV irradiation. Exponentially growing XP12RO (XPA^{-}) cells were grown on coverslips and subjected to UV irradiation (5 J/m^2). At 2 h post-UV, the cells were permeabilised followed by treatment with DNase I (100 U) and RNase A (1 mg/ml) enzymes to catalyse the degradation of DNA and RNA respectively (see 2.2.5). Cell nuclei are stained with DAPI and nucleophosmin was used as a nucleolar marker (Figure 3.4.1 (A)). The data shown is a representative result of three independent experiments.

In the mock- and triton-treated cells, p54^{nrb} protein is enriched in the nucleolus following UV irradiation. In the presence of DNase I, the localisation of p54^{nrb} to the nucleolus is not disrupted, indicating that DNA does not mediate the protein's association with the nucleolus. However, in the presence of RNase A, following UV irradiation (5 J/m^2), the nucleolar integrity of p54^{nrb} is disrupted as shown by the disrupted nucleolar pattern indicating that ongoing rDNA transcription is required for this response to occur. As a positive control for RNase A treatment, Fibrillarin and UBF 1/2 served as markers to prove that the RNA was successfully disrupted (Figure 3.4.1 (B) and (C)) since fibrillarin is a component of several ribonucleoproteins and is known to be associated with both rRNA and rDNA (Jamison et al., 2010). No positive control was used for DNase I treatment, however, as a control RPA or PCNA could be used as it interacts with DNA.

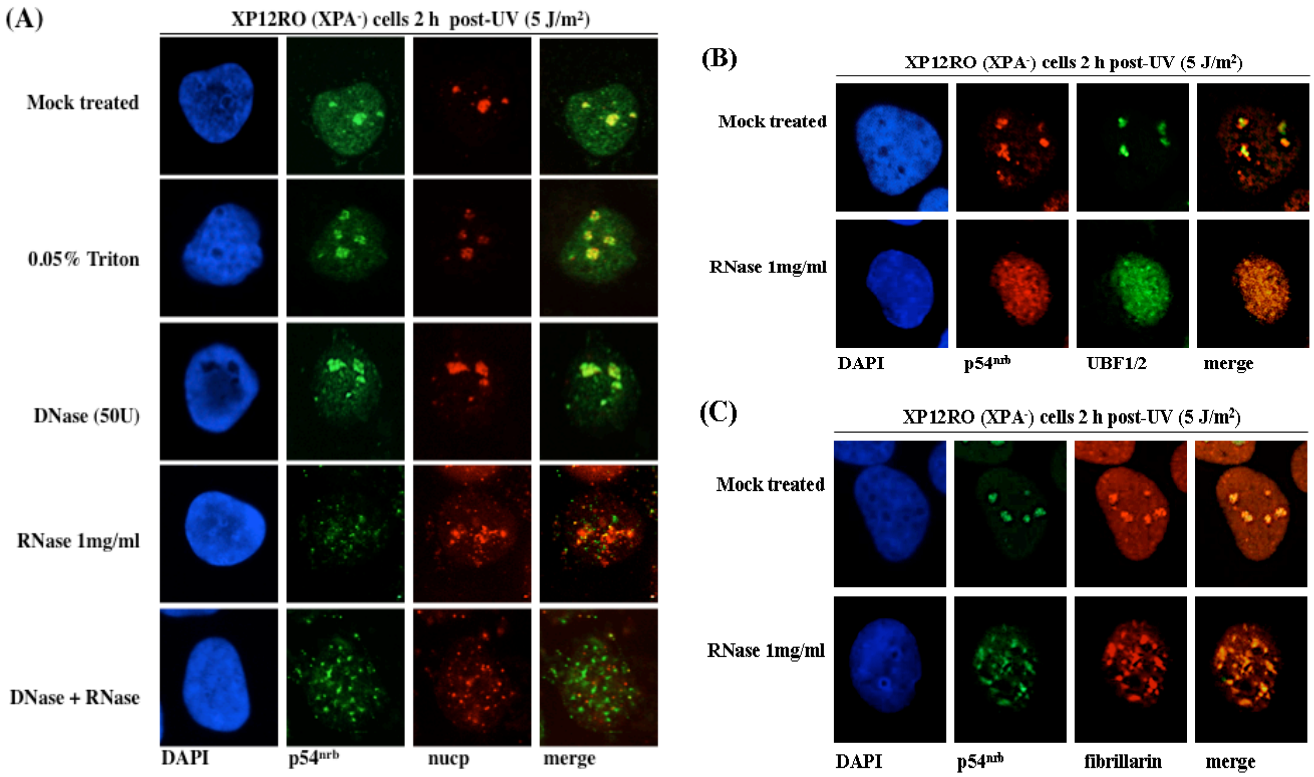

Figure 3.4.1 The presence of RNA is required for UV-induced nucleolar localisation of p54nrb. Exponentially growing XP12RO (XPA-) cells were grown on coverslips and subjected to UV irradiation (5 J/m^2). 2 h post-UV, the cells were permeabilised followed by treatment with DNase I and RNase A (panel **(A)**). Cells were then probed with p54nrb antibody followed by cy2-conjugated secondary mouse antibody (green colour). Nucleoli were stained with a nucleophosmin (Nucp) antibody followed by cy3-conjugated secondary rabbit antibody (red colour). Cell nuclei were stained with DAPI (blue). The immunofluorescence data of nucleophosmin and p54nrb were merged and presented in the fourth column highlighted as 'merge'. Immunofluorescence microscopy was performed using an Olympus IX51 microscope. As a control for the RNase A treatment XP12RO (XPA-) cells were also stained with a UBF 1/2 followed by a cy2-conjugated secondary sheep antibody (green; p54nrb was visualised finally with a cy3-conjugated secondary mouse antibody (red)). The immunofluorescence data of UBF 1/2 and p54nrb were merged and presented in the fourth column highlighted as 'merge' (panel **(B)**), and Fibrillarin followed by a cy3-conjugated secondary mouse antibody (red; p54nrb was again visualised finally with a cy2-conjugated secondary mouse antibody (green)). The immunofluorescence data of Fibrillarin and p54nrb were merged and presented in the fourth column highlighted as 'merge' (panel **(C)**).

3.4.2 Active transcription is required for p54^{nrb} accumulation in the nucleolus following UV irradiation

p54^{nrb} is a multi-functional nuclear protein that participates in the regulation of transcription (Shav-Tal and Zipori, 2002). As described previously, p54^{nrb} contains two RNA recognition motif (RRM) domains that carry out its function in RNA-processing and transport. Previous findings revealed that the deletion of the RRM domains (RRM1&2 1-228aa) causes the sequestration of p54^{nrb} to peri-nucleolar sites, however, its localisation in nucleoli following UV irradiation is not impaired suggesting that these domains do not play a critical role in the latter. In contrast, the recruitment of p54^{nrb} to nucleoli following UV irradiation is disrupted by RNase A treatment, indicating that the presence of RNA is required for p54^{nrb} nucleolar sequestration. Thus, these findings raised the question whether active transcription is required for the nucleolar enrichment of p54^{nrb} following UV irradiation.

Asynchronous XP12RO (XPA^{-}) and XP12RO clone 5 (XPA^{+}) cells were treated with Actinomycin-D (either 0.1 μg/ml or 1 μg/ml) and α-amanitin (30 μg/ml) followed by UV irradiation (5 J/m^2 of UVC) and fixed 2 h post-UV. The low concentration of Actinomycin-D results in the inhibition of RNA polymerase I alone whereas the high concentration inhibits both RNA polymerase I and II (Shav-Tal et al., 2005). α-amanitin specifically inhibits RNA polymerase II. The transcription factor UBF 1/2 was used as a positive control for inactivation of RNA polymerase II by Actinomycin-D as UBF 1/2 localises to nucleolar caps following transcriptional inhibition (Shav-Tal et al., 2005). Nucleolar caps are highlighted in Figure 3.4.2 (E) with white arrows. The data presented is a representative of three independent experiments.

In non-irradiated, mock treated, XP12RO (XPA^{-}) and XP12RO clone 5 (XPA^{+}) cells, p54^{nrb} is evenly distributed throughout the nucleoplasm **(**Figure 3.4.2 (A) and (C)). In the UV irradiated, mock treated cells, p54^{nrb} is enriched in the nucleoli XP12RO (XPA^{-}) cells following UV irradiation (Figure 3.4.2 (B) and (D)). Actinomycin-D treatment, at either a low or high concentration, recruits p54^{nrb} to nucleolar caps (Figure 3.4.2 (B) and (D)). At a high concentration of Actinomycin-D, the localisation of p54^{nrb} to nucleolar caps is more evident relative to the low concentration, indicating that this response is concentration-dependent and that complete inhibition of RNA synthesis is required for this relocalisation

to occur. To provide evidence whether this phenomenon is specific for RNA polymerase I or II, RNA polymerase II was inhibited with α-amanitin. After the addition of α-amanitin to cells, p54^{nrb} localises to areas surrounding the nucleolus (Figure 3.4.2 (B) and (D)). This redistribution of p54^{nrb} to the surrounding areas of nucleoli following drug treatment happens independently of UV irradiation and in both cell lines, indicating that this phenomenon is a global response. A reciprocal experiment was carried out whereby XP12RO (XPA^{-}) cells were UV irradiated at 5 J/m^2 and at 2 h post-UV, Actinomycin-D was added to the cells. In the UV irradiated, mock-treated cells, p54^{nrb} localises to nucleoli, however following drug treatment p54^{nrb} can be seen at nucleolar caps (data not shown). We conclude that the presence of p54^{nrb} protein in the nucleolus following UV irradiation is sensitive to transcriptional inhibition and RNase treatment, suggesting that ribonucleic acids play a role in its structural integrity in the nucleolus coinciding with work from (Fox et al., 2002).

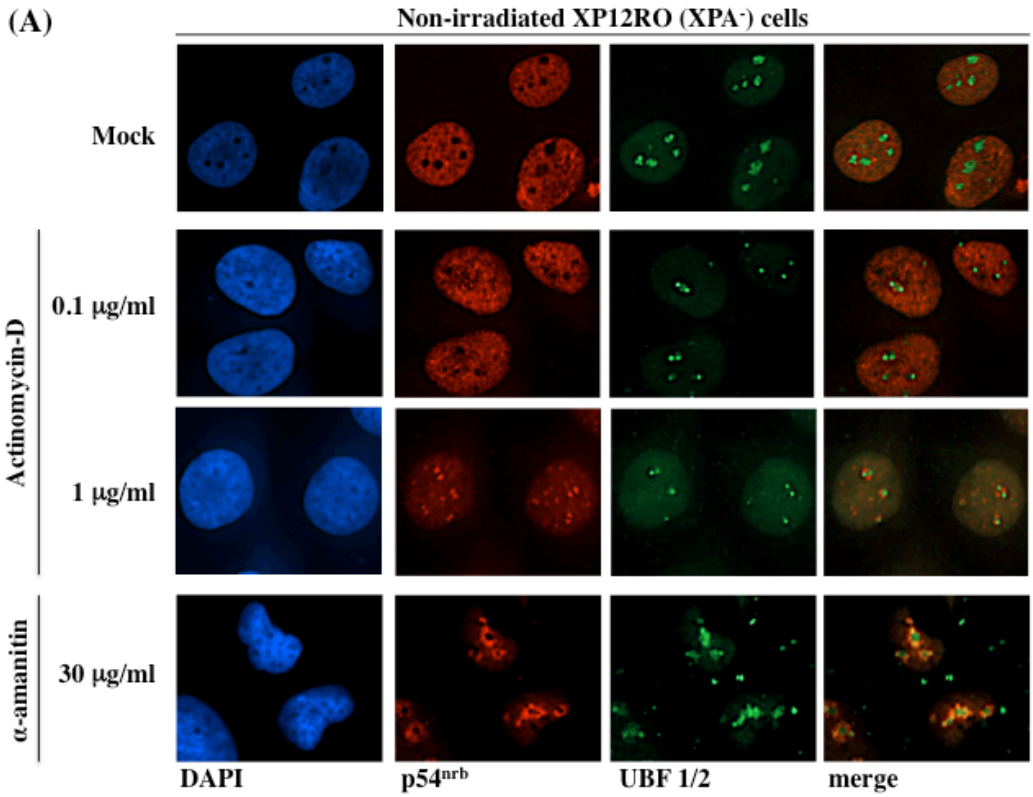

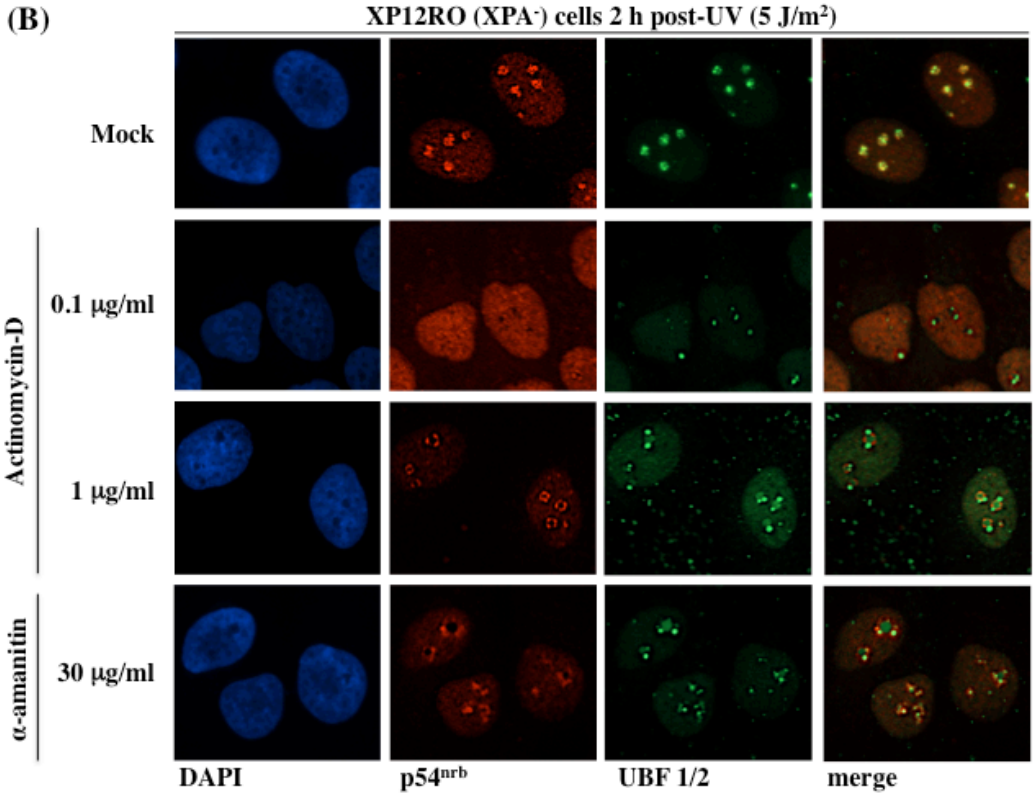
(B)
XP12RO (XPA-) cells 2 h post-UV (5 J/m2)
Mock
Actinomycin-D
0.1 µg/ml
1 µg/ml
α-amanitin
30 µg/ml
DAPI
p54nrb
UBF 1/2
merge

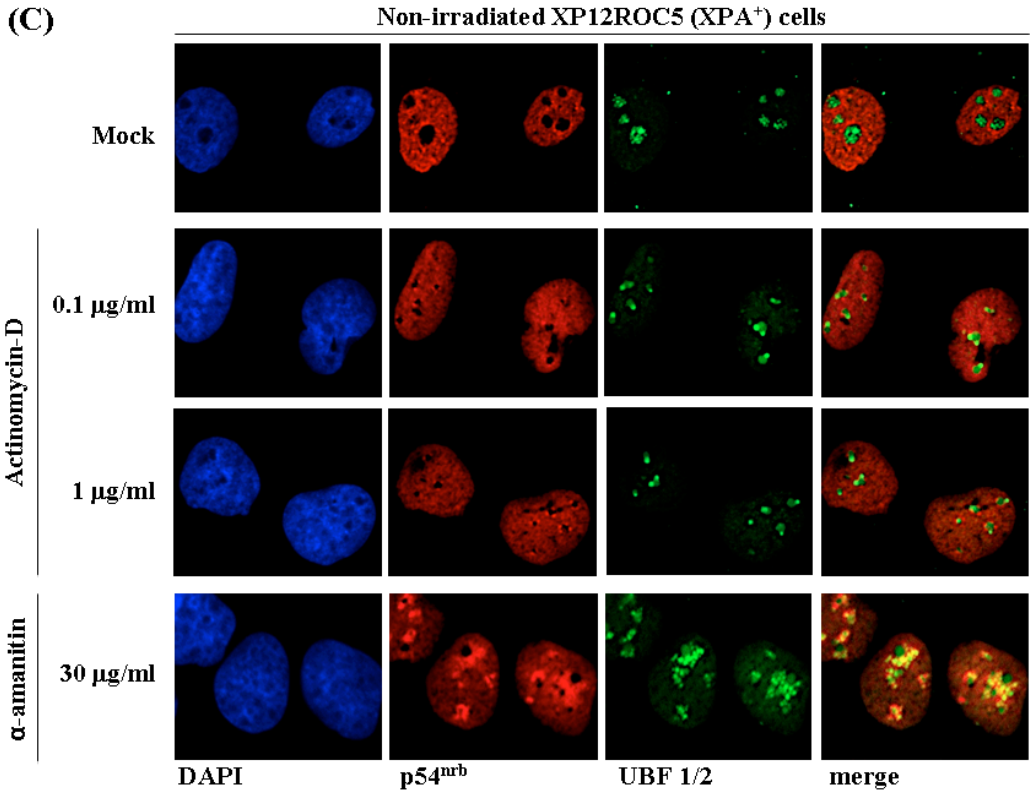
(C)
Non-irradiated XP12ROC5 (XPA+) cells
Mock
Actinomycin-D
0.1 µg/ml
1 µg/ml
α-amanitin
30 µg/ml
DAPI
p54nrb
UBF 1/2
merge

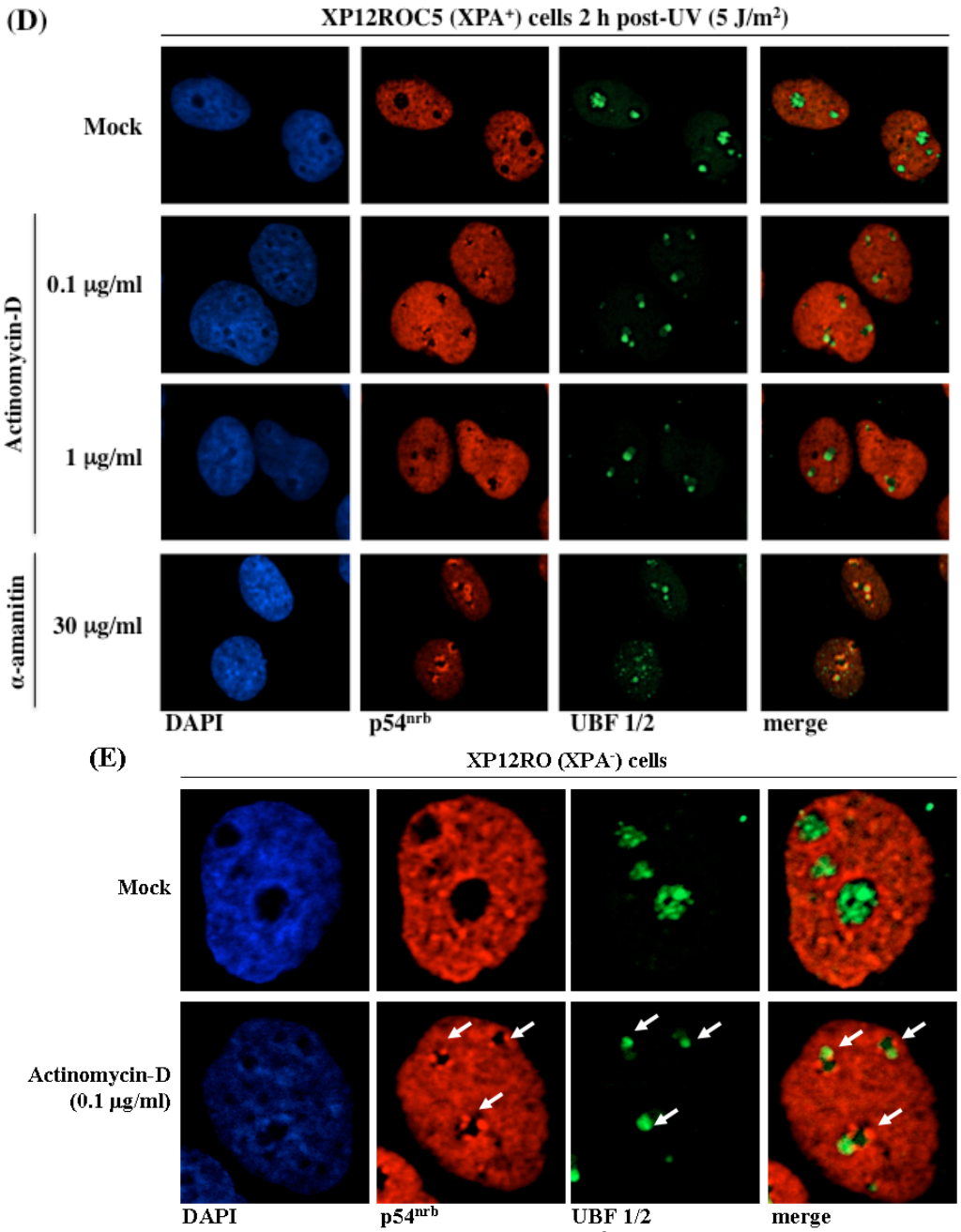

Figure 3.4.2 Inhibiting transcription abolishes p54nrb recruitment to nucleoli after UV irradiation.

Asynchronous XP12RO (XPA^-) cells (panels **(A)** and **(B)**) and XP12RO C5 (XPA^+) cells (panels **(C)** and **(D)**) were pre-treated with 30 µg/ml of α-amanitin, 0.1 µg/ml or 1 µg/ml of Actinomycin-D followed by UV irradiation (5 J/m^2 of UVC) and fixed 2 h post-UV. Cells were then probed with p54nrb antibody followed by cy3-conjugated secondary mouse antibody (red). UBF 1/2 antibody followed by cy2-conjugated secondary sheep antibody (green) was used to visualise transcription machinery. The immunofluorescence data of UBF 1/2 and p54nrb were merged and presented in the fourth column highlighted as 'merge'. Cell nuclei were stained with DAPI (blue). Immunofluorescence was performed using an Olympus IX51 microscope. Enlarged image and indicators (white arrows) showing an example of UBF 1/2 and p54nrb localisation to perinucleolar caps (panel **(E)**).

3.5 UV-induced DNA damage shows differential localisation of p54^{nrb}

Recent evidence suggests that p54^{nrb} is involved in the DNA damage response. p54^{nrb} in a complex with PSF is involved in DNA double-strand break (DSB) repair via non-homologous end joining (NHEJ) and the homologous recombination (HR) pathway (Bladen et al., 2005; Li et al., 2009). More recently, Kuhnert et al showed that p54^{nrb} and PSF migrate to sites of DNA damage induced by a UVA laser microbeam (Kuhnert et al., 2012). From these studies it could be hypothesised that p54^{nrb} may be recruited to sites of DNA damage following UVC irradiation.

3.5.1 p54^{nrb} does not associate with locally induced sites of DNA damage

To determine whether p54^{nrb} is recruited to sites of DNA damage, exponentially growing XP12RO (XPA^{-}) and XP12RO clone 5 (XPA^{+}) cells were grown on glass coverslips and UV irradiated after being covered with isopore polycarbonate 5.0 μm membrane filters. Green and Almouzni reported that the millipore filter absorbs ~98% of the applied dose and that the average dose applied to the cells is ~2 J/m^2 (Green and Almouzni, 2003). Antibodies that detect damage foci, specifically against thymine dimers, γH2AX, XPA and RPA foci, then detected the damage caused by UV irradiation. Localised damage was detected 2 h post-UV irradiation as seen in (Figure 3.5.1 (A), (B) and (C)), however p54^{nrb} remains evenly distributed throughout the nucleus. The data are a representative result of three independent experiments. We conclude that p54^{nrb} does not localise to sites of locally irradiated DNA damage under these experimental conditions.

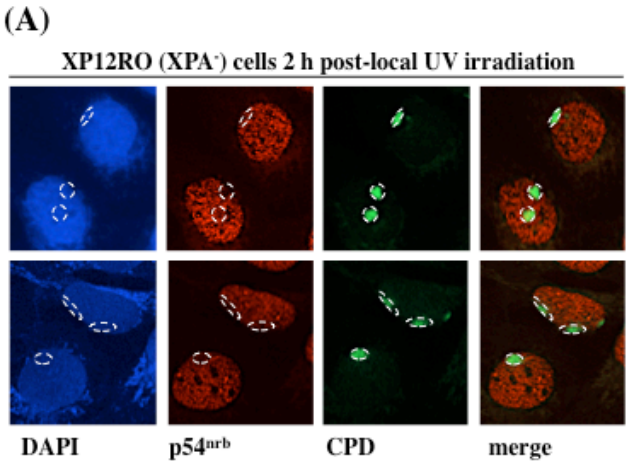

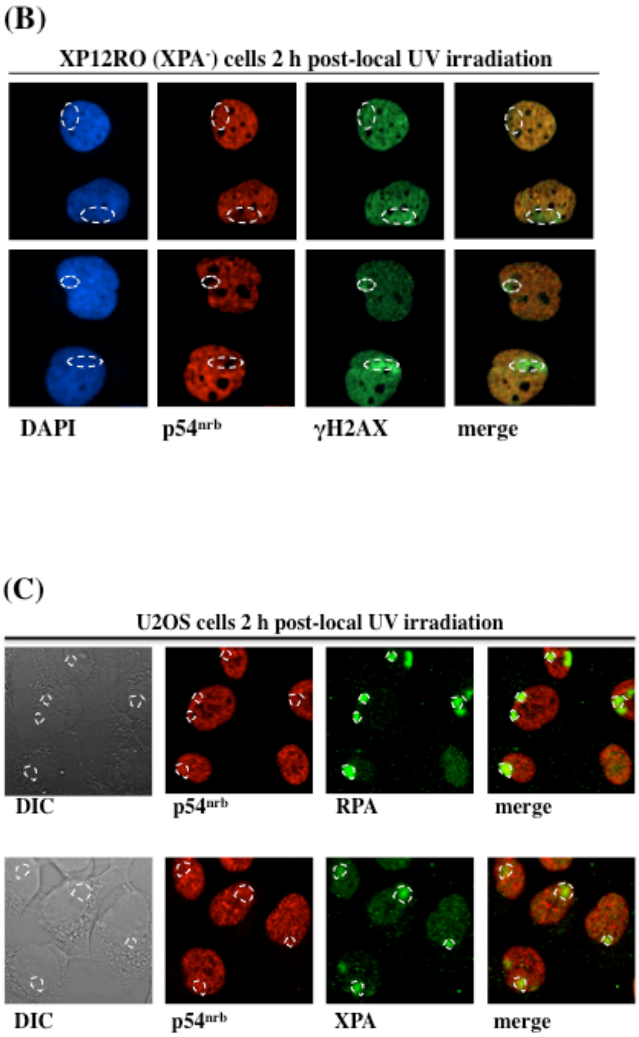

Figure 3.5.1 Locally induced DNA damage.
Exponentially growing XP12RO (XPA$^-$) or U2OS cells were grown on glass coverslips and individually covered with a piece of isopore polycarbonate 5.0 μm membrane filter (Millipore). The cells were irradiated (100 J/m^2) and fixed for analysis 2 h post-irradiation. Cells were then probed with a p54^{nrb} specific antibody followed by cy3-conjugated secondary rabbit antibody (red). The area of damage was detected in parallel by antibodies against CPD (green) (XP12RO (XPA$^-$) cells in panel **(A)**), γH2AX (green) (XP12RO (XPA$^-$) cells in panel **(B)**) and antibodies against XPA and RPA (both green) in panel (C) using U2OS cells as indicated. Cell nuclei of XP12RO (XPA$^-$) cells were stained with DAPI (blue) and U2OS cells nuclei are shown in DIC image. The immunofluorescence data of the various antibodies with p54^{nrb} were merged and presented in the fourth column highlighted as 'merge'. Immunofluorescence was performed using an Olympus IX51 microscope.

3.5.2 p54^{nrb} does not co-localise with laser-induced DNA damage foci

We have shown that p54^{nrb} localises to the nucleolus following UVC irradiation and that p54^{nrb} does not localise to sites of locally irradiated DNA damage using micropore filters and the experimental conditions we have used. Therefore, we wanted to determine whether specific cellular regions of the cell, particularly nucleoli, needed to be irradiated to cause p54^{nrb} to localise to nucleoli.

Exponentially growing XP12RO (XPA^{-}) cells were seeded on glass bottom 35 mm dishes (MatTek) and allowed to recover for 24 h. The cells were then irradiated with a 400 nm laser at 37°C on an integrated microscope system (DeltaVision). Using this technique, specific areas of the cells were irradiated, incubated at 37ºC and then fixed for analysis 2 h post-irradiation followed by immunofluorescence staining for p54^{nrb}, and γH2AX (sites of DNA damage). Using this technique, specific areas of the cell were irradiated with a laser beam; the irradiated areas of the cells are visible with γH2AX staining; however, p54^{nrb} remains evenly distributed throughout the nucleus (Figure 3.5.2). The data are a representative result of three independent experiments.

At the time this study was carried out various publications showed p54^{nrb} localising to site of DNA damage after UV laser induced DNA damage (Ha et al., 2011; Krietsch et al., 2012; Kuhnert et al., 2012; Salton et al., 2010). All of these studies induced localised DNA damage by laser micro irradiation resulting in the formation of DSB's and found that p54^{nrb} localised to these DSB induced foci. The reports used live cell imaging and fluorescently tagged p54^{nrb} to show the protein localised to these damaged induced foci and observed the same retention time of p54^{nrb} at these sites of DNA damage as early as 2 seconds and declines again after 2 – 10 min. Following these studies we irradiated XP12RO (XPA^{-}) cells at 5 J/m^2 and also locally irradiated XP12RO (XPA^{-}) cells using the micropore filter as described previously. The cells were fixed at 1 min post UV and sites of UV induced DNA damage were detected by XPA and CPD antibodies. However, p54^{nrb} remained evenly distributed in the nucleus at this time point and under these experimental conditions (data not shown). It would be interesting to perform an experiment whereby the localisation of p54^{nrb} to sites of DBSs is observed using the laser irradiation system used in this thesis (to successfully reproduce what is observed in other reports).

We conclude that p54^{nrb} does not associate with sites of UV damage induced by a laser at a time point when it usually is recruited to nucleoli after DNA damage. Moreover, specific areas of the cell, particularly the nucleolus, do not need to be irradiated for p54^{nrb} nucleolar localisation to occur. Although p54^{nrb} may not be recruited directly to sites of DNA damage under these experimental conditions, it does localise to the nucleolus after UV irradiation which suggests it may not play a direct role in the detection of sites of DNA damage but may help in the recruitment of other factors to sites of DNA damage or perhaps partake in the signalling of other DNA damage factors following UV irradiation.

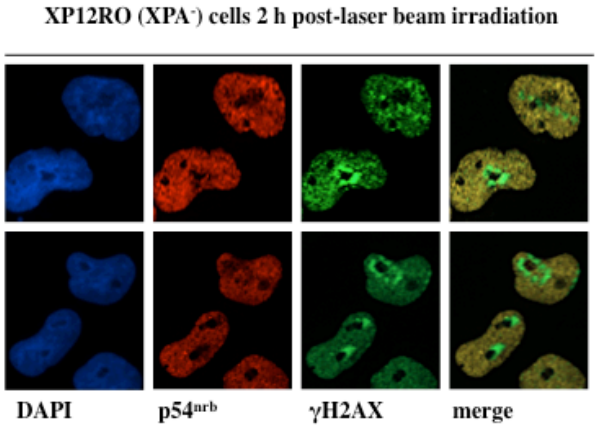

Figure 3.5.2 Laser-induced DNA damage.
Exponentially growing XP12RO (XPA$^-$) cells were seeded on glass bottom 35mm dishes (MatTek) and were allowed to recover at 37ºC for 24 h. The cells were then irradiated with a 400 nm laser at 37°C on an integrated microscope system (DeltaVision). The cells were allowed recover at 37ºC, before they were fixed for analysis 2 h post-irradiation. Cells were then probed with p54^{nrb} antibody followed by cy3-conjugated secondary rabbit antibody (red). The area of damage was then detected by antibodies detecting damaged-induced γ-H2AX foci (green). The immunofluorescence data of γH2AX and p54^{nrb} were merged and presented in the fourth column highlighted as 'merge'. Immunofluorescence was performed using an Olympus IX51 microscope.

3.6 p54^{nrb} localisation to the nucleolus is independent of S-phase

As previously shown, in XP12RO (XPA^{-}) cells p54^{nrb} begins to localise to the nucleolus at 2 h post 2.5 J/m^2 of UV irradiation. The recruitment of p54^{nrb} to nucleoli happens at an earlier time point (30 min) following higher doses of UV irradiation (5 and 10 J/m^2). p54^{nrb} persists to localise in nucleoli up until 8 h post UV irradiation (Figure 3.2.1 (B), (C) and (D)). In the XP12RO clone 5 (XPA^{+}) cells p54^{nrb} begins to target nucleoli at a later time-point and a higher UV dose (10 J/m^2) relative to the XP12RO (XPA^{-}) cells (Figure 3.2.1 (H)) and this localisation is observed in only a few cells (~5 out of 20 cells observed at 10 J/m^2). It was concluded that p54^{nrb} localisation to nucleoli is UV-dependent; next we wanted to determine whether cells were required to be in S-phase for this recruitment.

To investigate this hypothesis XP12RO (XPA^{-}) cells were subjected to UV irradiation followed by EdU labelling. EdU labelling was performed using a Click-iT^{TM} EdU imaging kit (Invitrogen) as discussed in section 2.10. EdU is a thymidine analogue that enables us to identify the cells that are in, or going in to, S-phase. Cells that are positive for EdU are clearly visible (cells shown in green) whereas cells that show p54^{nrb} nucleolar localisation are visible in red (Figure 3.6 (A)). The percentage of cells with positive staining for EdU was determined (49 %) followed by the percentage of cells showing p54^{nrb} in nucleoli (22 %). The percentage of cells that were positive for EdU labelling and positive for p54^{nrb} in nucleoli was 10%. The percentage of cells that were negative for EdU labelling and positive for p54^{nrb} in nucleoli was 12%. There seems to be no correlation between these two events as presented by the data suggesting that the recruitment of p54^{nrb} to nucleoli in independent of S-phase (Figure 3.6 (B)). These data are representative of three independent experiments.

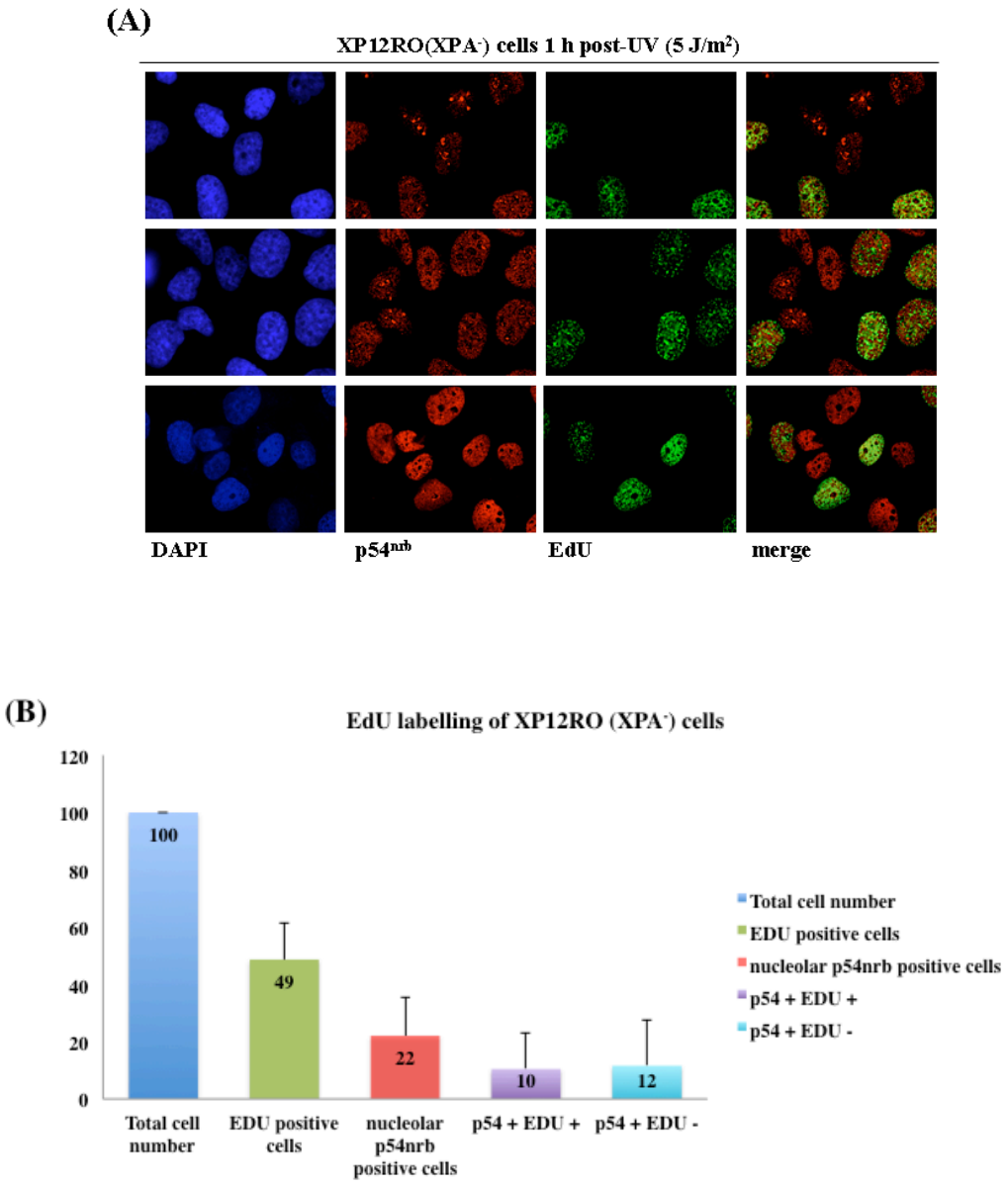

Figure 3.6 EdU labelled XP12RO (XPA$^-$) cells.
Asynchronous XP12RO (XPA$^-$) cells were subjected to UV irradiation (5 J/m^2) followed by EdU labelling and fixed 2 h post-irradiation (panel **(A)**). EdU labelling was performed using a Click-iT^{TM} EdU imaging kit (Invitrogen). Cells were then probed with p54^{nrb} antibody followed by cy3-conjugated secondary rabbit antibody (red). EdU labelled cells are visible in green. Cell nuclei were stained with DAPI (blue). The immunofluorescence data of EdU and p54^{nrb} were merged and presented in the fourth column highlighted as 'merge'. Immunofluorescence was performed using an Olympus IX51 microscope. A histogram representing the results obtained by immunofluorescence microscopy. Data represents the mean of three independent experiments. Error bar represent one standard deviation (panel **(B)**).

3.7 Elucidating DNA damage-dependent signalling factors essential for the localisation of p54^{nrb} protein to nucleoli following UV irradiation

3.7.1 p54^{nrb} recruitment to nucleoli is sensitive to inhibitors that target proteins of the phosphatidylinositol 3-kinase-like protein (PIKKs) family

We have demonstrated that p54^{nrb} localises to nucleoli following UV irradiation (Figure 3.2.1). We have also demonstrated that p54^{nrb} does not localise to locally induced sites of DNA damage (Figure 3.5.1). We hypothesised that the recruitment of p54^{nrb} to nucleoli is regulated by DNA damage-dependent signalling factors.

In mammalian cells, the phosphatidylinositol 3-kinase-like kinases (PIKKs) including DNA-dependent protein kinase (DNA-PK), Ataxia-telangiectasia-mutated protein (ATM) and Ataxia-telangiectasia and Rad3-related protein (ATR) play a key role in response to DNA damage (Ciccia and Elledge, 2010). More recently, Elledge and his lab identified new substrates of ATM and ATR by performing peptide IPs with phophotyrosine antibodies and mass spectrometry to identify new substrates. ATM and ATR share substrate specificity, recognising Ser-Gln (SQ) and Thr-Gln (TQ) motifs and they discovered a vast network of over 700 human and mouse proteins phosphorylated in response to DNA damage (Matsuoka et al., 2007). Although p54^{nrb} was not present in their novel data, it was investigated if p54^{nrb} was a possible substrate of these PIK kinases; this was done by using various databates such as NCBI, STRING, bioGRID and ConsensusPathDB however, no link was identified between p54^{nrb} and these PIK kinases.

To address our hypothesis, human cells were grown on coverslips and treated with Caffeine and Wortmannin followed by UV irradiation (5 J/m^2). Caffeine inhibits PIK kinase activity; it has been shown that Caffeine inhibits ATM and ATR at a concentration of 3 – 10 mM (Sarkaria et al., 1999). Wortmannin inhibits PIK kinase activity but it is more specific to ATM and DNA-PK, it has been shown that Wortmannin at a concentration of 20 μM efficiently inhibits ATM and DNA-PK, whereas ATR is only partially affected at this concentration ((Broderick et al., 2012; Cruet-Hennequart et al., 2008; Sarkaria et al., 1998).

Asynchronous XP12RO (XPA$^-$) cells were treated with Caffeine (2 mM or 5 mM) and Wortmannin (10 μM or 20 μM) 1 h prior to UV irradiation (5 J/m^2 of UVC) and fixed 2 h post-UV. In non-irradiated, mock-treated XP12RO (XPA$^-$) cells p54^{nrb} is evenly distributed throughout the nucleus (Figure 3.7.1 (A) and (C)); mock-treated is used in this section and

the following sections to address the addition of inhibitors. In UV irradiated, mock-treated cells, p54^{nrb} is enriched in nucleoli after UV irradiation (Figure 3.7.1 (B) and (D)). However, following Caffeine treatment, in UV irradiated cells, the localisation of p54^{nrb} in nucleoli is visibly reduced (Figure 3.7.1 (B)). At low inhibitor concentrations, the number of cells with nucleolar p54^{nrb} is reduced to ~70% of cells and this number is reduced nearly two-fold at a higher concentration of Caffeine to ~35% of cells, indicating that this recruitment of p54^{nrb} is inhibitor concentration-dependent, see figure 3.7.1 (E). Following Wortmannin treatment, at either a low or high concentration in UV irradiated cells, the localisation of p54^{nrb} to the nucleolus is also visibly reduced (Figure 3.7.1 (D). At a low concentration of Wortmannin the number of cells with nucleolar p54^{nrb} is reduced to ~40% of cells and this number is reduced nearly two-fold at the higher concentration to ~20% of cells, indicating that this localisation is also inhibitor concentration dependent, see figure 3.7.1 (E). The complete abrogation of p54^{nrb} translocation to the nucleolus following PIK kinase inhibitor treatment suggests that p54^{nrb} requires active PIK kinase activity to perform its role in the nucleolus following UV irradiation and that p54^{nrb} is a downstream factor of these signalling factors. The data presented are a representative result of three independent experiments.

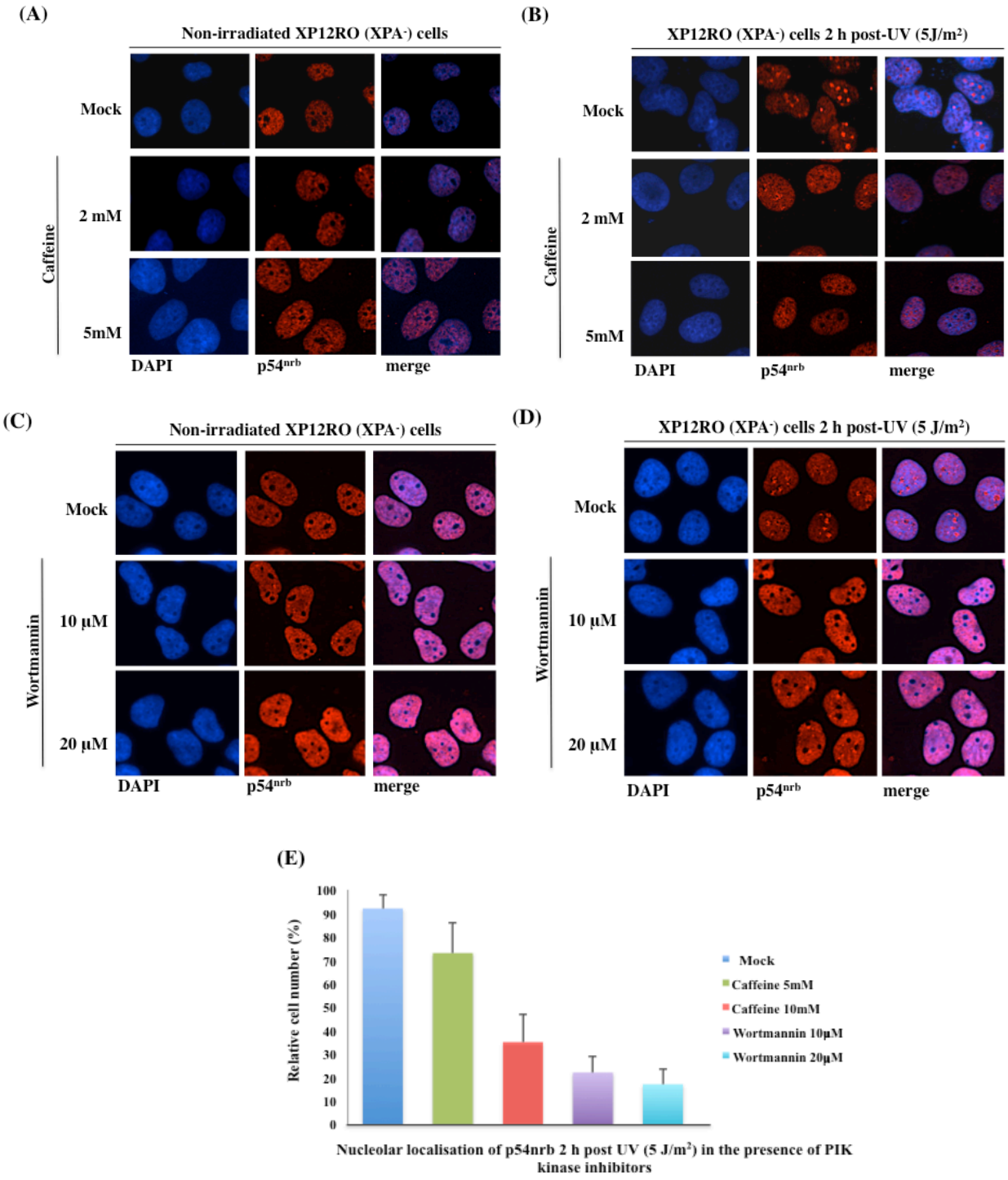

Figure 3.7.1 PIK kinase inhibitors and p54nrb nucleolar localisation.
Exponentially growing XP12RO (XPA-) cells were grown on coverslips and treated with two concentrations of Caffeine (2 mM or 5mM) and two concentrations of Wortmannin (10 µM or 20 µM). XP12RO (XPA-) cells were then either non-irradiated (panels **(A)** and **(C)**) or UV irradiated (5 J/m2) (panels **(B)** and **(D)**). The non-irradiated cells were exposed to the drugs in parallel to the UV irradiated cells to investigate the influence of these drugs on the localisation of p54nrb to nucleoli (panels **(A)** and **(C)**). The cells were fixed 2 h post UV irradiation. Cells were then probed with a

rabbit anti-p54^{nrb} antibody followed by cy3-conjugated secondary rabbit antibody (red). Cell nuclei were stained with DAPI (blue). The immunofluorescence data of DAPI and p54^{nrb} were merged and presented in the third column highlighted as 'merge'. Immunofluorescence was performed using an Olympus IX51 microscope. A histogram representing the results obtained by immunofluorescence microscopy. Results represent the mean of three independent experiments. Error bar show the standard deviation (panel **(E)**).

3.7.2 p54nrb recruitment to nucleoli is regulated by proteins of the phosphatidylinositol 3-kinase-like protein (PIKKs) family

The findings shown previously suggest that p54nrb localises to the nucleolus following UV irradiation (Figure 3.2.1) and that p54nrb is not recruited to locally induced sites of DNA damage (Figure 3.5.1). The PIK kinases ATM, ATR and DNA-PK play a key role in response to DNA damage (Ciccia and Elledge, 2010). We hypothesised that the recruitment of p54nrb to the nucleolus is regulated by DNA damage-dependent signalling factors. Following the discovery that the inhibition of members of the PIKK family reduced the enrichment of p54nrb in nucleoli, we wanted to investigate whether these signalling factors specifically played a role in the nucleolar enrichment of p54nrb. To elucidate the role of these kinases, exponentially growing cells were grown on coverslips and subjected to treatment with specific PIK kinase inhibitors for 1 h followed by UV irradiation (5 J/m^2). The ATM inhibitor (KU-55933) and DNA-PK inhibitor (NU7441) were used at a concentration of 10 μM, the IC_{50} values for inhibition of ATR kinase activity by KU-55933 and NU7441 are greater than 100 μM, so ATR activity should not be inhibited under the conditions used (Hickson et al., 2004; Veuger et al., 2003). The ATR inhibitor (compound 3, ETP-46464 (Toledo et al., 2011)) was tested at various concentrations, (data not shown) however we used the ATRi at a concentration of 10 μM in all experiments shown as it is at this concentration we observed the most significant changes in p54nrb localisation.

Asynchronous XP12RO (XPA$^-$) cells were treated with the specific ATRi, ATMi and DNA-PKi for 1 h followed by UV irradiation (5 J/m^2 of UVC) and fixed 2 h post-UV irradiation. In non-irradiated, mock- and drug-treated XP12RO (XPA$^-$) cells, p54nrb is evenly distributed throughout the nucleus (Figure 3.7.2.1 (A)). In UV irradiated, mock-treated cells, p54nrb is enriched in nucleoli following damage (Figure 3.7.2.1 (B)). The inhibitors ATMi and DNA-PKi, either together or separately, do not interfere with the recruitment of p54nrb to nucleoli after UV irradiation, as the same numbers of p54nrb enriched nucleoli were determined as represented by the histogram (~85%), figure 3.7.2.1 (D). In contrast, ATRi treatment inhibited the recruitment of p54nrb to nucleoli but an enrichment of p54nrb in the periphery of nucleoli was observed after UV irradiation, ~85% of cells showed perinucleolar localisation as determined by figure 3.7.2.1 (B) and (E). See figure 3.7.2.1 (D) for enlarged images. Treating cells with both DNA-PKi and ATRi

combined together showed similar results to that of treating cells with ATRi on its own, ~85-90% of cells showed perinucleolar localisation, see figure 3.7.2.1 (E). In contrast, treating cells with both ATMi and ATRi combined yielded that the localisation of p54^{nrb} is comparable to that of untreated cells, ~80% of cells showed p54^{nrb} in the nucleus and is exempt from the nucleolus, see figure 3.7.2.1 (C) and (E)). The incubation of cells with the ATM and ATR inhibitors combined resulted in similar inhibition as with the inhibitors Caffeine and Wortmannin, ~80% of cells show p54^{nrb} is exempt from the nucleolus, see figure 3.7.1 (D). To highlight the nucleolar localisation of p54^{nrb} following ATRi treatment, enlarged images of XP12RO (XPA^{-}) cells are shown in figure 3.7.1 panel (E). The nucleolus is shown with a white arrow to indicate the variation in p54^{nrb} localisation following inhibitor treatment; specifically the perinucleolar areas p54^{nrb} resides to following ATRi treatment. Although it is evident that the nucleolar localisation of p54^{nrb} is sensitive to these specific PIKK inhibitors, taken together, these results suggest that p54^{nrb} is a downstream target of ATR and ATM and that both kinases must be inactivated to prevent p54^{nrb} from localising to the nucleolus following UV irradiation.

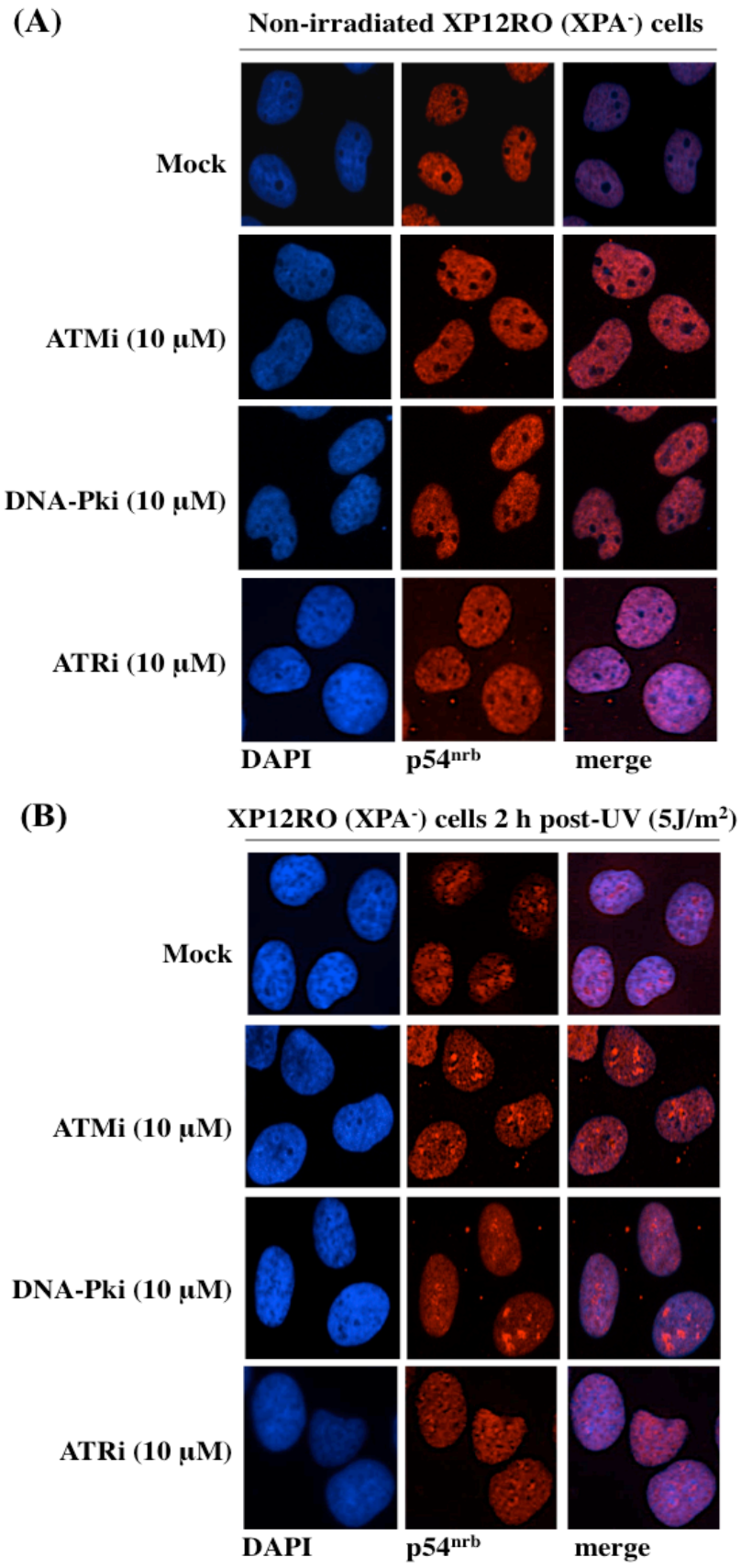
(A)
Non-irradiated XP12RO (XPA-) cells
Mock
ATMi (10 µM)
DNA-Pki (10 µM)
ATRi (10 µM)
DAPI
p54nrb
merge
(B)
XP12RO (XPA-) cells 2 h post-UV (5J/m2)
Mock
ATMi (10 µM)
DNA-Pki (10 µM)
ATRi (10 µM)
DAPI
p54nrb
merge

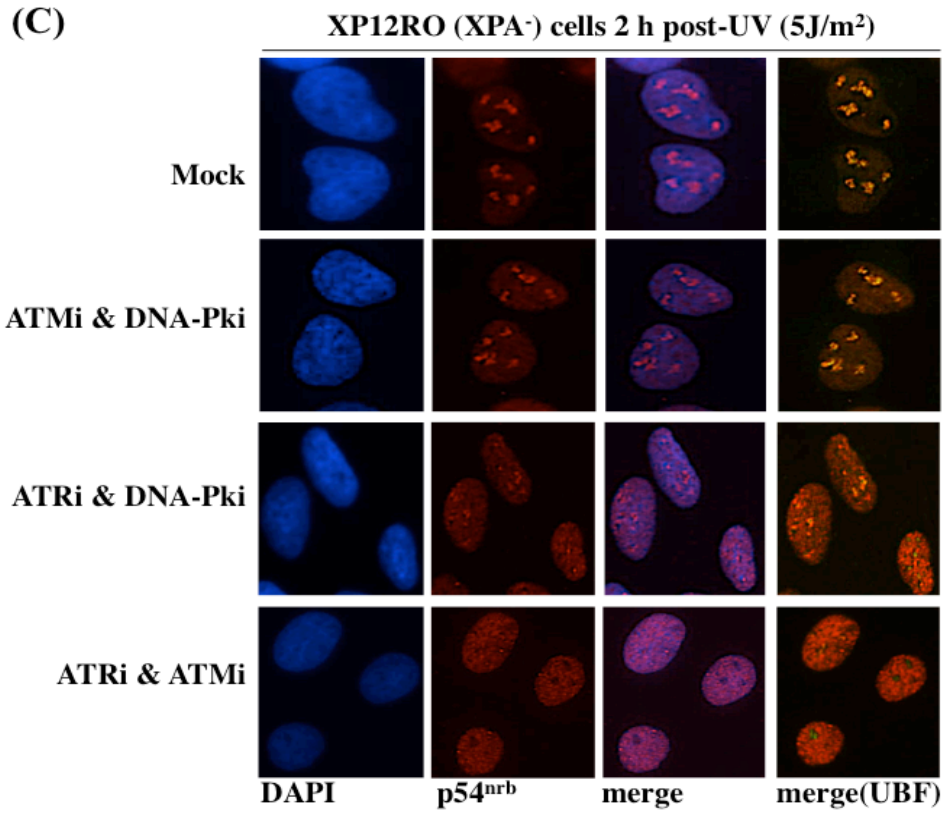
(C)
XP12RO (XPA-) cells 2 h post-UV (5J/m2)
Mock
ATMi & DNA-Pki
ATRi & DNA-Pki
ATRi & ATMi
DAPI
p54nrb
merge
merge(UBF)

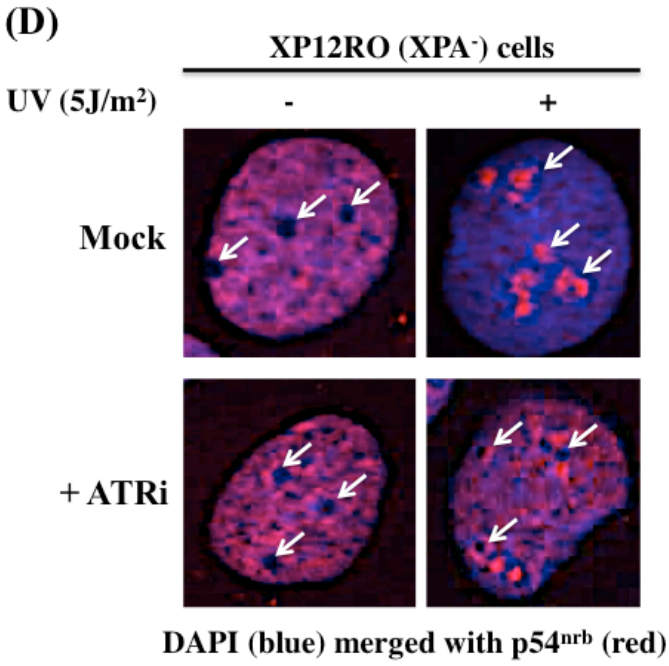
(D)
XP12RO (XPA-) cells
UV (5J/m2)
-
+
Mock
+ ATRi
DAPI (blue) merged with p54nrb (red)

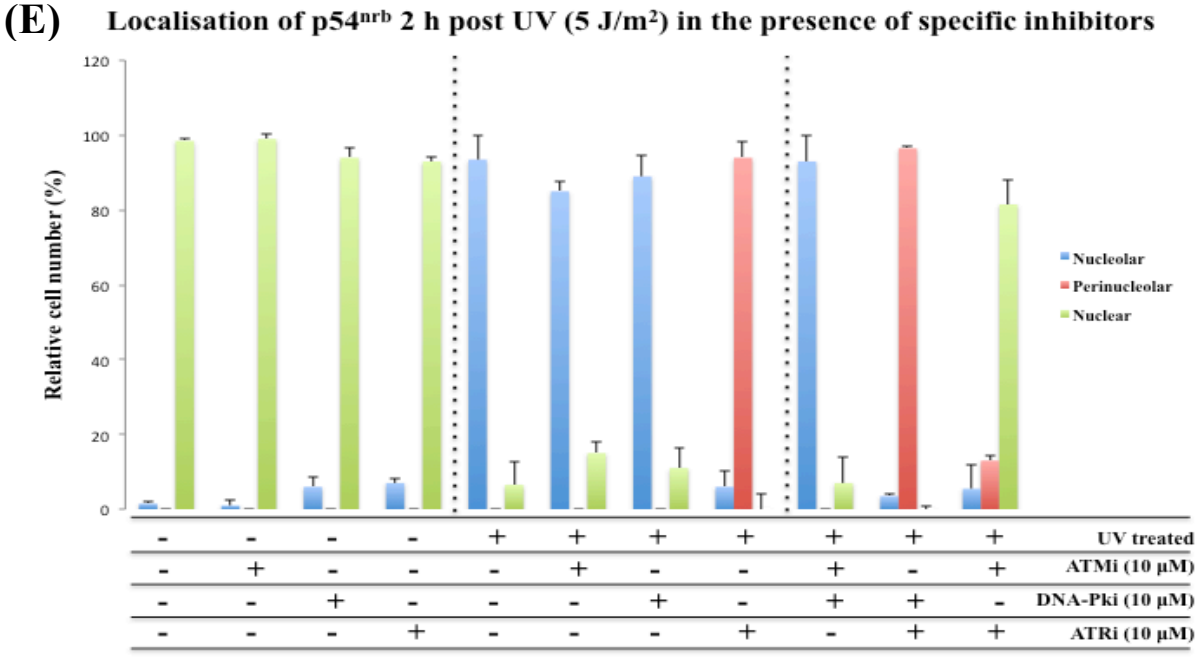

Figure 3.7.2.1 Specific cell signalling inhibitors and p54nrb nucleolar recruitment after UV irradiation.
Exponentially growing cells were grown on coverslips and treated with inhibitors as indicated. XP12RO (XPA-) cells were then either non-irradiated (panel **(A)),** or UV irradiated (5 J/m^2) (panels **(B)** and **(C)**). Cells were then probed with p54nrb antibody followed by cy3-conjugated secondary rabbit antibody (red). Cells were then probed with p54nrb antibody followed by cy3-conjugated secondary mouse antibody (red). UBF 1/2 antibody followed by cy2-conjugated secondary sheep antibody was used to visualise transcription machinery (panel **(C)**). Cell nuclei were stained with DAPI (blue). The immunofluorescence data of UBF 1/2 and p54nrb were merged and presented in the fourth column highlighted as 'merge' (panel **(C)**). Enlarged merged (DAPI and p54nrb) images with indicators (white arrows) highlighting the localisation of p54nrb in nucleoli before and after ATRi treatment (panel **(D)**). Immunofluorescence was performed using an Olympus IX51 microscope. Histogram representing the number of cells (obtained by immunofluorescence microscopy) showing nucleolar localisation of p54nrb following UV irradiation (5 J/m^2) and kinase inhibitor treatment (panel **(E)**). Data represents the mean of three independent experiments. Error bar represent one standard deviation.

As a control for the specificity of the various drug inhibitors used, XP12RO (XPA-) cells were pre-treated with the various PIK kinase drug inhibitors for 1 h followed by UV irradiation (5 J/m^2 of UVC), kept in drug-containing media and cells were harvested 2 h post-UV (for more details see 2.2.4.). Cell samples were then subjected to SDS-PAGE and western blot analysis. The blots were probed with anti-pChk1 (S317), anti-pChk2 (Thr68), and anti-pRPA32 (S4/8) antibodies, which are known phosphorylation sites of the downstream targets of ATR, ATM, and DNA-PK kinase activity (Ashwell and Zabludoff,

2008; Cruet-Hennequart et al., 2006; Cruet-Hennequart et al., 2008). As a control, the blots were probed with total Chk1, total Chk2, and total RPA32 to check for the relative levels of these proteins in the cell lysates. ATM and ATR have been identified as primary PIK kinase targets of Caffeine (Sarkaria et al., 1999), however, according to our western blot analysis, at the concentration we used, 10 mM, Caffeine does not exhibit an inhibitory effect on the activation of pChk1-S317 and pChk2-Thr68 after UV irradiation, in comparison to mock-treated cells, see figure 3.7.2.2 (A). Other reports have also highlighted the same phenomenon; Li et al showed that pChk2-Thr68 was insensitive to Caffeine treatment and Cortez et al showed that Caffeine treatment actually promoted phosphorylation of ATM/ATR downstream substrates (Cortez, 2003; Li and Stern, 2005). These results highlight that Caffeine is not a specific inhibitor of these PIK kinases alone and has other targets that it can inhibit. Wortmannin is a relatively effective inhibitor of ATM and DNA-PK kinases at a concentration of 10 μM; however, it is less inhibitory of ATR at this concentration (Sarkaria et al., 1998). In the presence of 10 μM of Wortmannin, a reduction of RPA32-S4/8 phosphorylation is visible after UV irradiation; however, there was no difference in pChk1-S317 and pChk2-Thr68 phosphorylation in comparison to mock-treated cells, see figure 3.7.2.2 (A). This result indicates that Wortmannin inhibits the activation of pRPA32-S4/8 at this concentration due to its inhibitory effect on DNA-PK at this concentration. We determine that at the concentration used (10 μM), Wortmannin targets DNA-PK and ATM kinase activity, and ATR less efficiently, rendering it still active, which gives an indication for the phosphorylation of pChk1-S317 and pChk2-Thr68 as ATM and ATR are known to cross-correlate for the activation of their downstream targets (Kerzendorfer and O'Driscoll, 2009; Stiff et al., 2008; Stiff et al., 2006). The specificity of DNA-PKi (10 μM) of its downstream target RPA32 as the catalytic subunit of DNA-PK (DNA-PKcs) is known to phosphorylate RPA32-S4/8 in response to replication stress (brought on by UV irradiation) (Liu et al., 2012). Treating cells with a DNA-PKi does reduce the activation of its downstream target RPA32-S4/8 relative to the mock-treated cells; see figure 3.7.2.2 (A). The specificity of the ATMi (10 μM), was also examined by the phosphorylation of its known downstream target, Chk2-Thr68. Treating cells with an ATMi shows a reduction in the phosphorylation of Chk2-Thr68 relative to the mock-treated cells; highlighting its specificity, see figure 3.7.2.2 (A). Similarly, treating

cells with an ATRi (10 μM) reduces the amount of pChk1-S317 and pChk2-Thr68, relative to the mock-treated cells, suggesting that the inhibitor successfully decreases the kinase activity of ATR, specifically using Chk1-S317 amino acid as a target sequence. However, after treating cells with an ATRi there is a marked increase in pRPA32-S4/8 activation. Toledo et al previously identified the accumulation of RPA foci after treating cells with the ATR inhibitor (5 μM), which might contribute to the increased level of pRPA32-S4/8 activation visible by western blot analysis (Toledo et al., 2011). However, when cells are treated with combined ATRi and DNA-PKi before UV irradiation, there is a reduction in the level of pChk1-S317, pChk2-Thr68, and pRPA32-S4/8 relative to the mock-treated cells; suggesting that together these inhibitors are more effective to inhibiting their downstream targets, see figure 3.7.2.2 (A). When cells are treated with combined ATRi and ATMi before UV irradiation, there is also a marked reduction in the activation of pChk1-S317, pChk2-Thr68, and pRPA32-S4/8 relative to the mock-treated cells; highlighting that combining these PIK kinase inhibitors is more effective to inhibiting the activation of the DNA damage signalling pathway, see figure 3.7.2.2 (A). A histogram (representing the number of cells obtained by immunofluorescence microscopy) showing the comparison of the various kinase inhibitors (described above) on nucleolar localisation of p54^{nrb} following UV irradiation (5 J/m^2), see figure 3.7.2.2 (B). These results, taken together with the immunofluorescence data (Figure 3.7.2.1 (A) – (C), strongly suggest that p54^{nrb} is a downstream target of ATR and ATM and that these kinases must be completely abrogated to prevent p54^{nrb} from localising to the nucleolus following UV irradiation. The data presented are a representative result of three independent experiments.

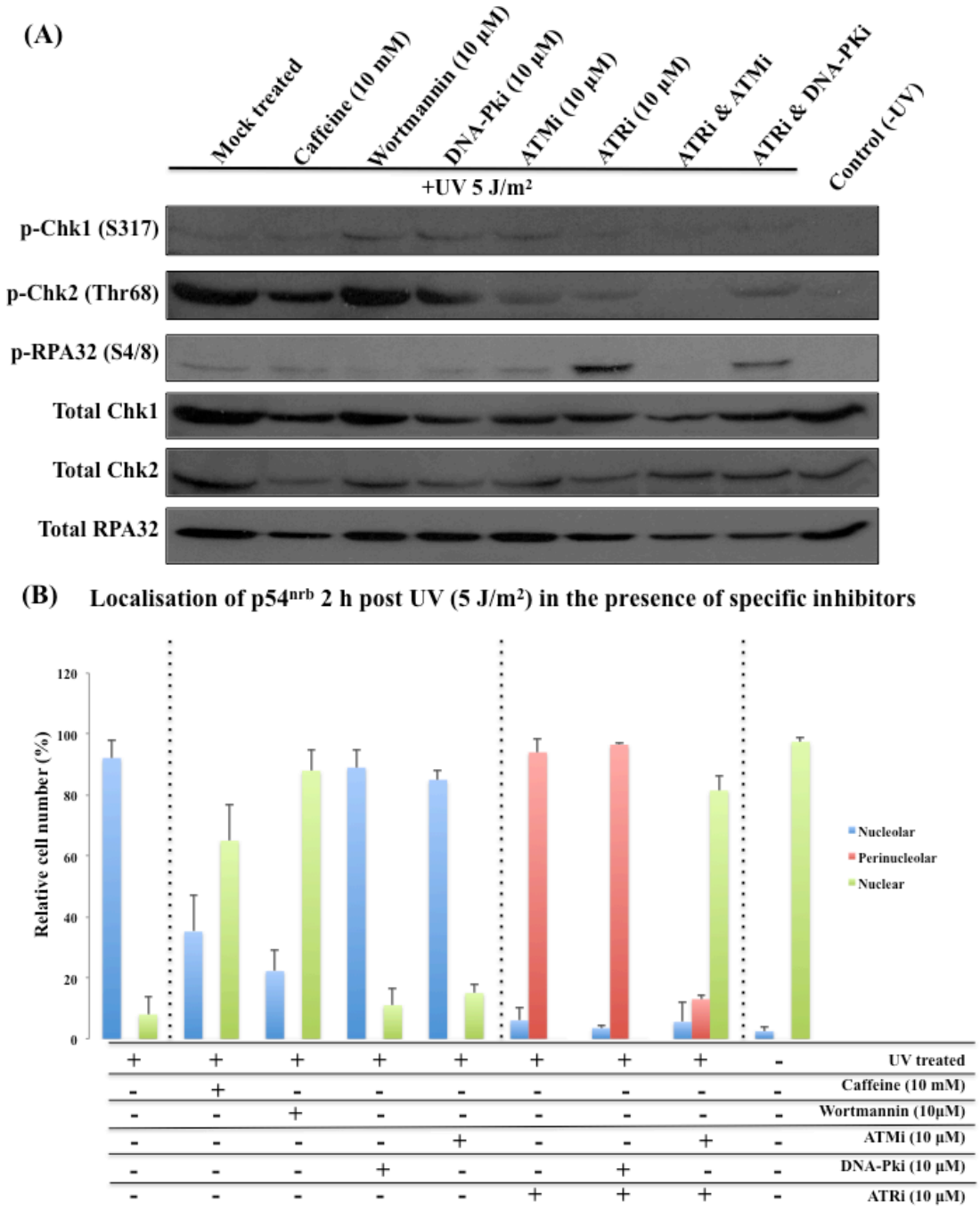

Figure 3.7.2.2 Comparison of PIK kinase inhibitors on p54nrb nucleolar recruitment after UV irradiation.

Cells exposed to PIK kinase inhibitor treatment followed by UV irradiation (5 J/m^2) were subjected to western blot analysis. The phosphorylation of Chk1 (S317), Chk2 (Thr68) and RPA 32 (S4/8) in response to various PIKK inhibitors treatment following UV irradiation (5 J/m^2) was analysed using specific antibodies. Total Chk1, total Chk2 and total RPA 32 expression levels were used as loading controls (panel **(A)**). Histogram representing the number of cells (obtained by immunofluorescence microscopy) showing nucleolar localisation of p54nrb following UV irradiation (5 J/m^2) and PIK kinase inhibitor treatment (described in above western blot) (panel **(B)**). Data represents the mean of three independent experiments. Error bar represent one standard deviation.

3.7.3 Chk2 checkpoint kinase plays a critcal role in determining p54^{nrb} cellular response to UV irradiation

ATR and ATM are phosphorylated following DNA damage, which in turn activate further downstream targets of the DDR signalling cascade specifically the Chk1 and Chk2 kinases (Zhou and Elledge, 2000). The discovery that the inhibition of members of the PIKK family reduced the enrichment of p54^{nrb} to nucleoli, specifically ATR and ATM, raises the question of which of their downstream checkpoint kinase, Chk1 and Chk2, or both regulates the recruitment of p54^{nrb} to nucleoli.

To investigate if these downstream kinases play a role in p54^{nrb} nucleolar recruitment, asynchronous XP12RO (XPA^{-}) cells were treated with a Chk2 inhibitor (5 μM) followed by UV irradiation (5 J/m^2 of UVC) and fixed 2 h post-UV. In non-irradiated, mock-treated, XP12RO (XPA^{-}) cells, p54^{nrb} is evenly distributed throughout the nucleus (Figure 3.7.3 (A)). In UV irradiated, mock-treated cells, p54^{nrb} is enriched in the nucleolus (Figure 3.7.3 (B)). Following treatment with the Chk2 inhibitor, in UV irradiated cells; the enrichment of p54^{nrb} to nucleoli is visibly reduced (Figure 3.7.3 (B)). At a low concentration of Chk2 inhibitor the number of cells with nucleolar p54^{nrb} is reduced to ~50% of cells and this number is reduced nearly two-fold at the higher concentration to ~25% of cells, indicating that this localisation is also concentration-dependent, see figure 3.7.3 (C). The data presented are a representative result of three independent experiments.

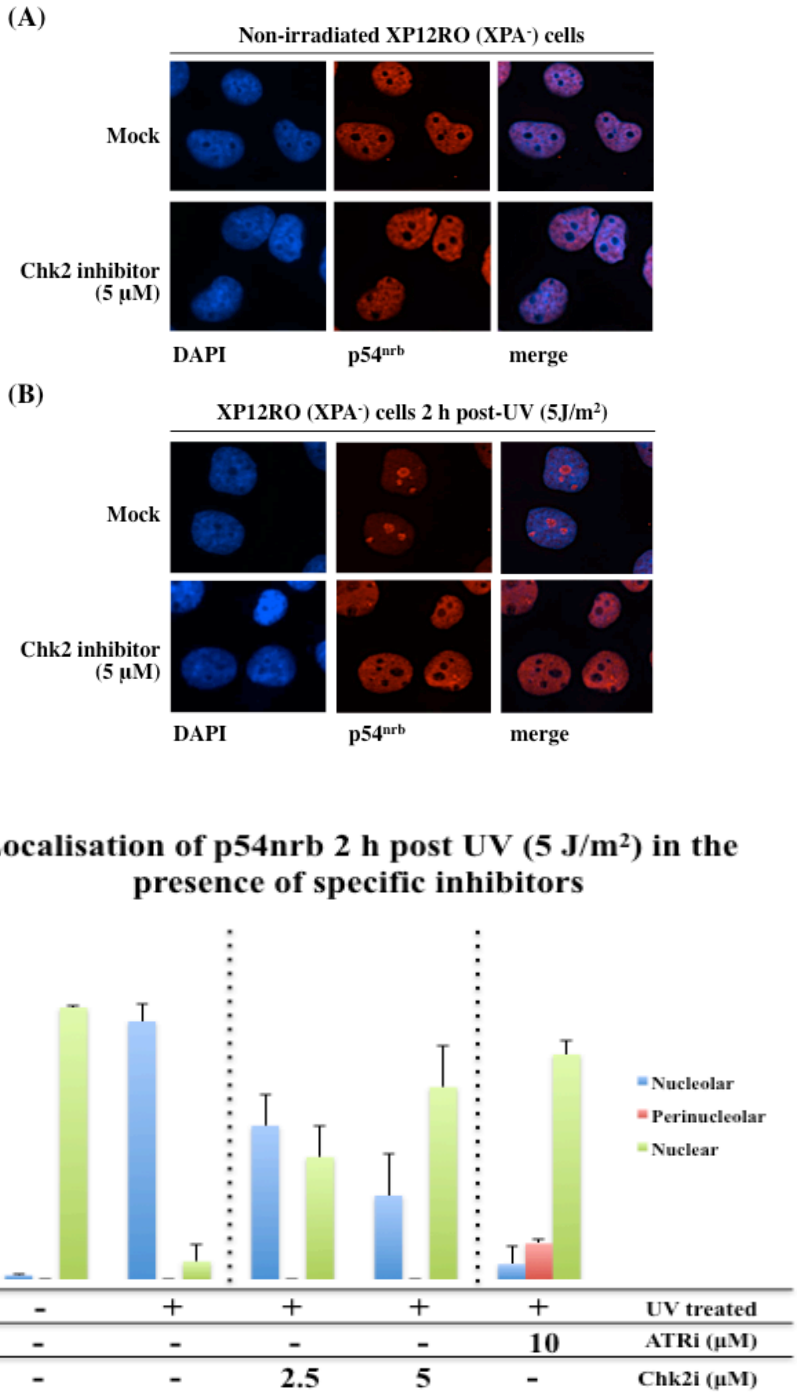

Figure 3.7.3.1 Chk2 signalling and p54nrb nucleolar recruitment.
Exponentially growing cells were grown on coverslips and treated with a Chk2 inhibitor (5 µM). XP12RO (XPA^-) and XP12ROC5 (XPA^+) cells were then non-irradiated (panel **(A)**), or UV irradiated (5 J/m^2) (panel **(B)**). Cells were fixed 2 h post UV irradiation and then probed with rabbit anti-p54nrb antibody followed by cy3-conjugated secondary rabbit antibody (red). Cell nuclei were stained with DAPI (blue). The immunofluorescence data of DAPI and p54nrb were merged and presented in the third column highlighted as 'merge'. Immunofluorescence was performed using an Olympus IX51 microscope. Diagram representing the number of cells (obtained by

immunofluorescence microscopy) showing nucleolar localisation of p54^{nrb} following UV irradiation (5 J/m^2) and kinase inhibitor treatment (panel **(C)**). Error bar represent one standard deviation.

Following these observations, we wanted to elucidate if the nucleolar localisation of p54^{nrb} was associated with Chk1 activity. To investigate this hypothesis, we silenced Chk1 using siRNA; see section 2.2.2, for procedure. Western blot analysis was performed using an antibody specific to Chk1 to detect the levels of the protein following siRNA. As a loading control an antibody raised against RPA32 was used, see figure 3.7.3.2 (B). We found that Chk1 protein was significantly reduced at 72 h post-siRNA treatment, see figure 3.7.3.2 (B). At 72 h post-siRNA treatment, the cells were subjected to UV irradiation (5 J/m^2 of UVC) and fixed 2 h post-UV. In siRNA transfected, non-irradiated, XP12RO (XPA$^-$) and U2OS cells, p54^{nrb} is evenly distributed throughout the nucleus (Figure 3.7.3.2 (A)). In siRNA transfected, UV irradiated cells, p54^{nrb} is enriched in the nucleolus (Figure 3.7.3.2 (A)). The number of cells with nucleolar p54^{nrb} is comparable in both siRNA treated and non-treated cells in both cell lines; see figure 3.7.3.2 (C). Other inhibitors that target specific downstream targets of PIKKs were used to establish if they play a role in p54^{nrb} localisation to nucleoli and were found to have a negative impact on p54^{nrb} nucleolar enrichment after UV irradiation, see table 3.7.3. A Chk1 inhibitor (UCN-01) was also used but treating cells with the inhibitor already caused recruitment of p54^{nrb} to nucleoli (data not shown), suggesting that Chk1 inhibitor is less specific than siRNA approach and therefore the inhibitor was not used furthermore in these experiments. The data presented is a representative result of three independent experiments.

Treating cells with a Chk2 inhibitor is comparable to that of treating cells with ATMi and ATRi together, ~80% of cells showed p54^{nrb} in the nucleus and is excluded from the nucleolus; see figure 3.7.3.1 (C). Collectively, these results suggest that p54^{nrb} recruitment to nucleoli depends on the kinase activity of ATR and ATM and together they control the nucleolar localisation of p54^{nrb} through their downstream target Chk2 and not through Chk1 as shown by siRNA analysis.

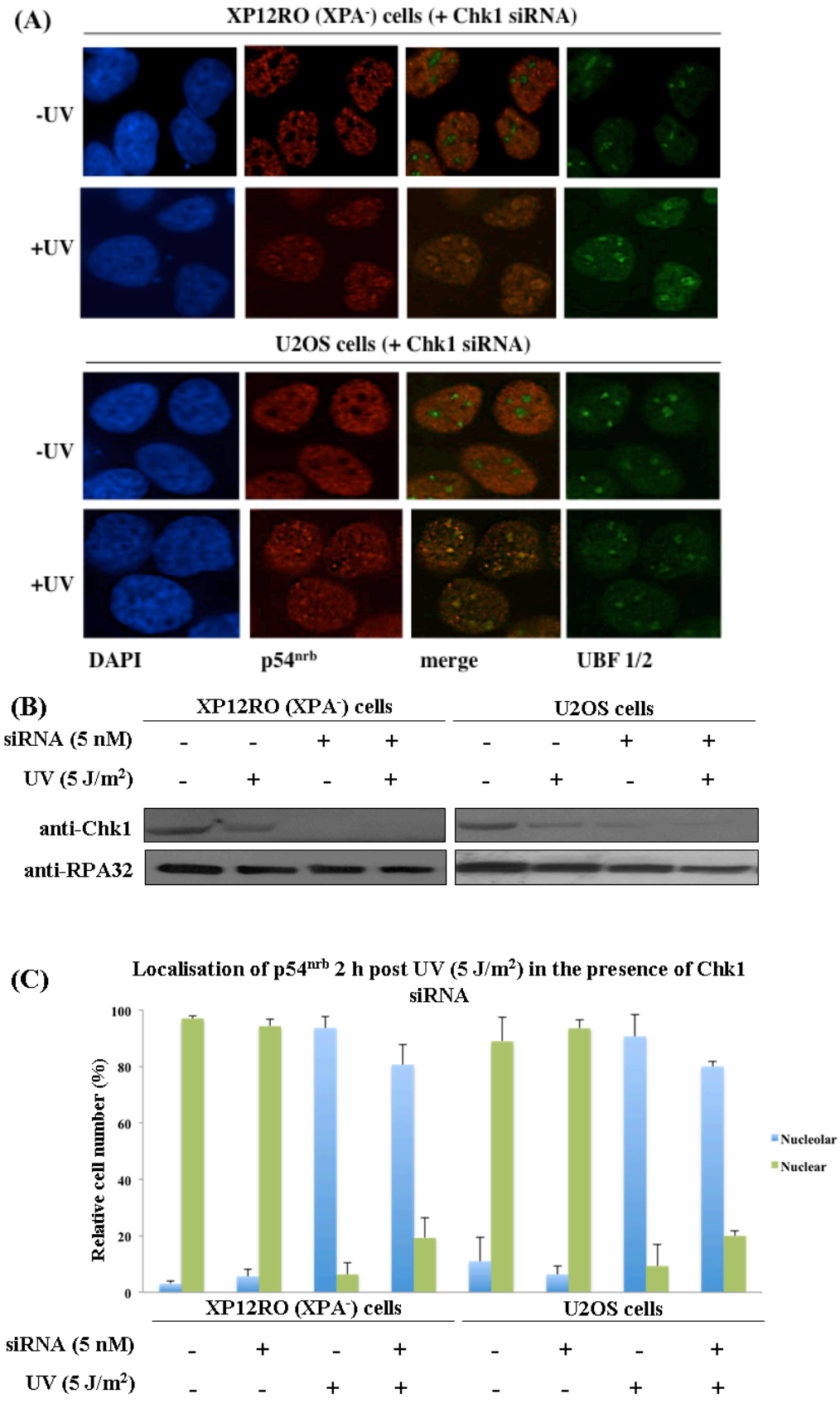
(A)
XP12RO (XPA-) cells (+ Chk1 siRNA)
-UV
+UV
U2OS cells (+ Chk1 siRNA)
-UV
+UV
DAPI
p54nrb
merge
UBF 1/2
(B)
XP12RO (XPA-) cells
U2OS cells
siRNA (5 nM)
UV (5 J/m2)
anti-Chk1
anti-RPA32
(C)
Localisation of p54nrb 2 h post UV (5 J/m2) in the presence of Chk1 siRNA
Relative cell number (%)
Nucleolar
Nuclear
XP12RO (XPA-) cells
U2OS cells
siRNA (5 nM)
UV (5 J/m2)

Figure 3.7.3.2 Chk1 signalling and p54^{nrb} nucleolar recruitment.
Exponentially growing cells were grown on coverslips and treated with Chk1 siRNA for 72 h. XP12RO (XPA^{-}) and U2OS cells were then non-irradiated or UV irradiated (5 J/m^2) Cells were fixed 2 h post UV irradiation and then probed with rabbit anti-p54^{nrb} antibody followed by cy3-conjugated secondary rabbit antibody (red). Cell nuclei were stained with DAPI (blue). The immunofluorescence data of UBF 1/2 and p54^{nrb} were merged and presented in the fourth column highlighted as 'merge'. Immunofluorescence was performed using an Olympus IX51 microscope (panel **(A)**). Western blot analysis was carried out using an antibody specific to Chk1 to detect the levels of the protein 72 h following siRNA. As a loading control an antibody raised against RPA32 was used. Membranes were developed using a horseradish peroxidase-conjugated secondary antibody and ECL system. Signal was detected with a Fuji LAS 3000 imager (panel **(B)**). Diagram representing the number of cells (obtained by immunofluorescence microscopy) showing nucleolar localisation of p54^{nrb} following UV irradiation (5 J/m^2) and siRNA treatment (panel **(C)**). The data presented is a representative result of three independent experiments. Error bar represent one standard deviation.

Table 3.7.3 Drug inhibitors used to target p54^{nrb} nucleolar enrichment.
A number of other kinase drug inhibitors were used and were found to have a negative impact on the localisation of p54^{nrb} to nucleoli.

	Reduction of p54^{nrb} localisation to the nucleolus after UV irradiation & kinase inhibitor treatment		
Caffeine	+	-	**Data represented in figure 3.7.1**
Wortmannin	+	-	
ATM Inhibitor	-	+	**Data represented in figure 3.7.2.1**
DNA-PK Inhibitor	-	+	
ATM & DNA-PK In.	-	+	
ATRi	++	-	
ATRi & DNA-PKi	++	-	
ATRi & ATMi	+	-	
Chk2 Inhibitor	+	-	**Data represented in figure 3.7.3.1**
UCN-01*	-	-	**Data not shown**
Roscovitine*	-	-	**Data not shown**

++ ATRi showed perinucleolar localisation of p54^{nrb}

*** UCN-01 and Roscovitine showed a relocalisation of p54^{nrb} but it was found to be drug mediated response**

3.7.4 Lymphoblastoid cells with defects in ATM and ATR show nucleolar recruitment of p54^{nrb} following UV irradiation

Following our discovery that various kinase inhibitors reduce the localisation of p54^{nrb} to nucleoli following UV irradiation we wanted to investigate whether cells with defects in ATM and ATR protein function showed the same phenomenon. To do this, we examined human lymphoblastoid cells with mutations in ATM and ATR kinases. The point mutation in ATR of SS cells causes a reduction in the protein level, but not its complete loss (O'Driscoll et al., 2003).

Human lymphoblastoid cells were exposed to 30 J/m^2 of UV irradiation and fixed 30 min - 4 h post-UV. A high dose of UV irradiation was used so that the localisation of p54^{nrb} could be readily observed in these cells, from previous experiments (see 3.2.1), it is evident that the localisation of p54^{nrb} to the nucleolus is dose-dependent. Immunofluorescence staining was performed using antibodies specific to p54^{nrb} (green) and nucleophosmin, which served as a nucleolar marker and is shown in red. Cell nuclei are stained with DAPI (Blue) (Figure 3.7.4.1 (A – C)). In all non-irradiated cells, p54^{nrb} is dispersed throughout the nucleoplasm of the cell with remarkable reduction in staining in nucleoli in the entire cell lines analysed. In the control lymphoblastoid cells, p54^{nrb} begins to enrich in nucleoli at 30 min post UV irradiation and remains there at least until 4 h after UV irradiation (Figure 3.7.4.1 (A)). In the Seckle Syndrome (SS) lymphoblastoid cells, p54^{nrb} targets the nucleolus at 30 min post UV irradiation and remains in the nucleolus up until 4 h (Figure 3.7.4.1 (B)). The same phenomenon is evident in AT lymphoblastoid cells as seen in (Figure 3.7.4.1 (C)); following UV irradiation, p54^{nrb} targets nucleoli and remains there up until 4 h post-UV. Human lymphoblastoid cells were also exposed to a lower dose of UV irradiation (5 J/m^2) and fixed 30 min - 4 h post-UV. In all the lymphoblastoid cell lines, p54^{nrb} begins to enrich in nucleoli at 2 h post 5 J/m^2 of UV irradiation, and remains there at least until 4 h after UV irradiation (data not shown). The data presented is a representative result of three independent experiments.

These results mirror our previous results that p54^{nrb} enrichment in nucleoli after UV irradiation is UV dose- and time-dependent. However, the SS cells used in this experiment highlight p54^{nrb} enrichment in nucleoli after UV irradiation indicating that even though these cells have minimal amounts of functional ATR protein, it is sufficient to allow

recruitment of p54^{nrb} to the nucleoli after UV irradiation. Again, these results are in agreement with our previous findings that ATR must be completely abolished to inhibit nucleolar enrichment of p54^{nrb} following UV irradiation, see previous figure 3.7.2.1 (C) and (D). The human lymphoblastoid cells are not an ideal cell line for immunofluorescence microscopy as variability can be observed in the staining of p54^{nrb} and nucleophosmin. The human lymphoblastoid cells are a suspension cell line and are round in shape, unlike the skin fibroblasts cells that are flat making them ideal candidates for immunofluorescence microscopy. The cells were attached to polylysine slides using a cytospin machine (cells were attachted to the slide by centrifugation (800 rpm) followed by fixation with 4% PFA before immunofluorescence microscopy was performed which may contribute to the variability in antibody staining.

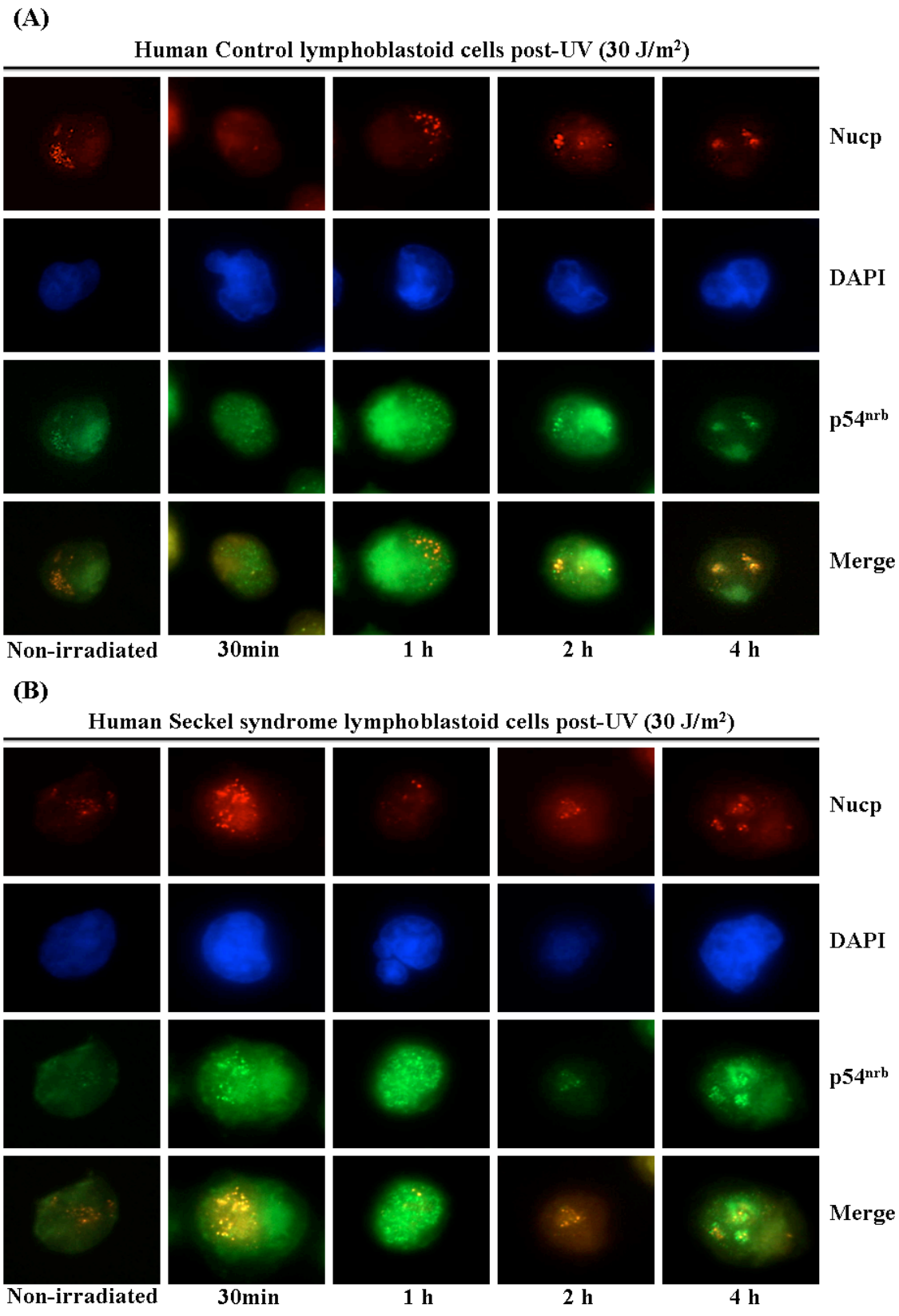
(A)
Human Control lymphoblastoid cells post-UV (30 J/m²)
Nucp
DAPI
p54nrb
Merge
Non-irradiated
30min
1 h
2 h
4 h
(B)
Human Seckel syndrome lymphoblastoid cells post-UV (30 J/m²)
Nucp
DAPI
p54nrb
Merge
Non-irradiated
30min
1 h
2 h
4 h

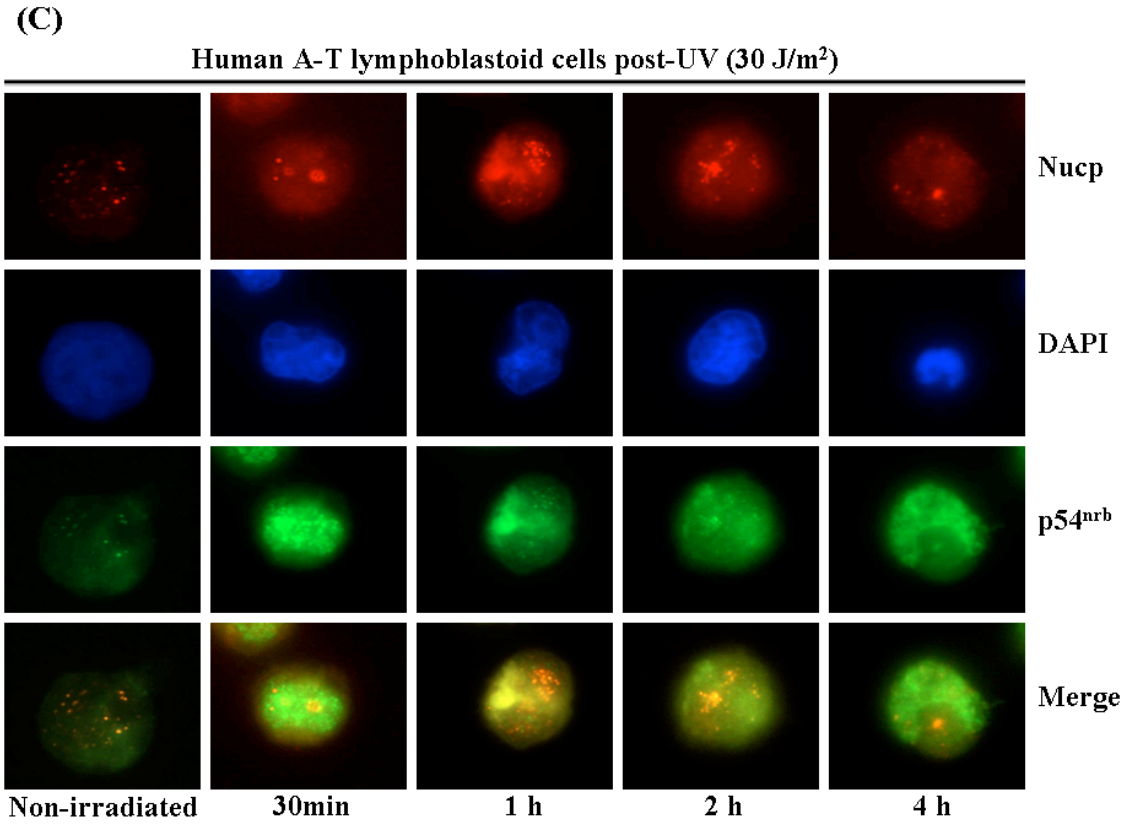

Figure 3.7.4.1 Localisation of p54^{nrb} to nucleoli following UV irradiation in human lymphoblastoid cell lines.
Human lymphoblastoid cell lines were either non-irradiated or UV irradiated with 30 J/m^2 of UVC. Cells were fixed 30 min - 4h post-UV and probed with p54^{nrb} antibody followed by cy2-conjugated secondary mouse antibody (green). Nucleoli were stained with a nucleophosmin (Nucp) antibody followed by cy3-conjugated secondary anti-rabbit antibody (red). Cell nuclei were stained with DAPI (blue). The immunofluorescence data of nucleophosmin and p54^{nrb} were merged and presented in the fourth column highlighted as 'merge'. Immunofluorescence was performed using an Olympus IX51 microscope (Lymphoblastoid cell lines are indicated at the top of panels **(A - C)**).

Our investigation into the recruitment of p54^{nrb} to nucleoli and its regulation by inhibitors of DNA damage-dependent signalling factors led us to investigate the loss of these PIK kinases *in vivo*. Asynchronous human lymphoblastoid cells were treated with Caffeine (2 mM or 5 mM) or a Chk2 inhibitor (2.5 μM or 5 μM) followed by UV irradiation (30 J/m^2 of UVC) and fixed 2 h post-UV. In non-irradiated lymphoblastoid cells, p54^{nrb} is evenly distributed throughout the nucleus (Figure 3.7.4.1 (A – C), non-irradiated panel of cells). In UV irradiated, mock-treated cells, p54^{nrb} is enriched in the nucleolus following UV irradiation in ~50 - 60% of cells, (Figure 3.7.4.2 (A - C)). Following treatment with Caffeine or a Chk2 inhibitor, this enrichment of p54^{nrb} in nucleoli is reduced significantly after UV irradiation, in the presence of a high concentration of both drugs the number of cells with nucleolar p54^{nrb} is reduced to ~25-30 % of cells, see (Figure 3.7.4.2 (A - C)). The data presented is a representative result of three independent experiments.

To conclude our findings, we have shown that treating these human cell lines with kinase inhibitors reduces the recruitment of p54^{nrb} to nucleoli following UV irradiation. This suggests that the enrichment of p54^{nrb} in nucleoli is sensitive to these different kinase inhibitors, thus indicating that the localisation of p54^{nrb} to the nucleolus is dependent on members of the phosphatidylinositol 3-kinase-like protein (PIKKs) kinase family and their downstream targets, particularly ATM and ATR, see figure 3.7.2.1 (C) and (D). However, by using human lymphoblastoid cells with defects in ATM and ATR kinases we see that p54^{nrb} still targets nucleoli following UV irradiation. From these findings, we hypothesise that the functional activity of ATR and ATM must be completely abolished to prevent p54^{nrb} from entering the nucleolus after UV irradiation.

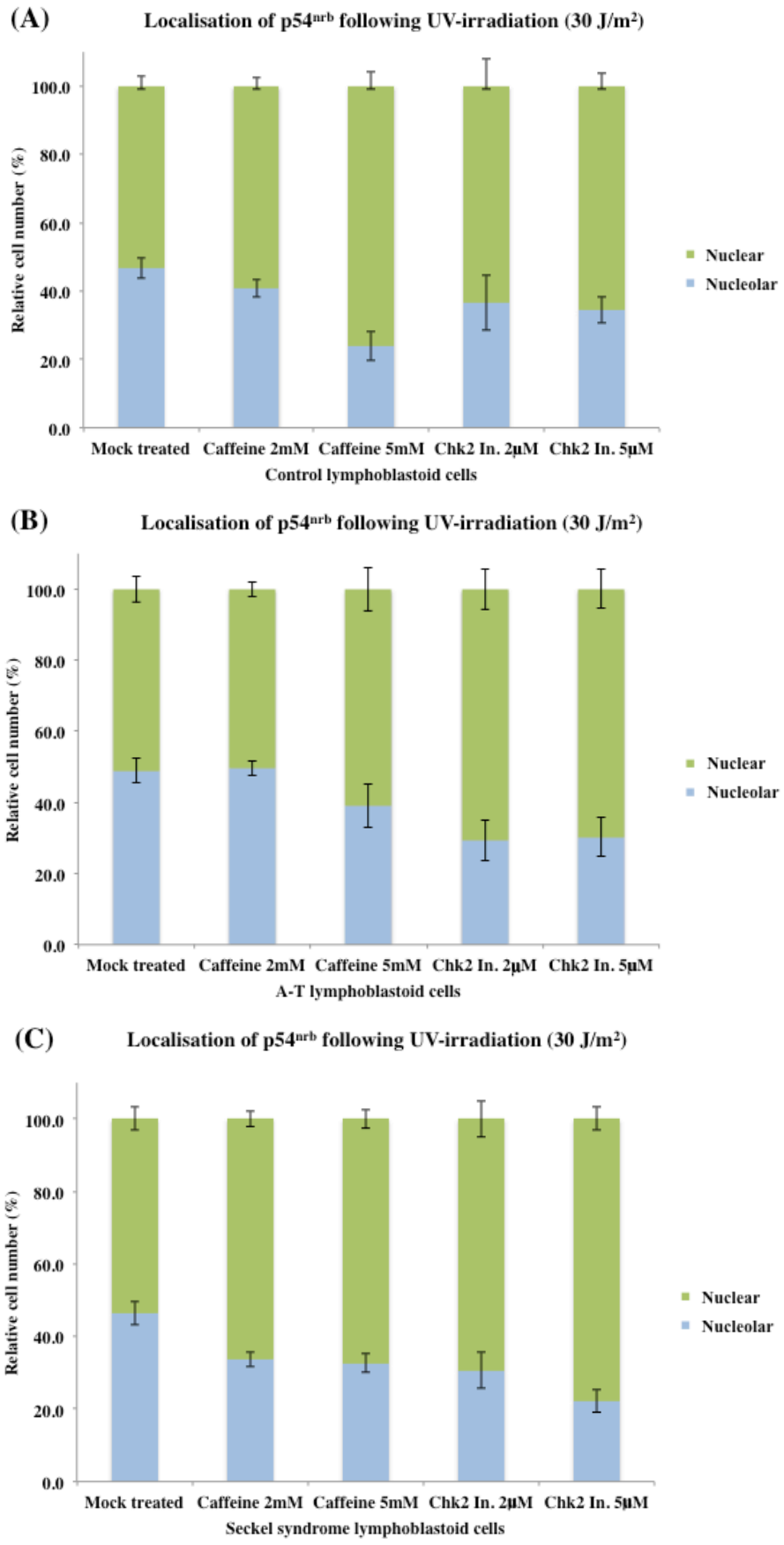

Figure 3.7.4.2 PIK kinase inhibitors and p54nrb nucleolar recruitment. Exponentially growing human lymphoblastoid cell lines were grown on coverslips and subjected to treatment with Caffeine (2 mM or 5mM) and Chk2 inhibitor (2 µM or 5 µM). The cells were then UV irradiated with 30 J/m^2 of UVC. The cells were fixed at 2 h post UV irradiation. Cells were then probed with p54nrb antibody. Immunofluorescence was performed using an Olympus IX51 microscope (see figure 3.7.4.1). Stacked columns represent the number of cells showing nucleolar localisation of p54nrb following UV irradiation and kinase inhibitor treatment, (panels **(A – C)**). Data represents the mean of three independent experiments. Error bar represent one standard deviation.

3.8 Interaction between p54^{nrb} and TopBP1 is reduced following UV irradiation as observed by co-immunoprecipitation

Our results strongly suggest that p54^{nrb} is a downstream target of ATR and ATM and that these kinases must be completely abrogated to prevent p54^{nrb} from localising to the nucleolus following UV irradiation (Figure 3.7.2.1 (A) – (C). TopBP1 is a BRCT domain-rich protein that has been shown to physically interact with ATR and enhance its kinase activity in response to DNA damage (Kumagai et al., 2006). Kuhnert et al showed that p54^{nrb} interacts with TopBP1 *in vivo* (Kuhnert et al., 2012). Kuhnert et al also showed that p54^{nrb} localises with TopBP1 to sites of DSB's as early as 2 seconds following damage induction, with subsequent disappearance about 10 minutes later (Kuhnert et al., 2012). Taking these findings into consideration, we wanted to investigate the relationship between p54^{nrb} and TopBP1 following UV irradiation.

To examine whether p54^{nrb} interacts with TopBP1 *in vivo* following UV irradiation, asynchronous XP12RO (XPA^{-}) cells were subjected to low (2.5 J/m^2) and high (10 J/m^2) doses of UV irradiation and the physical interaction of endogenous p54^{nrb} with TopBP1 was studied 1 min and 2 h post-treatment by co-immunoprecipitation. These two time points were chosen because at 1 min Kuhnert et al observed p54^{nrb} localising to sites of DNA damage (DSBs) with TopBP1 and at 2 h we observe a change in p54^{nrb} nucleolar localisation is detected by immunofluorescence microscopy in XP12RO (XPA^{-}) cells (Figure 3.2.1) and we wanted to observe the relationship between p54^{nrb} and TopBP1 at these timepoints following UV irradiation. Cell samples were then subjected to SDS-PAGE and western blot analysis (Figure 3.8).

We observed that p54^{nrb} interacted with TopBP1 in the non-irradiated (IP control) sample, mirroring the result observed by Kuhnert et al (see figure 3.8, lane 3). We found that the interaction between p54^{nrb} and TopBP1 is reduced 2 hrs-post 2.5 J/m^2 of UV irradiation (figure 3.8, lane 5) and that this reduction is even more pronounced after 10 J/m^2 of UV irradiation (see figure 3.8, lanes 6 and 7). We have shown that p54^{nrb} localises to the nucleolus following UV irradiation, however, we failed to identify p54^{nrb} at sites of UV induced damage. The results observed suggest that following UV irradiation the interaction between p54^{nrb} and TopBP1 is reduced because p54^{nrb} is enriched in the nucleolus and TopBP1 localises to sites of DNA damage to interact with ATR and the DNA damage

signalling pathway. We suggest that there is a loss of interaction between p54nrb and TopBP1 to allow for the DNA damage signalling process to take place.

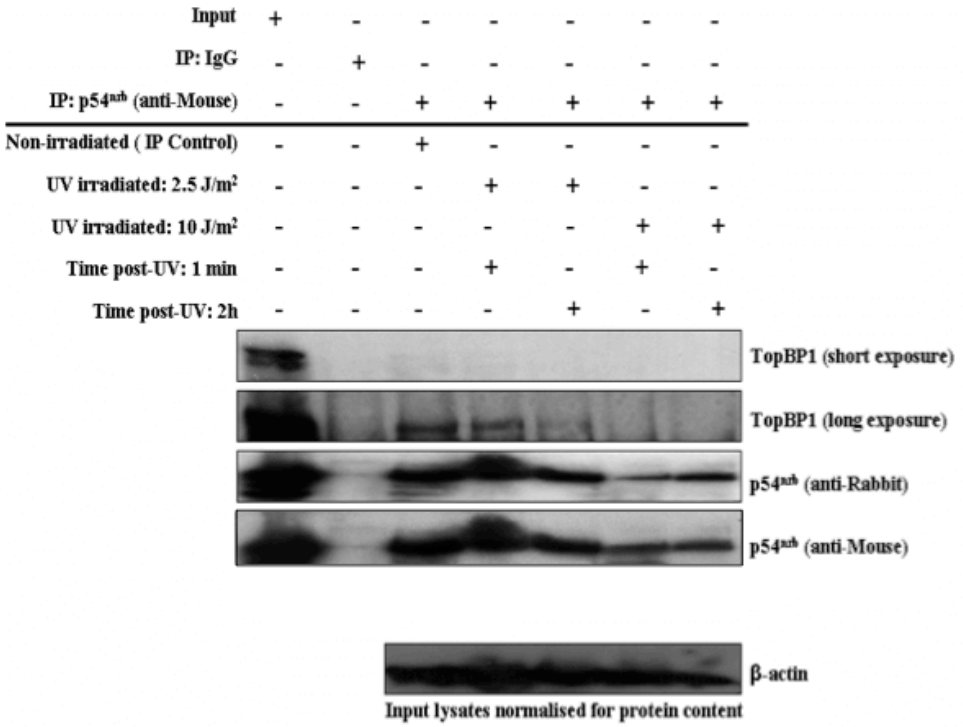

Figure 3.8 Interaction of p54nrb with TopBP1 is reduced following UV irradiation.
Asynchronous XP12RO (XPA-) cells were subjected to UV irradiation (2.5 J/m^2 and 10 J/m^2) and the interaction of endogenous p54nrb with TopBP1 was studied 1 min and 2 h post-treatment by co-immunoprecipitation. Lysate samples were subjected to SDS-PAGE and western blotting using antibodies specific to TopBP1 or p54nrb (anti-Rabbit). TopBP1 was immunoprecipitated as indicated with control IgG serving as negative control (IP: IgG) and eluates from each IP (IP: p54nrb) were analysed using antibodies specific to TopBP1 and p54nrb (anti-Rabbit). The data presented is a representative result of two independent experiments.

3.9 Human fibroblasts exhibit a radioresistant response UV irradiation to following p54^{nrb} siRNA

3.9.1 Attenuation of p54^{nrb}

Previous work has shown that silencing of p54^{nrb} in melanoma cells contributes to sensitivity of cells for apoptosis and reduction in cell migration (Schiffner et al., 2011). Li et al (2009) and (Krietsch et al., 2012) showed that the attenuation of p54^{nrb} in human cells leads to a decrease in survival of IR-treated cells and thus leads to a deficiency in NHEJ repair. Subsequent to our work on the role of p54^{nrb} in the DNA damage response pathway, we wanted to investigate whether or not p54^{nrb} is involved in the DNA damage response following UV irradiation.

To test this we knocked down p54^{nrb} using a siRNA method. XP12RO (XPA^{-}) cells were transfected with p54^{nrb} siRNA and harvested either 48 or 72 h post-transfection, procedure in 2.2.2, 3 - 20 nM of p54^{nrb} siRNA (ON-TARGET*plus* Target pool) and *20 nM* ON-TARGET*plus* Duplex were used and harvested either 48 or 72 h post-transfection. Western blot analysis was performed using an antibody specific to p54^{nrb} to detect the levels of the protein following siRNA. As a loading control an antibody raised against PCNA was used, see figure 3.9.1. The data presented are a representative result of three independent experiments.

We found that the amount of p54^{nrb} protein was significantly reduced after treatment with both types of p54^{nrb} siRNA used. However, the reduction of p54^{nrb} was most evident at 72 h post-siRNA treatment, see figure 3.9.1. Following this, we decided to transfect the cells with p54^{nrb} siRNA (ON-TARGET*plus* Target pool) for 72 h at a concentration of 5 nM in any further experiments carried out.

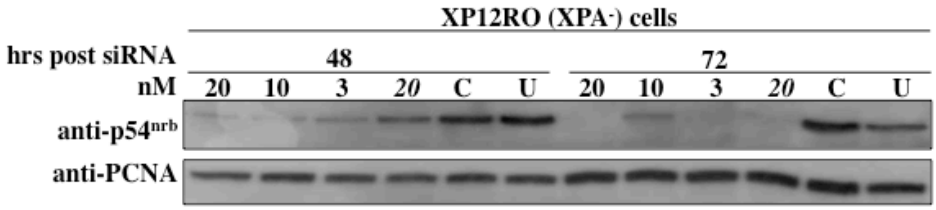

Figure 3.9.1 Attenuation of p54nrb expression using siRNA.
XP12RO (XPA-) cells were transfected with p54nrb siRNA and harvested either 48 or 72 h post-transfection. 3, 10 or 20 nM of p54nrb siRNA (ON-TARGET*plus* Target pool) and *20 nM* (Italics) ON-TARGET*plus* Duplex were used and harvested either 48 or 72 h post-transfection. C = Control, represents transfection with control siRNA (ON-TARGETplus Non-targeting Pool). U = Untreated, represents non-transfected cells. Western blot analysis was carried out using an antibody specific to p54nrb to detect the levels of the protein following siRNA. As a loading control an antibody raised against PCNA was used. Membranes were developed using a horseradish peroxidase-conjugated secondary antibody and ECL system. Signal was detected with a Fuji LAS 3000 imager.

3.9.2 Cell survival following UV irradiation

To analyse the influence of p54nrb on the cell survival of XP12RO (XPA-) and XP12ROC5 (XPA+) cells following UV irradiation these cells were treated with increasing doses of UV and cell survival was investigated. Asynchronous cells were seeded into 35 mm dishes (~1.5 x 10^5 cells/dish) and were subjected to increasing doses of UV irradiation (2.5 – 10 J/m^2) the following day (as described previously. 2.2.3). 48 h following UV irradiation, cells were trypsinised and then counted as described in section 2.3. Each dose of UV irradiation was performed in triplicate each time the experiment was carried out.

Figure 3.9.2.1 shows that under these conditions only ~25% of XP12RO (XPA-) cells survive at 2.5 J/m^2, in comparison to ~65 % of XP12ROC5 (XPA+) cells, the data presented are a representative result of three independent experiments. Increasing the dose even further decreases the number of viable XP12RO (XPA-) cells indicating that the cells are extremely sensitive to these doses so we decided to decrease the UV dose used for XP12RO (XPA-) cells to 0.5 – 2.5 J/m^2, (see figure 3.9.2.1). The rate of survival of XP12RO (XPA-) cells is ~50% at 0.5 J/m^2 and we used a maximal dose of 2.5 J/m^2 for these cells in any further experiments performed, see figure 3.9.2.2, the data presented is a representative result of two independent experiments.

The results presented here highlight that XPA protein is an essential part of the preincision complex of nucleotide excision repair. This crucial role implies that cells deficient in this

protein are unable to repair DNA lesions very efficiently that are induced by UV irradiation, resulting in severe anomalies in patients that are genetically XPA deficient.

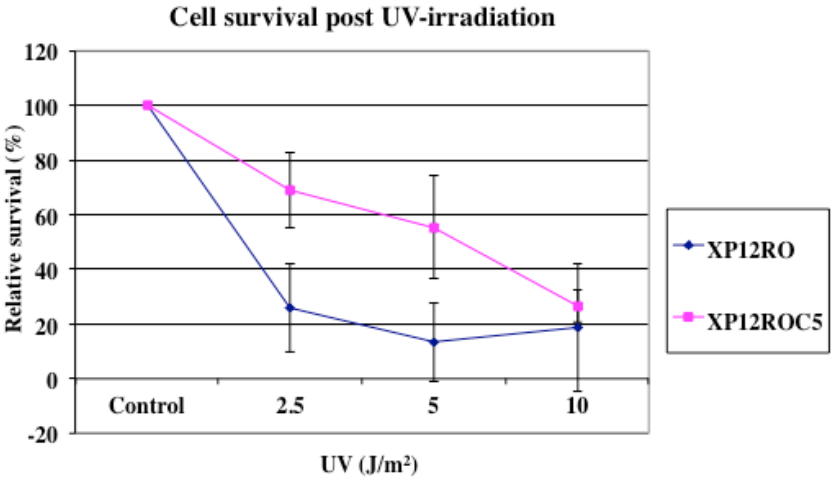

Figure 3.9.2.1 Effect of intermediate doses of UV irradiation on cell survival of XP12RO (XPA$^-$) and XP12ROC5 (XPA$^+$) cells.
Cell survival of XP12RO (XPA$^-$) and XP12ROC5 (XPA$^+$) cells following UV irradiation was assayed by counting cells using trypan blue 48 h after UV irradiation. Data represents the mean of three independent experiments. Error bar represent one standard deviation.

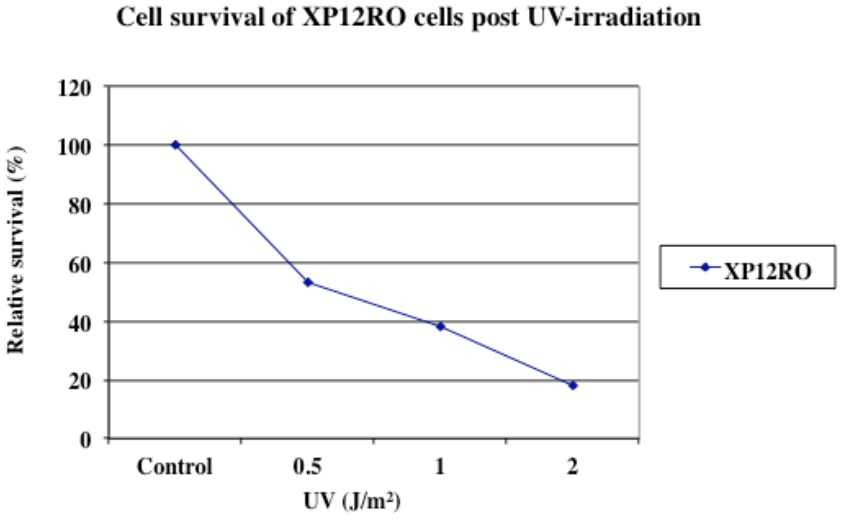

Figure 3.9.2.2 Effect of low doses of UV irradiation on XP12RO (XPA$^-$) cell survival.
Cell survival of XP12RO (XPA$^-$) cells following UV irradiation was assayed by counting cells using a trypan blue method 48 h after UV irradiation. Data represents the mean of two independent experiments.

3.9.3 Radioresistant response to p54nrb siRNA following UV irradiation.

Human cell lines were transfected with p54nrb siRNA (5 nM) and UV irradiated 72 h post-transfection. Cells were harvested at 0, 24 and 48 h post UV irradiation (72 h post-transfection = 0 h post UV irradiation) for western blot analysis.

To show that p54nrb was attenuated at 48 h post UV irradiation, western blot analysis was carried out using an antibody specific to p54nrb to detect the levels of the protein following siRNA. As a loading control an antibody raised against PCNA was used. From figure 3.9.3.1, it is evident that p54nrb protein is attenuated at 0, 24 and 48 h post UV irradiation in all of the cell lines used. Although there is an apparent accumulation of p54nrb following UV irradiation in the western blot shown, a nuclear extraction assay was performed in section 3.2.2 to address this observation and no increase of p54nrb was observed following UV irradiation. The data presented is a representative result of three independent experiments.

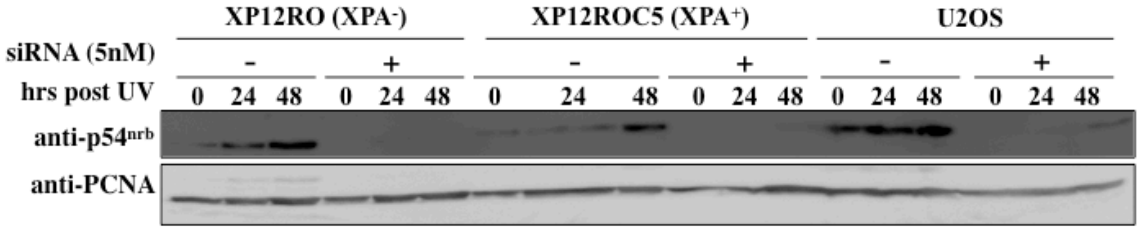

Figure 3.9.3.1 Attenuation of p54nrb expression using siRNA following UV irradiation.
Human cell lines were transfected with p54nrb siRNA (ON-TARGET*plus* Target pool) and UV irradiated 72 h post-transfection. Cells were harvested at 0, 24 and 48 h post UV irradiation to show that p54nrb was attenuated at 48 h post UV irradiation. Western blot analysis was carried out using an antibody specific to p54nrb to detect the levels of the protein following siRNA. As a loading control an antibody raised against PCNA was used. Membranes were developed using a horseradish peroxidase-conjugated secondary antibody and ECL system. Signal was detected with a Fuji LAS 3000 imager.

In order to address the issue of the attenuation of p54nrb protein on cell survival following UV irradiation in human cells, cell viability assays were performed on XP12RO (XPA-), XP12ROC5 (XPA+), and U2OS cells following siRNA.

There is a significant difference between the survival rate of siControl and sip54nrb transfected cells in the XP12RO (XPA-) cell line following UV irradiation. At 0.5 J/m^2 of UV irradiation 75% of sip54nrb cells survive in comparison to only 50% survival rate in siControl transfected cells. The difference is also evident at 1.25 J/m^2 with 33% siControl

transfected cell survival rate in comparison to 56% in sip54^{nrb} transfected cells. As the dose of UV irradiation increases to 2.5 J/m^2 there is no apparent difference between the transfected cells, see figure 3.9.3.2.

The same inclination is also evident in XP12ROC5 (XPA$^+$) cells, with a 66% survival rate of siControl transfected cells after 1.25 J/m^2 in comparison to an 88% survival rate of sip54^{nrb} transfected cells. The difference in survival rate is also evident at a higher dose of 2.5 J/m^2 with a 67% survival rate in siControl transfected cells and a 52% survival rate in sip54^{nrb} transfected cells. However, as the dose of UV irradiation increases to 5 - 10 J/m^2 there is no apparent difference between the transfected cells, See figure 3.9.3.3. This result is similar to the results obtained using the XP12RO (XPA$^-$) cells in that there is a more significant difference in the cell survival rate at a lower dose of UV irradiation. The results obtained in U2OS cells indicate that p54nrb ablation in these cells does not modify the survival to UV irradiation following transfection with siControl and sip54^{nrb}, see figure 3.9.3.4. The data presented are a representative result of three independent experiments.

These results taken together suggest that cells lacking p54^{nrb} remove UV induced DNA lesions more rapidly than those with p54^{nrb} as determined by their rate of survival. However, this is true for cells exposed to a low dose of UV irradiation, 0.5 - 1.25 J/m^2, in XP12RO (XPA$^-$) cells and 1.25 – 2.5 J/m^2 in XP12ROC5 (XPA$^+$) and U2OS cells. At a higher dose of UV irradiation the rate of survival seems to be comparable in siControl and sip54^{nrb} transfected cells in all cell lines, see figure 3.9.3.2 and figure 3.9.3.3. Our findings suggest that at a low dose of UV irradiation, the repair of DNA lesions is faster in cells lacking p54^{nrb} protein, this could indicate that p54^{nrb} plays a role in blocking access to sites of DNA damage thus operating via a distinct pathway leading to a delay in repair. Although, at a higher dose the rate of cell survival is the same in all transfected cells, which might indicate that, at a higher dose, a different repair pathway is used to carry out recognition and repair of UV induced DNA lesions. Our previous findings suggest that p54^{nrb} is a downstream target of DNA damage signalling pathway, our current findings highlight this interaction may be crucial for cell survival following UV irradiation. Alternativ suggestions for these findings are mentioned further in the thesis (see discussion section).

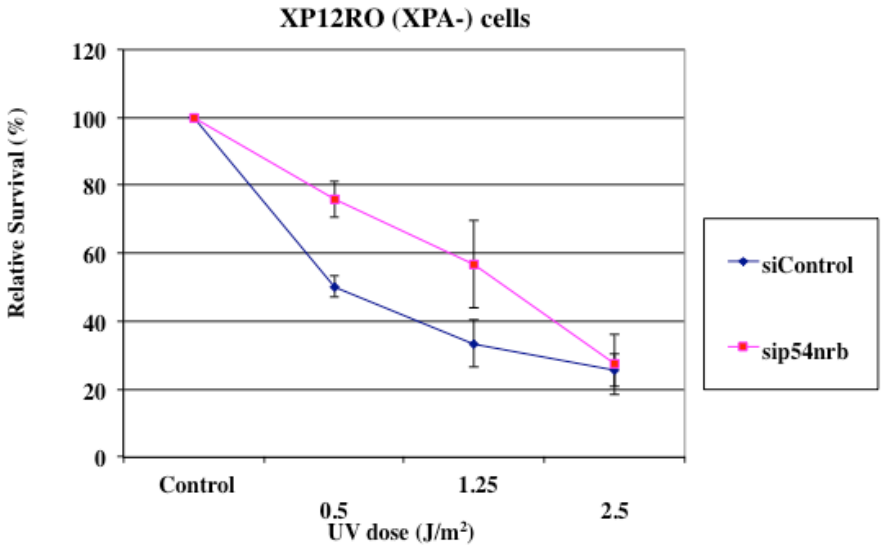

Figure 3.9.3.2 Effect of p54nrb depletion on cell survival following UV irradiation of XP12RO (XPA-) cells.
XP12RO (XPA-) cells were transfected with p54nrb siRNA (ON-TARGET*plus* Target pool) and UV irradiated 72 h post-transfection. Cell survival of XP12RO (XPA-) cells following UV irradiation was assayed by counting cells using a trypan blue method 48 h after UV irradiation. siControl represents transfection with control siRNA (ON-TARGETplus Non-targeting Pool); sip54nrb represents 5 nM of p54nrb siRNA (ON-TARGET*plus* Target pool). Data represents the mean of three independent experiments. Error bar represent the standard deviation.

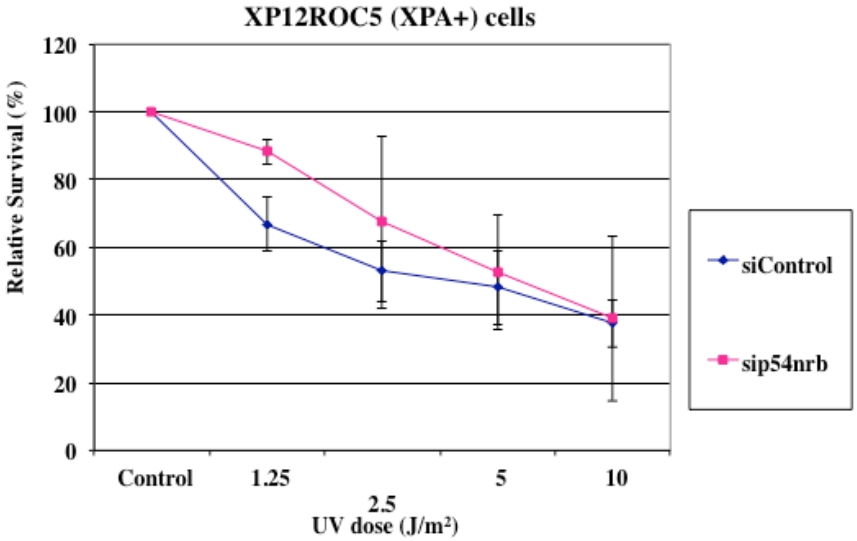

Figure 3.9.3.3 Effect of p54nrb depletion on cell survival following UV irradiation of XP12ROC5 (XPA+) cells.
XP12ROC5 (XPA+) cells were transfected with p54nrb siRNA (ON-TARGET*plus* Target pool) and UV irradiated 72 h post-transfection. Cell survival of XP12ROC5 (XPA+) cells following UV irradiation was assayed by counting cells using a trypan blue method 48 h after UV irradiation. siControl represents transfection with control siRNA (ON-TARGETplus Non-targeting Pool); sip54nrb represents 5 nM of p54nrb siRNA (ON-TARGET*plus* Target pool). Data represents the mean of three independent experiments. Error bar represent standard deviation.

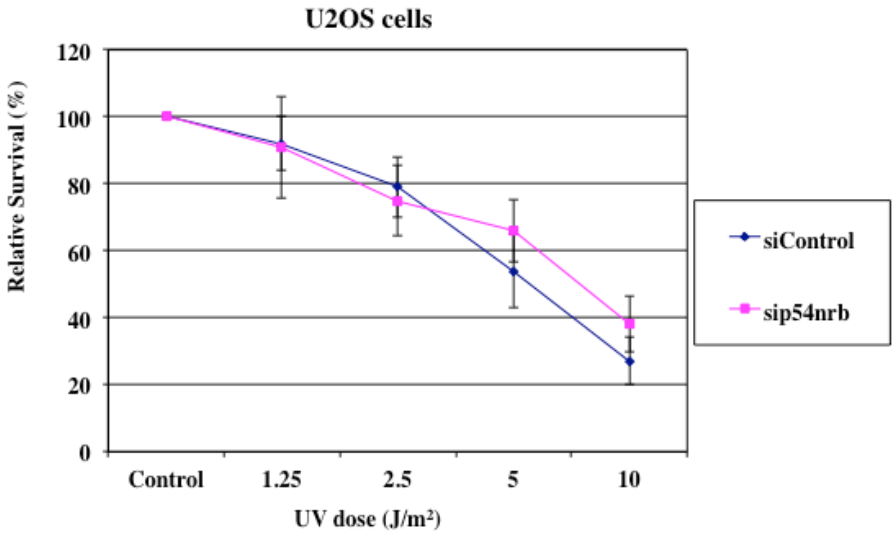

Figure 3.9.3.4 Effect of p54nrb depletion on cell survival following UV irradiation of U2OS cells.
U2OS cells were transfected with p54nrb siRNA (ON-TARGET*plus* Target pool) and UV irradiated 72 h post-transfection. Cell survival of U2OS cells following UV irradiation was assayed by counting cells using a trypan blue method 48 h after UV irradiation. siControl represents transfection with control siRNA (ON-TARGETplus Non-targeting Pool); sip54nrb represents 5 nM of p54nrb siRNA (ON-TARGET*plus* Target pool). Data represents the mean of three independent experiments. Error bar represent one standard deviation.

Chapter 4 - Discussion

The human genome codes for approximately 20,000 genes. The complex function of a human body requires that proteins possess dual or multiple roles from gene regulation to genomic stability through RNA biology and DNA repair, which has been more and more appreciated in recent years (Adamson et al., 2012; Beli et al., 2012; Polo et al., 2012). The protein p54^{nrb} is profoundly involved in transcription (see figure 4.1). Its roles in human cells ranges from activating mRNA splicing factors, to enhancing the activity of the CTD domain of RNA pol II for successful completion of gene expression (Emili et al., 2002; Peng et al., 2002). Recent reports have identified p54^{nrb} on its own, and as a heterodimer with PSF, is transiently recruited with the same kinetics to sites of DNA double-strand breaks (DSBs) induced by a laser track in human cells to allow non-homologous end joining (NHEJ) as well as homologous recombination (HR) to take place (Ha et al., 2011; Kuhnert et al., 2012; Salton et al., 2010).

Figure 4.1 p54^{nrb} performs multiple roles in RNA biogenesis
p54^{nrb} plays an integral role in RNA biogenesis. p54^{nrb} interacts with RNA pol II to perform various activities followed by roles in mRNA processing. Image adapted from (Karp, 2007).

Identification of the protein p54^{nrb} as a target of UV damage response pathways

Recently the laboratory identified p54^{nrb} as a protein being associated with minichromosomes after UV irradiation by performing mass spectrometry analysis (Anhold, 2007). p54^{nrb} protein has not previously been reported in the DNA damage response following UV irradiation. Data presented here show that p54^{nrb} translocates to the nucleolus

in a time- and dose-dependent manner after UV irradiation. However, it was found that $p54^{nrb}$ nucleolar enrichment is not limited to UV damage as immunofluorescence analyses showed that $p54^{nrb}$ also localises to the nucleolus in human cells in response to γ-irradiation (data not shown). These data, highlighting an enrichment of $p54^{nrb}$ in the nucleolus after UV irradiation, have not previously been reported and bring to light a number of possibilities for this protein's role in the UV DNA damage response pathway.

Damage induced by UV irradiation results in the formation of bulky adducts such as CPDs and 6-4 PPs. To deal with these UV-induced lesions cells trigger several processes to conserve their genomic integrity (see figure 4.2). UV-induced lesions are recognised by repair machinery, these are transcription-coupled repair (TCR) and global genome repair (GGR), to allow the cell to undergo normal gene expression and replication. The cellular response to DNA damage may activate cell-cycle checkpoints by a network of signaling pathways that gives cells extra time to repair the genomic lesions. Alternatively cells may induce apoptosis, which leads to cell death. UV irradiation may also disrupt the structure of the nucleolus and induces a nucleolar stress response. Using the above mentioned repair pathways as focal points for our investigation, we conducted detailed molecular and cellular analysis to characterise $p54^{nrb}$ in the UV DNA damage response pathway following UV irradiation. We specifically looked at the role of $p54^{nrb}$ at blocked transcription sites that leads to transcription coupled repair, the DNA-damage signaling pathway that recruits protein kinases such as ATM and ATR to investigate if $p54^{nrb}$ is a possible downstream target of these kinases and also the localisation of $p54^{nrb}$ in the nucleolus following UV irradiation and the domain required for this action (figure 4.2).

Figure 4.2 Proposed role of p54^{nrb} in DNA damage response pathways activated by UV-induced DNA lesions
UV-induced DNA lesions trigger various DNA damage response pathways such as transcription-coupled repair (TCR), DNA damage signalling yielding cell-cycle arrest or cell death, and nucleolar stress response. Image adapted from (Lindsey-Boltz and Sancar, 2007).

Protein regions of p54^{nrb} required for its recruitment to nucleoli after UV irradiation of cells

The 54-kDa nuclear RNA-binding protein called p54^{nrb} contains a *Drosophila* behaviour human splicing (DBHS) protein-core, two tandem RNA recognition motifs (RRM) and a 100-aa segment of a predicted helix-turn-helix (HTH) structure at its C terminus. The latter is putatively responsible for protein-protein interactions with itself and two other members of the DBHS family, namely PSF and PSP1 (see figure 4.3). N-terminally GFP-tagged p54^{nrb} deletion mutants were generated and their transient expression was analysed in human fibroblast cells. Full length p54^{nrb} fused to GFP behaves similarly to the wild type protein whereas the deletion mutant p54^{nrb}ΔRRM (deletion of the N-terminal half of p54^{nrb} including both RNA recognition motifs) fused to GFP is recruited to peri-nucleolar sites in unperturbed human cells, which differs to the endogenously expressed p54^{nrb}. However, following UV damage, GFP-p54^{nrb}ΔRRM is still recruited to the nucleolus. These investigations reveal that the RRM domain of p54^{nrb} is not critical for its localisation to the nucleolus following UV irradiation; however the RRM domain must play a role in the regulation of p54^{nrb} functions in the nucleus as the protein's distribution is disturbed when these domains are removed. Similarly, when Fox et al deleted the RRM domains of PSP1 the protein behaved similarly to the endogenous PSP1, however, PSP1 without RRM

domains was shown to localise to sites surrounding the nucleolus (Fox et al., 2005). This is consistent with the finding of Ha et al, that deleting the RRM1 domain of PSF leads to the accumulation of the protein at bright foci surrounding the nucleolus, but they did not observe this behaviour when the RRM2 domain was deleted (Ha et al., 2011). It is possible that deletion of the RRM domains of $p54^{nrb}$ enhances its ability to interact with another paraspeckle partner, however, not disrupting its nucleolar function following UV irradiation. In contrast, the GFP-$p54^{nrb}$ΔHTH construct (deletion of the C terminus including the helix-turn-helix domain) behaves differently to endogenous $p54^{nrb}$ protein and does not accumulate in the nucleus. By deleting the HTH domain of PSP1, its heterodimerisation with $p54^{nrb}$ was ablated (Fox et al., 2005). It has been previously shown that $p54^{nrb}$ interacts with PSF via its DBHS domain (Peng et al., 2002; Zhang et al., 1993). Other reports showed that sequences in PSF that interact with $p54^{nrb}$ are responsible for the recruitment of the $p54^{nrb}$/PSF complex to sites of DNA damage. Deleting the HTH domain of $p54^{nrb}$ leads to the disruption of its interaction with PSF, which could lead to the loss of nucleolar localisation of $p54^{nrb}$ following UV irradiation (Ha et al., 2011; Kuhnert et al., 2012).

Figure 4.3 $p54^{nrb}$ interacts with other paraspeckles via its DBHS domain
$p54^{nrb}$ performs various functions with its partner proteins PSP1 and PSF, with whom it interacts via its DBHS sequence conservation region. Image adapted from (Shav-Tal and Zipori, 2002).

RNA as a mediator of p54^{nrb} nucleolar recruitment after DNA damage

The findings observed in this work showed that active RNA, and not DNA, was required for the relocalisation of p54^{nrb} to the nucleolus following UV irradiation as it was determined that the nucleolar accumulation of p54^{nrb} was disturbed following RNase A treatment, suggesting that an interaction with active RNA plays a vital role for p54^{nrb} enrichment in the nucleolus. Similar work was performed by Fox et al., they showed that RNA was required for paraspeckle integrity (Fox et al., 2005). Also, using fibrillarin as a nucleolar marker, colocalisation of p54^{nrb} and fibrillarin in the nucleolus was observed after UV irradiation of cells. However, both proteins are dispersed throughout nuclei of UV-treated cells when treated with RNase A as oberved by immunofluorescence microscopy. Since fibrillarin is a snRNP protein that is located in the dense fibrillar centre (DFC) of the nucleolus and is required for splicing of rRNA, these immunofluorescence microscopy data present a possible link between p54^{nrb} and fibrillarin splicing activity in the nucleolus following UV irradiation.

Previous studies have investigated the relocalisation of p54^{nrb} to concave cap-like structures, known as peri-nucleolar caps, upon treatment of cells with actinomycin-D that inhibits RNA pol I (low concentration of actinomycin-D) or RNA pol I plus II together (high concentration of actinomycin-D) (Andersen et al., 2002; Fox and Lamond, 2010; Shav-Tal et al., 2005). UV irradiated cells that were pre-treated with low and high concentrations of actinomycin-D show that p54^{nrb} remains at peri-nucleolar caps indicating that active RNA pol I and II transcription is required for the enrichment of p54^{nrb} to nucleoli. However, p54^{nrb} has been shown to interact with the carboxy-terminal domain (CTD) of the largest subunit of RNA pol II to perform its transcriptional activities, (Emili et al., 2002), therefore we wanted to investigate if nucleolar enrichment of p54^{nrb} was specific to RNA pol II activity. UV irradiated cells that were pre-treated with α-amanitin show an enrichment of p54^{nrb} to surrounding areas of the nucleolus. Nucleolar integrity was completely disturbed following α-amanitin treatment, as observed by the disrupted staining pattern of UBF 1/2, a critical factor in the regulation of rDNA transcription, which normally resides in the nucleolus. Taken together these results suggest that factors involved in RNA biogenesis, particularly RNA pols I and II, and nucleolar integrity are required for sequestering and maintaining p54^{nrb} in the nucleolus after UV irradiation.

RNA pol II has a well established role in transcription, but in the last number of years extensive work has been carried out RNA pol II and its role in the DNA damage response (Lindsey-Boltz and Sancar, 2007). During transcription, RNA pol II stops when it encounters bulky lesions such as UV-induced thymine dimers (Selby et al., 1997). Stalled RNA pol II is recognised by a class of translocases called transcription-repair coupling factors that bind to both the stalled polymerase and nucleotide excision repair factors to recruit the repair factors to the site of damage and begin repair (Selby and Sancar, 2003). Brueckner et al provided a structure based mechanism for the CPD-induced stalling of RNA pol II (Brueckner et al., 2007). This work, taken together with our results, suggests that p54^{nrb} localises to nucleoli in response to UV irradiation in a RNA pols I and II-dependent manner. Our results also reveal that p54^{nrb} requires active RNA pols I and II to perform its nucleolar activity following UV irradiation.

We hypothesise that once RNA pol II encounters a DNA lesion it sequesters p54^{nrb} to the nucleolus to allow for transcription-coupled repair to take place (see figure 4.4). We hypothesise that p54^{nrb} blocks access to sites of DNA damage whilst binding to RNA pol II and the UV-induced lesions cannot be recognised efficiently by the transcription-coupled repair proteins.

Figure 4.4 p54^{nrb} nucleolar enrichment following UV irradiation.
p54^{nrb} requires active RNA pols I and II for recruitment to nucleoli following UV irradiation. We hypothesise that p54^{nrb} prevents RNA pol II from successfully activating the transcription-coupled repair (TCR) pathway and therefore p54^{nrb} is displaced to the nucleolus to allow RNA pol II to activate TCR efficiently (Vilmar and Sorensen, 2009)

Local UV damage and the p54^{nrb} response to sites of DNA damage

Recent reports have identified p54^{nrb} on its own and in a heterodimer with PSF, transiently recruited with the same kinetics to sites of DNA double-strand breaks (DSBs) induced by a laser track in human cells by means of non-homologous end joining (NHEJ) as well as homologous recombination (HR) (Ha et al., 2011; Kuhnert et al., 2012; Salton et al., 2010).

To test whether UV irradiation of specific nuclear regions recruit p54^{nrb} to these areas local UV irradiation experiments were performed but endogenously expressed p54^{nrb} protein could not be detected at DNA damaged sites under the conditions used (see Materials and Methods, chapter 2, section 2.9). To investigate the hypothesis that the nucleolus had to be irradiated specifically to instigate nucleolar enrichment of p54^{nrb} in response to UV induced DNA damage "laser stripe experiments" were performed whereby specific areas of the cell were subjected to laser-induced damage and these areas were identified by the phosphorylated form of histone H2AX, called γH2AX. Under the conditions used (see section 2.9), p54^{nrb} accumulation at laser induced damage areas was not observed.

Adamson et al identified that the RNA binding protein RBMX as a component of the DNA damage response by performing a genome-wide siRNA-based screen (Adamson et al., 2012). However, they failed to detect the accumulation of endogenously expressed RBMX protein at damage induced foci. In contrast, they found that 20-40% of cells showed GFP-RBMX localisation to DNA damage but when they depleted endogenous RBMX by siRNA, the number cells showing GFP-RBMX localisation to DNA damage increased. They suggest that background chromatin binding of the endogenous RBMX protein interferes with the detection of endogenous RBMX at DNA damage. Similarly, a change in distribution of endogenously expressed p54^{nrb} was not seen following the induction of localised sites of DNA damage and could be as a result of its chromatin binding properties. Beli et al identified the RNA-associated, THRAP3 protein as a DNA damage response factor but failed to identify the protein at DNA damage sites (Beli et al., 2012). Although many factors involved in the DDR are recruited to damage sites (Polo and Jackson, 2011), it is reasonable to assume that p54^{nrb}, although partakes in the DNA damage response, is absent from UV-induced damage sites and is not directly associated with UV-induced foci as observed by immunofluorescence microscopy under the conditions used. However, as

mentioned, other reports have identified p54^{nrb} at sites of laser induced DNA damage (DSB laser induced foci) within a short time frame directly after laser exposure of cells which is in a different time frame to the p54^{nrb} recruitment to nucleoli observed in this work (Krietsch et al., 2012; Kuhnert et al., 2012).

p54^{nrb} protein localised in the nucleolus following UV irradiation (as early as 30 min post-2.5 J/m^2 in XP12RO (XPA$^-$) cells) and this nucleolar enrichment occurs in a time- and dose-dependent manner. In contrast, after the induction of DSBs, p54^{nrb} is transiently recruited to sites of DNA damage as rapidly as 30 sec and only remains there for a short time (up to 10 min) (Krietsch et al., 2012; Kuhnert et al., 2012). By performing co-immunoprecipitation experiments we observed a loss of interaction between p54^{nrb} and TopBP1 following UV irradiation. Taking these results into consideration, it is reasonable to assume that p54^{nrb} may partake in opposite, yet interconnected functions in regards to the DNA damage response. Further investigations would need to be performed to address this hypothesis in further detail and to gain a better understanding into the mechanism and kinetics involved in the localisation of p54^{nrb} to the nucleolus after DNA damage in UV irradiated cells in comparison to localisation of p54^{nrb} to laser induced foci (particularly DSB foci).

p54^{nrb} negatively interferes with the UV DNA damage response pathway

This hypothesis is in agreement with the findings that cells with an attenuation of p54^{nrb} by siRNA, exhibited higher survival number after UV damage at low doses of UV irradiation. This result provides the base for the hypothesis that p54^{nrb} may have a negative impact on specific cells following UV exposure. Recently, various proteins have been shown to accumulate in nucleoli after UV damage. Rad9B, a protein that interacts with the 9-1-1 complex, localises to the nucleolus through ATR signalling and delays the G_1-S checkpoint transition; the report speculates that this localisation may have a function in maintaining genome stability (Perez-Castro and Freire, 2012). It is also important to note that Perez-Castro et al performed micropore experiments and did not observe a redistribution of Rad9B under these conditions. Similarly the tumour suppressor ING1 accumulates in the nucleolus after UV irradiation and sensitises cells to apoptosis (Scott et al., 2001). To add

to this, p21 and p53 proteins localises to the nucleolus by active signalling upon nucleolar stress (namely UV irradiation) (Abella et al., 2010; Karni-Schmidt et al., 2008).

The results observed here suggest that $p54^{nrb}$ negatively interferes with the response of cells to damaging DNA with UV and that sequestering of $p54^{nrb}$ to the nucleolus could be a cellular process to prevent distinct repair activities from taking place in the nucleolus. It is established that transcription-coupled repair takes place in mammalian genes transcribed by RNA pol II but not in ribosomal RNA genes (rDNA) and that the removal of UV-induced CPDs from rDNA in repair proficient human cells has been shown to be slower (Christians and Hanawalt, 1993; Christians and Hanawalt, 1994). The localisation of $p54^{nrb}$ to the nucleolus after UV irradiation may contribute to slowing down transcription-coupled repair or prevent the removal of CPDs in the nucleolus.

DNA damage signalling pathways involved in the recruitment of $p54^{nrb}$ to nucleoli

Following DNA damage, DNA repair and cell cycle checkpoints are the main processes of maintenance and stability of the genome. These processes are highly complex, involve many cellular factors and form an extensive signal transduction network. The DNA damage response is initiated by the activation of members of the phosphatidylinositol 3-kinase (PI-3) superfamily, namely ATR, ATM, and DNA-PK. Once activated, these kinases phosphorylate specific substrates, particularly Chk1 and Chk2, initiating signal transduction cascades that result in cell cycle arrest and DNA repair (Ciccia and Elledge, 2010; Zhou and Sausville, 2003). Collectively, it was aimed to elucidate if and which of these signalling factors influence the nucleolar localisation of $p54^{nrb}$ after UV-induced DNA damage occurred. The general PIK kinase inhibitors, Caffeine and Wortmannin, abrogated the enrichment of $p54^{nrb}$ to the nucleolus following UV irradiation. Caffeine and Wortmannin have been extensively used to study ATM, ATR and DNA-PK signalling and checkpoint kinases (Bode and Dong, 2007; Furgason and Bahassi, 2012; Sarkaria et al., 1999; Sarkaria et al., 1998). This result showed that $p54^{nrb}$ nucleolar recruitment was sensitive to these inhibitors and led us to believe that nucleolar localisation of $p54^{nrb}$ following UV damage was dependent on PIK kinase signalling. However, these inhibitors are relatively non-selective and have been shown to have many additional effects other than inhibiting PIK kinase signalling pathways (Sarkaria et al., 1999; Sarkaria et al., 1998).

Therefore, additional highly specific PIK kinase inhibitors were introduced and their influence on p54^{nrb} nucleolar localisation was investigated. Interestingly, ATM and DNA-PK inhibitors either alone or combined together, did not affect the localisation of p54^{nrb} to the nucleolus after UV induced DNA damage, suggesting that these PIK kinases alone did not play a role to in the translocation of p54^{nrb} to the nucleolus after DNA damage. Surprisingly, when cells were treated with a specific ATR inhibitor p54^{nrb} was redistributed to the periphery of the nucleolus after UV irradiation. This result revealed that the function of p54^{nrb} in the nucleolus was dependent on functional ATR activity, however, p54^{nrb} still aggregated to the periphery of the nucleolus indicating that perhaps its relocalisation was still induced by the presence of other PIK kinases. To eliminate this, cells were pre-treated with combined ATR and DNA-PK inhibitors before UV irradiating the cells and found that p54^{nrb} still accumulated to the periphery of the nucleolus. Interestingly, when the same experiment was performed with combined ATR and ATM inhibitors the localisation pattern of p54^{nrb} was comparable to that of untreated cells, diffuse staining in the nucleus with no apparent accumulation in the nucleolus, indicating that the dual function of ATR and ATM kinase activity regulated the nucleolar enrichment of p54^{nrb} after UV-induced DNA damage. These results showed that the nucleolar enrichment of p54^{nrb} is controlled via a distinct pathway that involved both transcription and DNA repair signalling pathway.

It has been well established that RNA pol II stalls when it encounters bulky lesions, such as UV-induced thymine dimers, and triggers the commencement of transcription-coupled repair factors (Selby et al., 1997). Specifically, Jiang et al showed that RPA and ATR preferentially accumulate on transcribed DNA sequences after UV irradiation presumably at sites of blocked RNA polymerases (Jiang and Sancar, 2006). To accentuate this recent report, RPA is known to play a role in transcription-coupled repair by binding to ssDNA at the transcription bubble although at the same time, is known to recruit ATR via ATRIP to sites of DNA damage thus activating the DNA damage response pathway (Derheimer et al., 2007). In addition, TopBP1 plays a crucial role in binding to ATR and enhancing its kinase activity (Kumagai et al., 2006). Recently, Kuhnert et al showed that TopBP1 interacted with p54^{nrb} *in vivo* (Kuhnert et al., 2012). By performing co-immunoprecipitation experiments we observed a loss of interaction between p54^{nrb} and TopBP1 following UV irradiation therefore it is reasonable to hypothesise that ATR through its interaction with

TopBP1 regulates the nucleolar enrichment of p54^{nrb} following UV irradiation and that enrichment of p54^{nrb} to the nucleolus allows DNA repair to occur. It is evident from the results presented here that both ATM and ATR activity need to be inhibited to abrogate p54^{nrb} nucleolar enrichment suggesting that they function together in controlling the recruitment of p54^{nrb} to nucleoli. This proposed model is consistent with the knowledge that they have overlapping functions in many processes (Abraham, 2001; Brown and Baltimore, 2003; Stiff et al., 2006).

Following the discovery that inhibition of ATR and ATM reduced the enrichment of p54^{nrb} to the nucleolus, the question was addressed about the involvement of p54^{nrb} in the downstream signal transduction cascade. ATR and ATM are phosphorylated following DNA damage, which in turn activate further downstream targets of the DDR signalling cascade specifically the Chk1 and Chk2 kinases (Abraham, 2001; Kastan and Bartek, 2004). Chk1 and Chk2 play a critical role in determining cellular responses to DNA damage. The inhibition of Chk2 kinase with a specific inhibitor abrogated nucleolar enrichment of p54^{nrb} after UV DNA damage of cells. In contrast, p54^{nrb} localised to the nucleolus after UV irradiation of cells in Chk1 siRNA-treated cells, suggesting that Chk1 does not play a direct role in the nucleolar enrichment of p54^{nrb}. This led us to believe that the activation of Chk2 via the ATM/ATR signalling pathway was responsible for the translocation of p54^{nrb} to the nucleolus. Although effects of Chk1 and Chk2 on downstream pathways share some similarities, inhibition of Chk1 and Chk2 have profoundly different outcomes as highlighted by our results on p54^{nrb} nucleolar enrichment which is consistent with previously shown findings of Ashwell and Zabludoff (Ashwell and Zabludoff, 2008). Our findings are also in agreement with the knowledge that both ATR and ATM sensors activate downstream effector target Chk2 and thus it is not unusual that Chk2 can be activated through ATR as well as ATM (Pabla et al., 2008; Stiff et al., 2008; Yang et al., 2003).

Taking our results into consideration, it is reasonable to assume that translocation of p54^{nrb} to the nucleolus is controlled by the dual acivation of ATR and ATM is initiated by transcriptional stress induced by UV irradiation and signals p54^{nrb} to localise in the nucleolus (see figure 4.5). However, it seems that the inhibition of ATR is a prerequisite for the initiation of the signal transduction cascade.

Figure 4.5 p54^{nrb} requires dual ATR/ATM signaling to localise to the nucleolus.
UV irradiation stalls transcription and triggers the initiation of transcription-coupled repair and DNA damage signalling pathways. The migration of p54^{nrb} to the nucleolus allows RNA pol II to perform its functions in transcription coupled repair. The migration of p54^{nrb} to the nucleolus also requires the dual acivation of ATR and ATM is initiated by transcriptional stress induced by UV irradiation. Image adapted from (Lindsey-Boltz and Sancar, 2007).

Chapter 5 - Conclusion and Future directions

The regulatory networks of the DNA damage response (DDR) encompass many proteins and distinctive repair pathways. These DNA repair processes are activated when the cell encounters DNA damage. UV-induced bulky lesions that distort the DNA backbone are mainly repaired by nucleotide excision repair (NER). NER is a complex multiprotein system that repairs DNA by two processes GGR and TCR that differ by their mechanisms of DNA lesion recognition. However, when NER is jeopardized by the inability to repair UV-induced lesions due to dysfunctional mutated proteins it has severe negative effects on the cell and results in diseases such as xeroderma pigmentosum and Cockayne syndrome. Although these inherited diseases display different phenotypes each defect can arise from mutations present in more than one gene. Conversely, different mutations in the same gene can give rise to a variety of clinical phenotypes. These findings highlight the broadness of the NER response pathway and the consequences of defects in this pathway.

Cells derived from a xeroderma pigmentosum type A patient were predominantly used in this study. Using these skin fibroblast cells it was determined that the transcription-associated $p54^{nrb}$ protein translocates to the nucleolus in a time- and dose-dependent manner following UV irradiation as determined by immunofluorescence microscopy and nucleolar purification procedures. Further to this, we determined that the C-terminus is required for the localisation of $p54^{nrb}$ to the nucleolus, highlighting the dual roles of $p54^{nrb}$ in RNA- and DNA-associated activities. The localisation of $p54^{nrb}$ to nucleoli after UV is sensitive to treatment with Caffeine and Wortmannin suggesting the involvement of kinases in the process, which are related to phosphatidylinositol kinases such as ATM and ATR. The use of ATM- and ATR-specific inhibitors revealed that both DNA damage response kinases co-operate in the regulation of $p54^{nrb}$ localisation in the nucleolus after UV treatment. Knocking down of $p54^{nrb}$ in human cells increased the survival of treated cells at low doses. These results suggest that $p54^{nrb}$ may negatively interfere with the response of cells to DNA damage via the NER and transcription-coupled repair pathway and that sequestering of $p54^{nrb}$ to the nucleolus could be a cellular process to allow an optimal response of cells to repair UV-induced DNA damage.

Figure 5.1 Schematic figure summarising the major findings.
The objective of this study was to gain a better insight into the mechanism(s) by which p54^{nrb} is involved in the DNA damage response following UV irradiation, primarily using human cells as a model system. Immunofluorescence microscopy using human cells showed that p54^{nrb}, a 54-kDa nuclear RNA-binding protein, is recruited to nucleoli after UV irradiation. This recruitment depends on transcription since inhibition of transcription abolishes the DNA damage-dependent recruitment of p54^{nrb}. We propose that once RNA pol II encounters a DNA lesion it sequesters p54^{nrb} to the nucleolus to allow for transcription-coupled repair to take place and that p54^{nrb} blocks access to sites of DNA damage whilst binding to RNA pol II and the UV-induced lesions cannot be recognised efficiently by the transcription-coupled repair proteins. DNA damage signalling (PIK kinases) drug inhibitors reduce p54^{nrb} nucleolar localisation following UV irradiation that suggests that p54^{nrb} could be a downstream target of these factors. Notably, the use of ATM- and ATR-specific inhibitors revealed that both DNA damage response kinases cooperate in the regulation of p54^{nrb} recruitment to the nucleolus after UV treatment. Depletion of p54^{nrb} demonstrates higher cell viability following UV irradiation. Model consistent with data is that sequestering of p54^{nrb} to the nucleolus could be a cellular mechanism to allow an optimal response of cells to repair DNA damage.

XP12RO (XPA^-) cells are more sensitive to UV damage due to their lack of XPA protein and are unable to cope with UV-induced lesions as a result of this. Using these cells $p54^{nrb}$ was observed in the nucleolus following UV irradiation. However, this phenomenon was not confined to these cells as this recruitment of $p54^{nrb}$ was observed in a number of cell lines. For future directions it would be of particular interest to investigate if all XP patients displayed $p54^{nrb}$ nucleolar accumulation at very low doses, for example XPC patients fail to recognise DNA lesions due to defective global genome repair. It would be interesting to investigate if $p54^{nrb}$ protein behaves similarly in these defective cell lines and if the recognition of a DNA lesion by NER proteins is imperative for the translocation of $p54^{nrb}$ to the nucleolus.

As a follow up to this, it would be worthwhile to investigate whether $p54^{nrb}$ nucleolar localisation plays a role in the differential mechanism in the recognition of CPDs and 6-4 PPs in rDNA. It is known that transcription-coupled repair and CPDs are recognized less efficiently in the nucleolus. The translocation of $p54^{nrb}$ to the nucleolus may prevent repair of DNA lesions, particularly CPD lesions induced on rDNA. Since $p54^{nrb}$ recruitment itself to UV induced damage sites was not detected under the conditions used it is assumed that $p54^{nrb}$ binding to damaged sites does not play a role in the DNA damage-signalling pathways studied.

The PIK kinases are key signal transducers in controlling cellular responses to genotoxic stress. The issue of $p54^{nrb}$ as a target of PIK kinase signalling is an intriguing one that could be usefully explored in further research. However, considerably more work will need to be done to determine the connection between $p54^{nrb}$ and the DNA damage signalling response pathway following UV irradiation. Although the study presented here gives an indication that $p54^{nrb}$ is a target of ATR/ATM kinase activity and their downstream target Chk2, to prove that $p54^{nrb}$ presents itself as a checkpoint regulator further work will need to be performed to tackle this issue. It would be interesting to assess whether a direct interaction exists between $p54^{nrb}$ protein and these signalling kinase proteins. This would allow us to investigate if these kinases or other members of the signalling cascade instigate the localisation of $p54^{nrb}$ to the nucleolus. One method would be to use a peptide IP with phosphotyrosine antibodies, ATM and ATR share substrate specificity and both recognise (SQ) and (TQ) motifs. This would address the question of $p54^{nrb}$ being phosphorylated as a

downstream target of these kinases. Another method would be to perform a kinase assay with ATR and ATM and recombinant p54^{nrb}.

Reports by other groups have explored the possibility that the cellular function of p54^{nrb} depends on the localisation of p54^{nrb} (Krietsch et al., 2012; Kuhnert et al., 2012). It is well established that p54^{nrb} functions in many processes in the cell, here we provide evidence that after UV irradiation p54^{nrb} is recruited to the nucleolus. The migration of p54^{nrb} to the nucleolus could represent a quality control mechanism of the cell to allow the cell to deal with UV lesions present on the DNA. Perhaps the cell reaches a certain threshold (of damage induced lesions) before it requires nucleolar accumulation of p54^{nrb} to sustain or disrupt the protein's other functions in the cell and p54^{nrb} recruitment serves as a balance or 'switch" between (1) to continue transcription and splicing activities with RNA pol II or (2) localising to the nucleolus to allow repair the UV-induced lesions. Thus, p54^{nrb} may act as a regulator to decide if the cell should repair a UV-induced lesion or to continue transcription, p54^{nrb} may decide which is more detrimental to the cell. Together these future directions may culminate in further proof of our hypothesis that lesion specific proteins required for signaling are recruited to sites damage via p54^{nrb} as a regulator.

The translocation of p54^{nrb} to the nucleolus after UV induced DNA damage having a positive impact on cell survival raised the posibility of the protein functioning in apoptosis. The nucleolus is an organelle that partakes in the early events of RNA processing and may be a prefered intracellular target for apoptotic events because if you inhibit these processes it would prevent the formation of ribosomes and consequently block further cellular activities. It would be of interest to examine if the attenuation of p54^{nrb} renders the cells ability to activate the apoptotic pathway successfully. To follow this up, proteomic analysis such as a western blot could be performed to detect proteins that posses roles in the apoptotic pathway such as, a caspase 3 protein, which is a key apoptotic player. Together these future directions as well as those proposed above may culminate in further proof of our hypothesis that sequestering of p54^{nrb} to the nucleolus could be a cellular mechanism to allow an optimal response of cells to repair DNA damage.

References

Abella, N., S. Brun, M. Calvo, O. Tapia, J.D. Weber, M.T. Berciano, M. Lafarga, O. Bachs, and N. Agell. 2010. Nucleolar disruption ensures nuclear accumulation of p21 upon DNA damage. *Traffic*. 11:743-755.

Abraham, R.T. 2001. Cell cycle checkpoint signaling through the ATM and ATR kinases. *Genes Dev*. 15:2177-2196.

Adamson, B., A. Smogorzewska, F.D. Sigoillot, R.W. King, and S.J. Elledge. 2012. A genome-wide homologous recombination screen identifies the RNA-binding protein RBMX as a component of the DNA-damage response. *Nat Cell Biol*. 14:318-328.

Al-Baker, E.A., J. Boyle, R. Harry, and I.R. Kill. 2004. A p53-independent pathway regulates nucleolar segregation and antigen translocation in response to DNA damage induced by UV irradiation. *Exp Cell Res*. 292:179-186.

Andersen, J.S., Y.W. Lam, A.K.L. Leung, S.-E. Ong, C.E. Lyon, A.I. Lamond, and M. Mann. 2005. Nucleolar proteome dynamics. *Nature*. 433:77-83.

Andersen, J.S., C.E. Lyon, A.H. Fox, A.K.L. Leung, Y.W. Lam, H. Steen, M. Mann, and A.I. Lamond. 2002. Directed proteomic analysis of the human nucleolus. *Curr Biol*. 12:1-11.

Anhold, H. 2007. Protein recruitment to chromatin after UV damage of DNA. *In* Biochemistry. National University of Ireland, Galway, Galway.

Ashwell, S., and S. Zabludoff. 2008. DNA damage detection and repair pathways--recent advances with inhibitors of checkpoint kinases in cancer therapy. *Clin Cancer Res*. 14:4032-4037.

Basu, A., B. Dong, A.R. Krainer, and C.C. Howe. 1997. The intracisternal A-particle proximal enhancer-binding protein activates transcription and is identical to the RNA- and DNA-binding protein p54nrb/NonO. *Mol Cell Biol*. 17:677-686.

Batty, D., V. Rapic'-Otrin, A.S. Levine, and R.D. Wood. 2000. Stable binding of human XPC complex to irradiated DNA confers strong discrimination for damaged sites. *J Mol Biol*. 300:275-290.

Beli, P., N. Lukashchuk, S.A. Wagner, B.T. Weinert, J.V. Olsen, L. Baskcomb, M. Mann, S.P. Jackson, and C. Choudhary. 2012. Proteomic investigations reveal a role for RNA processing factor THRAP3 in the DNA damage response. *Mol Cell*. 46:212-225.

Berg, J.M., Tymoczko, J.L, Stryer, L. 2002. Eukaryotic transcription and translation are separated in space and time. *In* Biochemistry. W H Freeman, New York.

Bernstein, K.A., and R. Rothstein. 2009. At loose ends: Resecting a double-strand break. *Cell*. 137:807-810.

Bladen, C.L., D. Udayakumar, Y. Takeda, and W.S. Dynan. 2005. Identification of the polypyrimidine tract binding protein-associated splicing factor.p54(nrb) complex as a candidate DNA double-strand break rejoining factor. *J Biol Chem*. 280:5205-5210.

Blow, J.J., and X. Quan Ge. 2009. Conserved steps in eukaryotic DNA replication. *In* Molecular themes in DNA replication. Royal Society of Chemistry, Lynne S. Cox.

Bode, A.M., and Z. Dong. 2007. The enigmatic effects of caffeine in cell cycle and cancer. *Cancer Lett*. 247:26-39.

Bomgarden, R.D., P.J. Lupardus, D.V. Soni, M.C. Yee, J.M. Ford, and K.A. Cimprich. 2006. Opposing effects of the UV lesion repair protein XPA and UV bypass polymerase eta on ATR checkpoint signaling. *EMBO J*. 25:2605-2614.

Bond, C.S., and A.H. Fox. 2009. Paraspeckles: nuclear bodies built on long noncoding RNA. *J Cell Biol*. 186:637-644.

Broderick, R., and H.P. Nasheuer. 2009. Regulation of Cdc45 in the cell cycle and after DNA damage. *Biochem Soc Trans*. 37:926-930.

Broderick, R., S. Ramadurai, K. Toth, D.M. Togashi, A.G. Ryder, J. Langowski, and H.P. Nasheuer. 2012. Cell cycle-dependent mobility of Cdc45 determined in vivo by fluorescence correlation spectroscopy. *PLoS One*. 7:e35537.

Brown, E.J., and D. Baltimore. 2003. Essential and dispensable roles of ATR in cell cycle arrest and genome maintenance. *Genes Dev*. 17:615-628.

Brueckner, F., U. Hennecke, T. Carell, and P. Cramer. 2007. CPD damage recognition by transcribing RNA polymerase II. *Science*. 315:859-862.

Burtelow, M.A., S.H. Kaufmann, and L.M. Karnitz. 2000. Retention of the human Rad9 checkpoint complex in extraction-resistant nuclear complexes after DNA damage. *J Biol Chem*. 275:26343-26348.

Cardinale, S., B. Cisterna, P. Bonetti, C. Aringhieri, M. Biggiogera, and S.M. Barabino. 2007. Subnuclear localization and dynamics of the Pre-mRNA 3' end processing factor mammalian cleavage factor I 68-kDa subunit. *Mol Biol Cell*. 18:1282-1292.

Christians, F.C., and P.C. Hanawalt. 1993. Lack of transcription-coupled repair in mammalian ribosomal RNA genes. *Biochemistry*. 32:10512-10518.

Christians, F.C., and P.C. Hanawalt. 1994. Repair in ribosomal RNA genes is deficient in xeroderma pigmentosum group C and in Cockayne's syndrome cells. *Mutat Res*. 323:179-187.

Ciccia, A., and S.J. Elledge. 2010. The DNA damage response: making it safe to play with knives. *Mol Cell*. 40:179-204.

Clancy, S. 2008. DNA transcription. *Nature Education*. 1:1-5.

Cleaver, J.E. 1969. Xeroderma Pigmentosum: A human disease in which an initial stage of DNA repair is defective. *PNAS*. 63:428-435.

Cleaver, J.E., F. Cortes, L.H. Lutze, W.F. Morgan, A.N. Player, and D.L. Mitchell. 1987. Unique DNA repair properties of a xeroderma pigmentosum revertant. *Mol Cell Biol*. 7:3353-3357.

Clemson, C.M., J.N. Hutchinson, S.A. Sara, A.W. Ensminger, A.H. Fox, A. Chess, and J.B. Lawrence. 2009. An architectural role for a nuclear noncoding RNA: NEAT1 RNA is essential for the structure of paraspeckles. *Mol Cell*. 33:717-726.

Cohen, T.V., L. Hernandez, and C.L. Stewart. 2008. Functions of the nuclear envelope and lamina in development and disease. *Biochem Soc Trans*. 36:1329-1334.

Cooper, G. 2000. Eukaryotic RNA polymerases and general transcription factors. *In* The cell: A molecular approach. Sinauer Associates, Sunderland (MA).

Cortez, D. 2003. Caffeine inhibits checkpoint responses without inhibiting the ataxia-telangiectasia-mutated (ATM) and ATM- and Rad3-related (ATR) protein kinases. *J Biol Chem*. 278:37139-37145.

Costa, R.M., V. Chigancas, S. Galhardo Rda, H. Carvalho, and C.F. Menck. 2003. The eukaryotic nucleotide excision repair pathway. *Biochimie*. 85:1083-1099.

Coverley, D., H. Laman, and R.A. Laskey. 2002. Distinct roles for cyclins E and A during DNA replication complex assembly and activation. *Nat Cell Biol*. 4:523-528.

Cruet-Hennequart, S., S. Coyne, M.T. Glynn, G.G. Oakley, and M.P. Carty. 2006. UV-induced RPA phosphorylation is increased in the absence of DNA polymerase eta and requires DNA-PK. *DNA Repair (Amst)*. 5:491-504.

Cruet-Hennequart, S., M.T. Glynn, L.S. Murillo, S. Coyne, and M.P. Carty. 2008. Enhanced DNA-PK-mediated RPA2 hyperphosphorylation in DNA polymerase eta-deficient human cells treated with cisplatin and oxaliplatin. *DNA Repair (Amst)*. 7:582-596.

Dammer, E.B., A. Leon, and M.B. Sewer. 2007. Coregulator exchange and sphingosine-sensitive cooperativity of steroidogenic factor-1, general control nonderepressed 5, p54, and p160 coactivators regulate cyclic adenosine 3',5'-monophosphate-dependent cytochrome P450c17 transcription rate. *Mol Endocrinol*. 21:415-438.

Daniely, Y., D.D. Dimitrova, and J.A. Borowiec. 2002. Stress-dependent nucleolin mobilization mediated by p53-nucleolin complex formation. *Mol Cell Biol*. 22:6014-6022.

de Boer, J., and J.H.J. Hoeijmakers. 2000. Nucleotide excision repair and human syndromes. *Carcinogenesis*. 21:453-460.

de Lima-Bessa, K.M., M.G. Armelini, V. Chigancas, J.F. Jacysyn, G.P. Amarante-Mendes, A. Sarasin, and C.F. Menck. 2008. CPDs and 6-4PPs play different roles in UV-induced cell death in normal and NER-deficient human cells. *DNA Repair (Amst)*. 7:303-312.

Dellaire, G., and D.P. Bazett-Jones. 2007. Beyond repair foci: subnuclear domains and the cellular response to DNA damage. *Cell Cycle*. 6:1864-1872.

Dellaire, G., R. Farrall, and W.A. Bickmore. 2003. The Nuclear Protein Database (NPD): sub-nuclear localisation and functional annotation of the nuclear proteome. *Nucleic Acids Res*. 31:328-330.

Derheimer, F.A., H.M. O'Hagan, H.M. Krueger, S. Hanasoge, M.T. Paulsen, and M. Ljungman. 2007. RPA and ATR link transcriptional stress to p53. *PNAS*. 104:12778-12783.

Dettwiler, S., C. Aringhieri, S. Cardinale, W. Keller, and S.M. Barabino. 2004. Distinct sequence motifs within the 68-kDa subunit of cleavage factor Im mediate RNA binding, protein-protein interactions, and subcellular localization. *J Biol Chem*. 279:35788-35797.

Dong, B., D.S. Horowitz, R. Kobayashi, and A.R. Krainer. 1993. Purification and cDNA cloning of HeLa cell p54nrb, a nuclear protein with two RNA recognition motifs and extensive homology to human splicing factor PSF and *Drosophila* NONA/BJ6. *Nucleic Acids Res*. 21:4085-4092.

Emili, A., M. Shales, S. McCracken, W. Xie, P.W. Tucker, R. Kobayashi, B.J. Blencowe, and C.J. Ingles. 2002. Splicing and transcription-associated proteins PSF and p54nrb/nonO bind to the RNA polymerase II CTD. *RNA*. 8:1102-1111.

Fox, A.H., C.S. Bond, and A.I. Lamond. 2005. P54nrb forms a heterodimer with PSP1 that localizes to paraspeckles in an RNA-dependent manner. *Mol Biol Cell*. 16:5304-5315.

Fox, A.H., Y.W. Lam, A.K. Leung, C.E. Lyon, J. Andersen, M. Mann, and A.I. Lamond. 2002. Paraspeckles: a novel nuclear domain. *Curr Biol*. 12:13-25.

Fox, A.H., and A.I. Lamond. 2010. Paraspeckles. *Cold Spring Harb Perspect Biol*. 2:1-14.

Friedberg, E.C., Walker, G.C., Siede,W, Wood, R.D.,Schultz, R.A., Ellenburger, T. . 2006. DNA repair and mutagenesis. American Society for Microbiology Washington, D.C. 1,118.

Furgason, J.M., and E.M. Bahassi. 2012. Targeting DNA repair mechanisms in cancer. *Pharmacol Ther*. 137:298-308.

Furuta, T., H. Takemura, Z.-Y. Liao, G.J. Aune, C. Redon, O.A. Sedelnikova, D.R. Pilch, E.P. Rogakou, A. Celeste, H.T. Chen, A. Nussenzweig, M.I. Aladjem, W.M. Bonner, and Y. Pommier. 2003. Phosphorylation of histone H2AX and activation of Mre11, Rad50, and

Nbs1 in response to replication-dependent DNA double-strand breaks Induced by mammalian DNA topoisomerase I cleavage complexes. *J Biol Chem*. 278:20303-20312.

Gatei, M., K. Sloper, C. Sorensen, R. Syljuasen, J. Falck, K. Hobson, K. Savage, J. Lukas, B.B. Zhou, J. Bartek, and K.K. Khanna. 2003. Ataxia-telangiectasia-mutated (ATM) and NBS1-dependent phosphorylation of Chk1 on Ser-317 in response to ionizing radiation. *J Biol Chem*. 278:14806-14811.

Gerbi, S.A., Borovjagin, A.V. 2000. Pre-ribosomal RNA processing in multicellular organisms. M.C. Bioscience, editor. Landes Bioscience, Austin (TX).

Giannattasio, M., F. Lazzaro, M.P. Longhese, P. Plevani, and M. Muzi-Falconi. 2004. Physical and functional interactions between nucleotide excision repair and DNA damage checkpoint. *EMBO J*. 23:429-438.

Govoni, M., F. Farabegoli, A. Pession, and F. Novello. 1994. Inhibition of topoisomerase II activity and its effect on nucleolar structure and function. *Exp Cell Res*. 211:36-41.

Green, C.M., and G. Almouzni. 2003. Local action of the chromatin assembly factor CAF-1 at sites of nucleotide excision repair in vivo. *Embo J*. 22:5163-5174.

Grummt, I. 2003. Life on a planet of its own: regulation of RNA polymerase I transcription in the nucleolus. *Genes Dev*. 17:1691-1702.

Guo, R., J. Chen, F. Zhu, A.K. Biswas, T.R. Berton, D.L. Mitchell, and D.G. Johnson. 2010. E2F1 localizes to sites of UV-induced DNA damage to enhance nucleotide excision repair. *J Biol Chem*. 285:19308-19315.

Ha, K., Y. Takeda, and W.S. Dynan. 2011. Sequences in PSF/SFPQ mediate radioresistance and recruitment of PSF/SFPQ-containing complexes to DNA damage sites in human cells. *DNA Repair (Amst)*. 10:252-259.

Haley, B., T. Paunesku, M. Protic, and G.E. Woloschak. 2009. Response of heterogeneous ribonuclear proteins (hnRNP) to ionising radiation and their involvement in DNA damage repair. *Int J Radiat Biol*. 85:643-655.

Hallier, M., A. Tavitian, and F. Moreau-Gachelin. 1996. The transcription factor Spi-1/PU.1 binds RNA and interferes with the RNA-binding protein p54nrb. *J Biol Chem*. 271:11177-11181.

Hata, K., R. Nishimura, S. Muramatsu, A. Matsuda, T. Matsubara, K. Amano, F. Ikeda, V.R. Harley, and T. Yoneda. 2008. Paraspeckle protein p54nrb links Sox9-mediated transcription with RNA processing during chondrogenesis in mice. *J Clin Invest*. 118:3098-3108.

Hickson, I., Y. Zhao, C.J. Richardson, S.J. Green, N.M.B. Martin, A.I. Orr, P.M. Reaper, S.P. Jackson, N.J. Curtin, and G.C.M. Smith. 2004. Identification and characterization of a

novel and specific inhibitor of the ataxia-telangiectasia mutated kinase (ATM). *Cancer Res*. 64:9152-9159.

Hirao, A., Y.-Y. Kong, S. Matsuoka, A. Wakeham, J.r. Ruland, H. Yoshida, D. Liu, S.J. Elledge, and T.W. Mak. 2000. DNA damage-induced activation of p53 by the checkpoint kinase Chk2. *Science*. 287:1824-1827.

Hirose, Y., and J.L. Manley. 2000. RNA polymerase II and the integration of nuclear events. *Genes Dev*. 14:1415-1429.

Horowitz, D.S., and J. Abelson. 1993. A U5 small nuclear ribonucleoprotein particle protein involved only in the second step of pre-mRNA splicing in *Saccharomyces cerevisiae*. *Mol Cell Biol*. 13:2959-2970.

Huang, J., and W.S. Dynan. 2002. Reconstitution of the mammalian DNA double-strand break end-joining reaction reveals a requirement for an Mre11/Rad50/NBS1-containing fraction. *Nucl Acids Res*. 30:667-674.

Huber, A., P. Bai, J.M. de Murcia, and G. de Murcia. 2004. PARP-1, PARP-2 and ATM in the DNA damage response: functional synergy in mouse development. *DNA Repair (Amst)*. 3:1103-1108.

Hwang, B.J., S. Toering, U. Francke, and G. Chu. 1998. p48 Activates a UV-damaged-DNA binding factor and is defective in xeroderma pigmentosum group E cells that lack binding activity. *Mol Cell Biol*. 18:4391-4399.

Jamison, J.M., J. Gilloteaux, L. Perlaky, M. Thiry, K. Smetana, D. Neal, K. McGuire, and J.L. Summers. 2010. Nucleolar changes and fibrillarin redistribution following apatone treatment of human bladder carcinoma cells. *J Histochem Cytochem*. 58:635-651.

Jazayeri, A., J. Falck, C. Lukas, J. Bartek, G.C.M. Smith, J. Lukas, and S.P. Jackson. 2006. ATM- and cell cycle-dependent regulation of ATR in response to DNA double-strand breaks. *Nat Cell Biol*. 8:37-45.

Jiang, G., and A. Sancar. 2006. Recruitment of DNA damage checkpoint proteins to damage in transcribed and nontranscribed sequences. *Mol Cell Biol*. 26:39-49.

Jones, K.R., and G.M. Rubin. 1990. Molecular analysis of no-on-transient A, a gene required for normal vision in *Drosophila*. *Neuron*. 4:711-723.

Kameoka, S., P. Duque, and M.M. Konarska. 2004. p54(nrb) associates with the 5' splice site within large transcription/splicing complexes. *EMBO J*. 23:1782-1791.

Kamileri, I., I. Karakasilioti, and G.A. Garinis. 2012. Nucleotide excision repair: new tricks with old bricks. *Trends Genet*. 28:566-573.

Kaneko, S., O. Rozenblatt-Rosen, M. Meyerson, and J.L. Manley. 2007. The multifunctional protein p54nrb/PSF recruits the exonuclease XRN2 to facilitate pre-mRNA 3' processing and transcription termination. *Genes Dev*. 21:1779-1789.

Karni-Schmidt, O., A. Zupnick, M. Castillo, A. Ahmed, T. Matos, P. Bouvet, C. Cordon-Cardo, and C. Prives. 2008. p53 is localized to a sub-nucleolar compartment after proteasomal inhibition in an energy-dependent manner. *J Cell Sci*. 121:4098-4105.

Karp, G. 2007. Cell and molecular biology. John Wiley and Sons, U.S.A.

Kastan, M.B., and J. Bartek. 2004. Cell-cycle checkpoints and cancer. *Nature*. 432:316-323.

Kerzendorfer, C., and M. O'Driscoll. 2009. Human DNA damage response and repair deficiency syndromes: Linking genomic instability and cell cycle checkpoint proficiency. *DNA Repair (Amst)*. 8:1139-1152.

Kiesler, E., M.E. Hase, D. Brodin, and N. Visa. 2005. Hrp59, an hnRNP M protein in *Chironomus* and *Drosophila*, binds to exonic splicing enhancers and is required for expression of a subset of mRNAs. *J Cell Biol*. 168:1013-1025.

Koberle, B., V. Roginskaya, and R.D. Wood. 2006. XPA protein as a limiting factor for nucleotide excision repair and UV sensitivity in human cells. *DNA Repair (Amst)*. 5:641-648.

Krietsch, J., M.C. Caron, J.P. Gagne, C. Ethier, J. Vignard, M. Vincent, M. Rouleau, M.J. Hendzel, G.G. Poirier, and J.Y. Masson. 2012. PARP activation regulates the RNA-binding protein NONO in the DNA damage response to DNA double-strand breaks. *Nucl Acids Res*.

Krishnakumar, R., and W.L. Kraus. 2010. The PARP side of the nucleus: molecular actions, physiological outcomes, and clinical targets. *Mol Cell*. 39:8.

Krude, T., and R. Knippers. 1991. Transfer of nucleosomes from parental to replicated chromatin. *Mol Cell Biol*. 11:6257-6267.

Kuhnert, A., U. Schmidt, S. Monajembashi, C. Franke, B. Schlott, F. Grosse, K.O. Greulich, H.-P. Saluz, and F. Hänel. 2012. Proteomic identification of PSF and p54(nrb) as topBP1-interacting proteins. *J Cell Biol*. 113:1744-1753.

Kumagai, A., J. Lee, H.Y. Yoo, and W.G. Dunphy. 2006. TopBP1 activates the ATR-ATRIP complex. *Cell*. 124:943-955.

Kurki, S., K. Peltonen, and M. Laiho. 2004. Nucleophosmin, HDM2 and p53: players in UV damage incited nucleolar stress response. *Cell Cycle*. 3:976-979.

Laine, J.P., and J.M. Egly. 2006. When transcription and repair meet: a complex system. *Trends Genet*. 22:430-436.

Lazzaro, F., M. Giannattasio, F. Puddu, M. Granata, A. Pellicioli, P. Plevani, and M. Muzi-Falconi. 2009. Checkpoint mechanisms at the intersection between DNA damage and repair. *DNA Repair (Amst)*. 8:1055-1067.

Leibeling, D., P. Laspe, and S. Emmert. 2006. Nucleotide excision repair and cancer. *J Mol Hist*. 37:225-238.

Leung-Pineda, V., C.E. Ryan, and H. Piwnica-Worms. 2006. Phosphorylation of Chk1 by ATR is antagonized by a Chk1-regulated protein phosphatase 2A circuit. *Mol Cell Biol*. 26:7529-7538.

Li, J., and D.F. Stern. 2005. Regulation of Chk2 by DNA-dependent protein kinase. *Journal of Biological Chemistry*. 280:12041-12050.

Li, J., T. Uchida, T. Todo, and T. Kitagawa. 2006. Similarities and differences between cyclobutane pyrimidine dimer photolyase and (6-4) photolyase as revealed by resonance raman spectroscopy: Electron transfer from the fad cofactor to ultraviolet-damaged DNA. *J Biol Chem*. 281:25551-25559.

Li, S., W.W. Kuhne, A. Kulharya, F.Z. Hudson, K. Ha, Z. Cao, and W.S. Dynan. 2009. Involvement of p54(nrb), a PSF partner protein, in DNA double-strand break repair and radioresistance. *In* Nucl Acids Res. Vol. 37. 6746-6753.

Lindahl, T., and D.E. Barnes. 2000. Repair of endogenous DNA damage. *Cold Spring Harb Symp Quant Biol.* 65:127-134.

Lindsey-Boltz, L.A., and A. Sancar. 2007. RNA polymerase: the most specific damage recognition protein in cellular responses to DNA damage? *Proc Natl Acad Sci U S A*. 104:13213-13214.

Liu, S., S.O. Opiyo, K. Manthey, J.G. Glanzer, A.K. Ashley, C. Amerin, K. Troksa, M. Shrivastav, J.A. Nickoloff, and G.G. Oakley. 2012. Distinct roles for DNA-PK, ATM and ATR in RPA phosphorylation and checkpoint activation in response to replication stress. *Nucl Acids Res*. 40:10780-10794.

Mahaney, B.L., K. Meek, and S.P. Lees-Miller. 2009. Repair of ionizing radiation-induced DNA double-strand breaks by non-homologous end-joining. *Biochem J*. 417:639-650.

Marko, M., M. Leichter, M. Patrinou-Georgoula, and A. Guialis. 2010. hnRNP M interacts with PSF and p54(nrb) and co-localizes within defined nuclear structures. *Exp Cell Res*. 316:390-400.

Masai, H., Z. You, and K. Arai. 2005. Control of DNA replication: regulation and activation of eukaryotic replicative helicase, MCM. *IUBMB Life*. 57:323-335.

Matsuoka, S., B.A. Ballif, A. Smogorzewska, E.R. McDonald, K.E. Hurov, J. Luo, C.E. Bakalarski, Z. Zhao, N. Solimini, Y. Lerenthal, Y. Shiloh, S.P. Gygi, and S.J. Elledge.

2007. ATM and ATR substrate analysis reveals extensive protein networks responsive to DNA damage. *Science*. 316:1160-1166.

Matsuoka, S., G. Rotman, A. Ogawa, Y. Shiloh, K. Tamai, and S.J. Elledge. 2000. Ataxia telangiectasia-mutated phosphorylates Chk2 in vivo and in vitro. *PNAS*. 97:10389-10394.

Morishima, K., S. Sakamoto, J. Kobayashi, H. Izumi, T. Suda, Y. Matsumoto, H. Tauchi, H. Ide, K. Komatsu, and S. Matsuura. 2007. TopBP1 associates with NBS1 and is involved in homologous recombination repair. *BBRC*. 362:872-879.

Morozumi, Y., Y. Takizawa, M. Takaku, and H. Kurumizaka. 2009. Human PSF binds to RAD51 and modulates its homologous-pairing and strand-exchange activities. *Nucl Acids Res*. 37:4296-4307.

Moser, J., H. Kool, I. Giakzidis, K. Caldecott, L.H.F. Mullenders, and M.I. Fousteri. 2007. Sealing of chromosomal DNA nicks during nucleotide excision repair requires XRCC1 and DNA ligase III alpha in a cell-cycle-specific manner. *Mol Cell*. 27:311-323.

Mullenders, L.S., A;, Sarasin, A.;. 2001. Nucleotide excision repair. *Atlas Genet Cytogenet Oncol Haematol.* 2:347-353.

Muotri, A.R., M.C. Marchetto, M.F. Suzuki, K. Okazaki, C.F. Lotfi, G. Brumatti, G.P. Amarante-Mendes, and C.F. Menck. 2002. Low amounts of the DNA repair XPA protein are sufficient to recover UV-resistance. *Carcinogenesis*. 23:1039-1046.

Murthy, U.M., and P.N. Rangarajan. 2010. Identification of protein interaction regions of VINC/NEAT1/Men epsilon RNA. *FEBS Lett*. 584:1531-1535.

Nakagawa, S., and T. Hirose. 2012. Paraspeckle nuclear bodies—useful uselessness? *CMLS*. 69:3027-3036.

Nanninga, N. 2001. Cytokinesis in prokaryotes and eukaryotes: common principles and different solutions. *Microbiol Mol Biol Rev*. 65:319-333

Nasheuer, H.P., R. Smith, C. Bauerschmidt, F. Grosse, and K. Weisshart. 2002. Initiation of eukaryotic DNA replication: regulation and mechanisms. *Prog Nucl Acid Res Mol Biol*. 72:41-94.

Neugebauer, K.M., and M.B. Roth. 1997. Transcription units as RNA processing units. *Genes Dev*. 11:3279-3285.

O'Driscoll, M., V.L. Ruiz-Perez, C.G. Woods, P.A. Jeggo, and J.A. Goodship. 2003. A splicing mutation affecting expression of ataxia-telangiectasia and Rad3-related protein (ATR) results in Seckel syndrome. *Nat Genet*. 33:497-501.

Pabla, N., S. Huang, Q.S. Mi, R. Daniel, and Z. Dong. 2008. ATR-Chk2 signaling in p53 activation and DNA damage response during cisplatin-induced apoptosis. *J Biol Chem*. 283:6572-6583.

Page, T., M.A. Gitcho, S. Mosaheb, D. Carter, S. Chakraverty, R.H. Perry, E.H. Bigio, M. Gearing, I. Ferrer, A.M. Goate, N.J. Cairns, and J.R. Thorpe. 2011. FUS immunogold labeling TEM analysis of the neuronal cytoplasmic inclusions of neuronal intermediate filament inclusion disease: a frontotemporal lobar degeneration with FUS proteinopathy. *J Mol Neurosci*. 45:409-421.

Pang, D., S. Yoo, W.S. Dynan, M. Jung, and A. Dritschilo. 1997. Ku proteins join DNA fragments as shown by atomic force microscopy. *Cancer Res*. 57:1412-1415.

Pederson, T. 1998. The plurifunctional nucleolus. *Nucl Acids Res*. 26:3871-3876.

Peng, C.Y., P.R. Graves, R.S. Thoma, Z. Wu, A.S. Shaw, and H. Piwnica-Worms. 1997. Mitotic and G2 checkpoint control: regulation of 14-3-3 protein binding by phosphorylation of Cdc25C on serine-216. *Science*. 277:1501-1505.

Peng, R., B.T. Dye, I. Perez, D.C. Barnard, A.B. Thompson, and J.G. Patton. 2002. PSF and p54nrb bind a conserved stem in U5 snRNA. *RNA*. 8:1334-1347.

Perez-Castro, A.J., and R. Freire. 2012. Rad9B responds to nucleolar stress through ATR and JNK signalling, and delays the G1-S transition. *J Cell Sci*. 125:1152-1164.

Polo, S.E., A.N. Blackford, J.R. Chapman, L. Baskcomb, S. Gravel, A. Rusch, A. Thomas, R. Blundred, P. Smith, and J. Kzhyshkowska. 2012. Regulation of DNA-end resection by hnRNPU-like proteins promotes DNA double-strand break signaling and repair. *Mol Cell*. 45:505-516.

Polo, S.E., and S.P. Jackson. 2011. Dynamics of DNA damage response proteins at DNA breaks: a focus on protein modifications. *Genes Dev*. 25:409-433.

Prasanth, K.V., S.G. Prasanth, Z. Xuan, S. Hearn, S.M. Freier, C.F. Bennett, M.Q. Zhang, and D.L. Spector. 2005. Regulating gene expression through RNA nuclear retention. *Cell*. 123:249-263.

Proudfoot, N. 2000. Connecting transcription to messenger RNA processing. *Trends Biochem Sci*. 25:290-293.

Proudfoot, N.J., A. Furger, and M.J. Dye. 2002. Integrating mRNA processing with transcription. *Cell*. 108:501-512.

Rajesh, C., D.K. Baker, A.J. Pierce, and D.L. Pittman. 2011. The splicing-factor related protein SFPQ/PSF interacts with RAD51D and is necessary for homology-directed repair and sister chromatid cohesion. *Nucl Acids Res*. 39:132-145.

Raska, I., P.J. Shaw, and D. Cmarko. 2006. New insights into nucleolar architecture and activity. *Int Rev Cytol*. 255:177-235.

Rytkönen, A.K., M. Vaara, T. Nethanel, G. Kaufmann, R. Sormunen, E. Läärä, H.-P. Nasheuer, A. Rahmeh, M.Y.W.T. Lee, J.E. Syväoja, and H. Pospiech. 2006. Distinctive

activities of DNA polymerases during human DNA replication. *FEBS Journal*. 273:2984-3001.

Salton, M., Y. Lerenthal, S.Y. Wang, D.J. Chen, and Y. Shiloh. 2010. Involvement of Matrin 3 and SFPQ/NONO in the DNA damage response. *Cell Cycle*. 9:1568-1576.

Sarkaria, J.N., E.C. Busby, R.S. Tibbetts, P. Roos, Y. Taya, L.M. Karnitz, and R.T. Abraham. 1999. Inhibition of ATM and ATR kinase activities by the radiosensitizing agent, caffeine. *Cancer Res*. 59:4375-4382.

Sarkaria, J.N., R.S. Tibbetts, E.C. Busby, A.P. Kennedy, D.E. Hill, and R.T. Abraham. 1998. Inhibition of phosphoinositide 3-kinase related kinases by the radiosensitizing agent wortmannin. *Cancer Res*. 58:4375-4382.

Sasaki, Y.T., T. Ideue, M. Sano, T. Mituyama, and T. Hirose. 2009. MENepsilon/beta noncoding RNAs are essential for structural integrity of nuclear paraspeckles. *Proc Natl Acad Sci U S A*. 106:2525-2530.

Schiffner, S., N. Zimara, R. Schmid, and A.-K. Bosserhoff. 2011. p54nrb is a new regulator of progression of malignant melanoma. *Carcinogenesis*. 32:1176-1182.

Scott, M., F.M. Boisvert, D. Vieyra, R.N. Johnston, D.P. Bazett-Jones, and K. Riabowol. 2001. UV induces nucleolar translocation of ING1 through two distinct nucleolar targeting sequences. *Nucl Acids Res*. 29:2052-2058.

Selby, C.P., R. Drapkin, D. Reinberg, and A. Sancar. 1997. RNA polymerase II stalled at a thymine dimer: footprint and effect on excision repair. *Nucl Acids Res*. 25:787-793.

Selby, C.P., and A. Sancar. 2003. Characterization of transcription-repair coupling factors in E. coli and humans. *Methods Enzymol*. 371:300-324.

Sewer, M.B., V.Q. Nguyen, C.J. Huang, P.W. Tucker, N. Kagawa, and M.R. Waterman. 2002. Transcriptional activation of human CYP17 in H295R adrenocortical cells depends on complex formation among p54(nrb)/NonO, protein-associated splicing factor, and SF-1, a complex that also participates in repression of transcription. *Endocrinology*. 143:1280-1290.

Shav-Tal, Y., J. Blechman, X. Darzacq, C. Montagna, B.T. Dye, J.G. Patton, R.H. Singer, and D. Zipori. 2005. Dynamic sorting of nuclear components into distinct nucleolar caps during transcriptional inhibition. *Mol Biol Cell*. 16:2395-2413.

Shav-Tal, Y., and D. Zipori. 2002. PSF and p54(nrb)/NonO--multi-functional nuclear proteins. *FEBS Lett*. 531:109-114.

Shaw, P.J., and E.G. Jordan. 1995. The nucleolus. *Annu Rev Cell Dev Biol*. 11:93-121.

Shell, S.M., Z. Li, N. Shkriabai, M. Kvaratskhelia, C. Brosey, M.A. Serrano, W.J. Chazin, P.R. Musich, and Y. Zou. 2009. Checkpoint kinase ATR promotes nucleotide excision repair of UV-induced DNA damage via physical interaction with XPA. *J Biol Chem*.

Sherr, C.J., and J.M. Roberts. 2004. Living with or without cyclins and cyclin-dependent kinases. *Genes Dev*. 18:2699-2711.

Sorensen, C.S., R.G. Syljuasen, J. Falck, T. Schroeder, L. Ronnstrand, K.K. Khanna, B.B. Zhou, J. Bartek, and J. Lukas. 2003. Chk1 regulates the S phase checkpoint by coupling the physiological turnover and ionizing radiation-induced accelerated proteolysis of Cdc25A. *Cancer Cell*. 3:247-258.

Souquere, S., G. Beauclair, F. Harper, A. Fox, and G. Pierron. 2010. Highly ordered spatial organization of the structural long noncoding NEAT1 RNAs within paraspeckle nuclear bodies. *Mol Biol Cell*. 21:4020-4027.

Spector, D.L., and A.I. Lamond. 2011. Nuclear speckles. *Cold Spring Harb Perspect Biol*. 3:12.

Stiff, T., K. Cerosaletti, P. Concannon, M. O'Driscoll, and P.A. Jeggo. 2008. Replication independent ATR signalling leads to G2/M arrest requiring Nbs1, 53BP1 and MDC1. *Hum Mol Genet*. 17:3247-3253.

Stiff, T., S.A. Walker, K. Cerosaletti, A.A. Goodarzi, E. Petermann, P. Concannon, M. O'Driscoll, and P.A. Jeggo. 2006. ATR-dependent phosphorylation and activation of ATM in response to UV treatment or replication fork stalling. *EMBO J*. 25:5775-5782.

Sunwoo, H., M.E. Dinger, J.E. Wilusz, P.P. Amaral, J.S. Mattick, and D.L. Spector. 2009. MEN epsilon/beta nuclear-retained non-coding RNAs are up-regulated upon muscle differentiation and are essential components of paraspeckles. *Genome Res*. 19:347-359.

Takebe, H., Y. Miki, T. Kozuka, J.-i. Furuyama, K. Tanaka, M.S. Sasaki, Y. Fujiwara, and H. Akiba. 1977. DNA repair characteristics and skin cancers of xeroderma pigmentosum patients in Japan. *Cancer Res*. 37:490-495.

Toledo, L.I., M. Murga, R. Zur, R. Soria, A. Rodriguez, S. Martinez, J. Oyarzabal, J. Pastor, J.R. Bischoff, and O. Fernandez-Capetillo. 2011. A cell-based screen identifies ATR inhibitors with synthetic lethal properties for cancer-associated mutations. *Nat Struct Mol Biol*. 18:721-727.

van Hoffen, A., A. Balajee, A.A. van Zeeland, and L.H.F. Mullenders. 2003. Nucleotide excision repair and its interplay with transcription. *Toxicology*. 193:79-90.

Veuger, S.J., N.J. Curtin, C.J. Richardson, G.C.M. Smith, and B.W. Durkacz. 2003. Radiosensitization and DNA repair inhibition by the combined use of novel inhibitors of DNA-dependent protein kinase and poly(ADP-Ribose) polymerase-1. *Cancer Res*. 63:6008-6015.

Vilmar, A., and J.B. Sorensen. 2009. Excision repair cross-complementation group 1 (ERCC1) in platinum-based treatment of non-small cell lung cancer with special emphasis on carboplatin: a review of current literature. *Lung Cancer*. 64:131-139.

Volker, M., M.J. MonÈ, P. Karmakar, A. van Hoffen, W. Schul, W. Vermeulen, J.H.J. Hoeijmakers, R. van Driel, A.A. van Zeeland, and L.H.F. Mullenders. 2001. Sequential assembly of the nucleotide excision repair factors in vivo. *Mol cell*. 8:213-224.

Vrouwe, M., and L.F. Mullenders. 2009. Nucleotide excision repair: from DNA damage processing to human disease. *In* The DNA damage response: Implications on cancer formation and treatment. K.K. Khanna and Y. Shiloh, editors. Springer Netherlands. 235-259.

Wang, X.Q., J.L. Redpath, S.T. Fan, and E.J. Stanbridge. 2006. ATR dependent activation of Chk2. *J Cell Physiol*. 208:613-619.

Wollmann, Y., U. Schmidt, G.D. Wieland, P.F. Zipfel, H.-P. Saluz, and F. Hänel. 2007. The DNA topoisomerase IIβ binding protein 1 (TopBP1) interacts with poly (ADP-ribose) polymerase (PARP-1). *J Cell Biol*. 102:171-182.

Woodard, R.L., K. Lee, J. Huang, and W.S. Dynan. 2001. Distinct roles for Ku protein in transcriptional reinitiation and DNA repair. *J Biol Chem*. 276:15423-15433.

Wu, X., S.M. Shell, Y. Liu, and Y. Zou. 2007. ATR-dependent checkpoint modulates XPA nuclear import in response to UV irradiation. *Oncogene*. 26:757-764.

Yang, J., Y. Yu, H.E. Hamrick, and P.J. Duerksen-Hughes. 2003. ATM, ATR and DNA-PK: initiators of the cellular genotoxic stress responses. *Carcinogenesis*. 24:1571-1580.

Yang, Y.S., J.H. Hanke, L. Carayannopoulos, C.M. Craft, J.D. Capra, and P.W. Tucker. 1993. NonO, a non-POU-domain-containing, octamer-binding protein, is the mammalian homolog of *Drosophila* nonA. *Mol Cell Biol*. 13:5593-5603.

Zhang, W.W., L.X. Zhang, R.K. Busch, J. Farres, and H. Busch. 1993. Purification and characterization of a DNA-binding heterodimer of 52 and 100 kDa from HeLa cells. *Biochem J*. 290 (Pt 1):267-272.

Zhang, Z., and G.G. Carmichael. 2001. The fate of dsRNA in the nucleus: a p54(nrb)-containing complex mediates the nuclear retention of promiscuously A-to-I edited RNAs. *Cell*. 106:465-475.

Zhou, B.-B.S., and S.J. Elledge. 2000. The DNA damage response: putting checkpoints in perspective. *Nature*. 408:433-439.

Zhou, B.B., and E.A. Sausville. 2003. Drug discovery targeting Chk1 and Chk2 kinases. *Prog Cell Cycle Res*. 5:413-421.

Zou, L., D. Cortez, and S.J. Elledge. 2002. Regulation of ATR substrate selection by Rad17-dependent loading of Rad9 complexes onto chromatin. *Genes Dev*. 16:198-208.

Zou, L., and S.J. Elledge. 2003. Sensing DNA damage through ATRIP recognition of RPA-ssDNA complexes. *Science*. 300:1542-1548.